Estimating Aboveground Biomass Based on Forest Volume from Als and Fcd Mapper in Berkelah Tropical Rainforest, Malaysia

EXAVERY KIGOSI
February 2018

SUPERVISORS:
Drs. E.H. Kloosterman
Dr. Y.A. Hussin

ADVISOR:
Dr. Zulkiflee Abd Latif (University Technology Mara Malaysia – UiTM)

Estimating Aboveground Biomass Based on Forest Volume from Als and Fcd Mapper in Berkelah Tropical Rainforest, Malaysia

EXAVERY KIGOSI

Enschede, The Netherlands, February 2018

Thesis submitted to the Faculty of Geo-Information Science and Earth Observation of the University of Twente in partial fulfilment of the requirements for the degree of Master of Science in Geo-Information Science and Earth Observation.

Specialization: Natural Resources Management

SUPERVISORS:

Drs. E.H. Kloosterman

Dr. Y.A. Hussin

ADVISOR:

Dr. Zulkiflee Abd Latif (University Technology Mara Malaysia - UiTM)

THESIS ASSESSMENT BOARD:

Prof. Dr. A.D. Nelson (Chair)

Dr. T. Kauranne (External Examiner, LUT School of Engineering Science, Finland)

ABSTRACT

Forests regulate climate by absorbing greenhouse gases from the atmosphere and storing it. Anthropogenic activities threaten this type of ecosystem service due to deforestation and as a result there is a flux for carbon dioxide in the atmosphere. The United Nations Frame Work Convention for Climate Change (UNFCCC) through REDD+ program is aiming to control carbon dioxide emissions through payments to communities or institutions that have managed to control deforestation and increase carbon sequestration.

Consequently, UNFCCC is seeking best methods that can be applied for Measuring, Report and Verifying (MRF) aboveground biomass from different types of forests including tropical rain forests. This method must be cheap, accurate and, in terms of coverage, must cover large areas during aboveground biomass estimations. This will improve REDD+ governance in terms of carbon estimations.

In this study, aboveground biomass from a tropical rain forest has been estimated in terms of forest canopy volume derived from airborne LiDAR data. Different conditions have been applied to estimate forest canopy volume: non-slice canopy, sliced canopy (using a threshold for the lower boundary of the canopy), non-smoothed canopy and smoothed canopy (without pits in the canopy surface). All four conditions have been applied into three different canopy pixel sizes: 0.5m*0.5m, 1m*1m and 2m*2m. In addition, forest canopy volume has been combined with forest canopy density derived from a forest canopy density mapper to get an adjusted forest canopy volume. Forest canopy volume and adjusted forest volume were assessed the relationship with above biomass using regression analysis model.

For a non-sliced and smoothed forest canopy of 2m*2m pixel size has predicted aboveground biomass with a coefficient of determination (r^2) of 0.715 for a linear regression and 0.781 for a exponential regression while adjusted forest volume, the coefficient of determination (r^2) decreased were 0.668 – linear and 0.694 exponential. This decrease resulted in all adjusted forest canopy volumes in all conditions that were used. The hypothesis of the study was assessing the significance of forest canopy volume in predicting AGB.

Smoothed forest canopies have a high coefficient of determination (r^2) with aboveground biomass compared to non-smoothed forest canopies. This is due to the fact that smoothed canopies have estimated a bigger forest volume compared to non-smoothed canopies. Higher amounts of forest volume are due to the removal of effects of neighbouring pixel differences within forest canopy.

The study faces some limitations in aboveground estimation due to shift errors on the location of individual trees and plot centre locations. Moreover, the calculations of forest canopy density in setting some parameters thresholds is subjective depending on the analyser's perceptions. It is better to consider the use of static GPS for recording locations of individual trees and centre locations. Lastly, algorithms can be used to estimate forest canopy density which could remove subjectivity from forest canopy density mapping.

Keywords: Forest Canopy Volume, Adjusted Forest Canopy Volume, Forest Canopy Density, Aboveground Biomass and Airborne LiDAR.

ACKNOWLEDGEMENTS

First, I thank Almighty GOD for this grace, mercy and blessings throughout my studies. I would also like to thank the University of Twente, Geoinformation Science and Earth Observation Faculty (ITC) for giving me this opportunity to undertake my master's studies and make my dream come true. This has been made possible through the Dutch government scholarship (NUFFIC) and so I am grateful to the Dutch tax payers. I also recognize the help of MJUMITA country director, Madam Rahima Njaidi, for permitting me to come pursue my studies. Drs. Raymond Nijmeijer, Course Director, thank you for your support in the whole period of my studies.

The support and encouragement from my lovely Mother, Father, brothers and sisters has also given me the strength to successfully complete my studies. My brothers and sisters were behind me towards my studies, I recognize your contributions and support toward my studies. Truly, I saw strong family unity. Thanks very much my lovely parents, brothers and sisters.

Completing this study was not my own effort, as I stood on the shoulders of giants: Drs. E. H. Kloosterman (Henk), first supervisor and Dr. Y. A. Hussin (Yousif), second supervisor. I would like to express my sincere appreciation for the material and moral support. Your ideas, criticism, advice, guidance and encouragement during my studies and research have helped me immeasurably. It has been a great experience working with you. Thank you very much for your guidance and support.

My appreciation to Dr. Zulfiflee Abd Latif from University Technology Mara Malysia and Ms. Syaza Rozali, Phd candidate at University Technology Mara Malaysia for the help and support they provided during the fieldwork. This included the collection of Airborne Laser Scanner data and the different logistical support such as transport, accommodation and access to the Berkelah Forest. To the fieldwork team members, Robert Masolele, Edward Justine, Solomon Begashaw, Tiegsti Hadush, Agerie Nega and Belinda Odia, I appreciate your team work spirit and encouragement during the fieldwork and thesis writing. Lastly, I give credit to our drivers who took us daily from Kuantan town to our study area which was more than 120 km I could not have done it alone, thank you all very much.

Special thanks to my fellow Tanzanians and Kenyans our neighbours for their hospitality during my studies. Lyidia Biri has always been so close to me, your time, ideas, critics, moral and material support has had great impacts to my studies. Thank you very much. Last but not least to the ITC students, NRM in particular the class of 2018, your ideas and critics have been constructive towards my studies. Thank You All.

Exavery Kigosi
Faculty of Geo-information and Earth Observation – University of Twente
Enschede, Netherlands
February 2018.

TABLE OF CONTENTS

LIST OF FIGURES

LIST OF TABLES

APPENDICES

EQUATIONS

ACRONYMS

AGB	Aboveground Biomass
LiDAR	Light Detection And Ranging
ALS	Airborne Laser Scanner
TLS	Terrestrial Laser scanner
FCD	Forest canopy Density
FCD Mapper	Forest Canopy Density Mapper
UNFCCC	United Nations Framework Convection for Climate Change
REDD+	Reducing Emission from Deforestation and Degradation
MVR	Monitoring, Verifying and Reporting
SAR	Synthetic Aperture Radar
RADAR	Radio Detection and Ranging
DBH	Diameter at Breast Height
IMU	Inertial Measuring Unit
DTM	Digital Terrain Model
DSM	Digital Surface Model
CHM	Canopy Height Model

1. INTRODUCTION

1.1. Background

Globally, forests cover more than 4 billion hectares, which is 31% of the total land surface. Forest resources, originating from tropical rainforests, boreal, temperate and tree-grass savannah, are very important to human and other living organisms. These resources provide many ecosystem services such as fresh water, wood, food, and timber, nutrient cycles and, regulation of climate and soil, not to mention cultural services, including recreational activities and aesthetics (Millennium Ecosystem Assessment, 2005; Phan et al., 2017; Alamgir et al., 2016 and Achad et al., 2016). These ecosystem services are threatened by anthropogenic activities such as deforestation and almost 13 million hectares of forest are being converted into other land cover types such as farmlands and bare lands every year (FAO, 2010). This conversion leads to the contribution of greenhouse gases in the atmosphere. Cutting down tropical rainforests contribute to 12 – 20% global anthropogenic greenhouse gases emission (Le Quéré et al., 2015). Therefore, the decline of forest ecosystem services contributes to climate effects such as climate change.

As a result, forest regulation services play a crucial role in mitigating the effects of climate change by acting as a carbon pool or sink in terrestrial ecosystems. The United Nations Framework Convention on Climate Change (UNFCC) has developed global initiatives under Reducing Emission from Degradation and Deforestation (REDD+) which ensures will reducing greenhouse gases emissions resulting from forest degradation and deforestation. The REDD+ programme is implementing payment mechanisms to communities who have degraded their forests once they have controlled the forest degradation and deforestation. Hence, the REDD+ programme is looking for efficient and effective methods for measuring, reporting, and verifying (MRV) the emission and carbon sequestrations from forests which will make the payment initiatives more transparent to all stakeholders (Neba et al., 2014).

Identifying the capacity of a forest to sequester carbon or to estimate the amount of carbon that has been released by a degraded forest is done through estimating aboveground biomass of a forest area. Aboveground biomass can be estimated using either a destructive method or non–destructive method. A destructive method involves cutting, oven drying and weighing a tree to estimate the aboveground biomass. Clearly, this method has some limitations as it is time-consuming, destructive, expensive and subject to sampling bias (Stovall et al., 2017). A non-destructive method uses an allometric equation and biophysical tree measurements to estimate aboveground biomass (Djomo & Chimi, 2017). Remote Sensing (RS) and Geographic Information Systems (GIS) approaches are among these non–destructive methods that can be used to asses and estimate aboveground biomass. They can provide spatial information and allow for monitoring, especially of inaccessible areas (Dengsheng Lu, 2006). As remote sensing provides spatial and temporal information, it is seen as a means of estimating carbon sequestered in the forest and as a method which meets the Kyoto Protocol and the United Nation's REDD+ requirements (Karna et al., 2015).

Based on these technologies, UNFCC, through the REDD+ programme, recommends the use of different techniques such as very high-resolution satellite images, SAR backscatter and LiDAR to assess aboveground biomass and carbon stock, because it is considered a cheap and effective methods (FFPRI, 2012). Moreover, optical sensors, Radio Detection and Ranging (RADAR) and light detection and ranging (LiDAR) are among remote sensing techniques that can be used for biomass estimation (Kumar et al., 2015).

LiDAR remote sensing can be used to derive tree biophysical information because it measures a tree in three dimensions and at the same time records the location (Lim et al., 2003). The information measured can be used to quantify forest ecosystem services such as carbon sequestration by assessing the amount of biomass it contains, (Van Leeuwen et al., 2011). From LiDAR, it is possible to derive tree or stand height, tree volume, leaf area index and foliage amount (Farid et al., 2008; van Leeuwen & Nieuwenhuis, 2010). The tree parameters (DBH and tree height) that have been derived with LiDAR can be used in estimating and mapping aboveground biomass and carbon.

Similarly, estimating aboveground biomass from optical remote sensing data through spectral reflectance and vegetation indices with field data, such as DBH, is being used to estimate biomass (Foody et al., 2003; Joshi, 2006; Dittmann et al.,2017). It should be noted that using optical remote sensing images, "biomass cannot be directly measured from space, but the remotely sensed reflectance can be related to the biomass estimates based on the field measurements" (Muukkonen & Heiskanen, 2005). Statistical regression models are applied in estimation and prediction of tree biomass by using optical image pixel spectral band values (Muukkonen & Heiskanen, 2005). The application of optical images appears to be the best option decision for exploring a general overview of the amount of biomass over a large area of homogeneous stands by using exploratory power (R^2) and Root Mean Square Error (RMSE) (Muukkonen & Heiskanen, 2007).

1.2. Problem Statement

Biomass estimation for tropical forests received substantial attention in recent years because of the role of these forests in carbon sequestration in climate regulations (Lu et al., 2002) and the contribution of forest degradation and deforestation in the emissions of carbon dioxide. Different techniques and approaches have been applied in estimating aboveground biomass in tropical rainforests such as traditional, which are field-based measurements and remote sensing methods, such as LiDAR, Synthetic Aperture RADAR (SAR) backscatters and optical satellite images. In combining LiDAR with field measurements such as diameter at breast height (DBH), tree height and wood density, the method becomes more accurate in estimating aboveground biomass (Englhart et al., 2012). Although this method provides very precise AGB values, it is difficult to implement in remote areas, labour demand, time-consuming and lacks information on the spatial distribution especially when a terrestrial laser scanner (TLS) is used (Englhart et al., 2012).

Aboveground biomass estimation requires tree diameter at breast height but is not captured by remote sensing techniques from above, whereas tree crown projection areas, which can be obtained from very high-resolution images, can serve as a proxy for tree DBH. Nonetheless the relationship between crown projected area and field measured DBH is weak according to studies conducted by Shrestha (2011) and Nandin-Erdene (2011) with a coefficient (r^2) of 0.35 and 0.16 respectively. Other remote sensing techniques such as using optical satellite observation measurements, are less accurate, but they have advantages of large spatial coverage and can even work in remote areas. Less accuracy is due to forest structure complexity (Lu et al., 2002), saturation in vegetation indices and wavelength reflection (Dong et al., 2003; Muukkonen & Heiskanen, 2007; Englhart et al., 2012). However, still these methods are advantageous for preliminary exploration for the amount of biomass in inaccessible areas.

In addition, using optical remote sensing satellite images, forest canopy density assessments can be derived by combining biophysical indices: advanced vegetation index (AVI), bare soil index (BI), canopy shadow index (SI) and thermal index (TI) which can be used to study the structure and quality of a forest canopy (Chandrashekhar et al., 2005; Lu et al., 2002). According to Joshi (2006), the Forest Canopy Density mapper technique can be used to derive forest canopy density but is 54.5% and the artificial neural network (ANN) while ANN estimated by 63.1% forest canopy density.

On the other hand, LiDAR data (ALS and TLS) is another remote sensing technique that can be used to derive individual tree volume, lower forest canopy volume for TLS and upper canopy volume for ALS (Liang et al., 2016; Nelson, 1984). Mathematical relationships may be established between forest or tree volume derived from ALS and FCD mapper and forest biomass (Nelson et al., 1997). Estimating aboveground biomass could be based on the use of mathematical relationships of some of the forest parameters such as forest volume derived from LiDAR data, forest canopy density and wood density.

Biomass estimation using the allometric equation is generally accepted as a non-destructive method to assess tree aboveground biomass and carbon stock. The most important tree parameter in the equation is DBH, unfortunately, the DBH cannot be seen with remote sensing techniques that capture data from above and it is a very challenging task to measure DBH due to forest accessibility complexities. Shrestha (2011) and Nandin-Erdene (2011) in their studies have shown that there is weak correlation coefficient (r) between crown projected area (CPA) and tree diameter at breast height (DBH) because it is less than between 0.1 and 0.3 respectively. Karna et al., (2015) has used crown projected area as a proxy for aboveground biomass estimation for different species in Kayar Khola watershed in Nepal and the correlation coefficient was between 0.76 to 0.94. Crown Projected area approach is successful in temperate forests and plantation forests which have a simple vertical canopy structure. However, this approach loses significance in tropical rain forests as they have interlocking canopies of multiple layers and consist of different varieties of species in one location. These characteristics affect the predictive capabilities of CPA.

From Airborne LiDAR remote sensing technology is accurate in extracting upper forest canopy height which is used in estimating aboveground biomass through allometric equation (Liang et al., 2016). Liang et al. (2016) also describe that LiDAR technology can be used to measure tree volume, and tree DBH by using TLS and not ALS. The aim of this research is to investigate if airborne data can be used to estimate forest volume in combination with forest canopy density derived from forest canopy density model which can be used as a proxy for aboveground biomass and carbon stock.

1.3. Research Objectives

1.3.1. Main Objective

This study aims to investigate if foliage forest volume from ALS point clouds in combination with FCD mapper can act as a proxy for aboveground biomass estimation in a tropical rainforest.

1.3.2. Specific Objectives

1. Derive forest volume using ALS point clouds and FCD mapper in a tropical rainforest

2. Assess the aboveground biomass of the field plots (AGB_{field})

3. Assess the relationship between ALS/FCD mapper forest volume and AGB_{field}.

4. Map AGB of the study area using forest volume

1.4. Research Questions

1. What is the forest volume derived from ALS and FCD mapper in a tropical rainforest?
2. What is aboveground biomass of the field plots ($AGB_{field)}$ used in this research?
3. What is the relation between forest volume derived from ALS and FCD mapper and AGB_{field}?
4. How accurately does the AGB map predict the actual AGB in the field?

1.5. Hypothesis

1. H0 = There is no significant relation between AGB_{field} and forest volume from ALS * FCD in a tropical rainforest.

H1 = There is a significant relation between AGB_{field} and forest volume from ALS * FCD tropical rain forest

2. REFERENCED LITERATURE OF KEY CONCEPTS AND TECHNOLOGIES

Chapter 2 discusses key concepts, data and technologies that have been used in this research. Tropical rainforest, aboveground biomass, carbon, allometric equation, forest canopy volume and forest canopy density are the key concepts that have been applied in this research. LiDAR technology is the main source of data, so this chapter has described the way can be acquired and used.

2.1. Tropical Rain Forest

Tropical rainforests are characterized by tall, evergreen, variety of tree species composition and dense forests and multilayer canopy in which the climate is always hot and has a short dry season (Sato, 2009, Corlett & Primack, 2011). Tropical rainforests are located around the equator between latitudes 5^0 – 10^0 North and South, its rainfall ranges between 1500 mm to 1800 mm per annum and the mean annual temperature is about 25^0C – 26^0C (Corlett & Primack, 2011). In addition, tropical rainforests contain almost two thirds of the world's biodiversity (Haven, 1988), they store approximately 60% of the world's aboveground biomass and almost 27% of global soil carbon. The contribution of the net primary production (NPP) of tropical rainforests is estimated to be almost 20 – 40% of the global NPP (Olivas et al., 2013).

2.2. Forest Aboveground Biomass and Carbon

Aboveground biomass comprises all plant living materials such as stump, stem, branches, bark, leaves and foliage (IPCC, 1996). Edson & Wing (2011) defines aboveground biomass as "mass of live or dead organic matter and its unit of measure is weight (tons)/area (ha)". Plant biomass can be measured by using destructive method, non-destructive method, remote sensing, or modelling. Tree aboveground biomass can be derived from tree parameters such as diameter at the breast height (DBH), tree height and using the allometric equation, or by using vegetation indices, forest volume and wood density of a specific tree(Chave et al., 2006). Carbon content describes the amount of carbon a plant has stored after sequestering it from the atmosphere and can amount to approximately 50% of the dry weight (Eckert, 2012; Holdaway et al., 2014; Nogueira et al., 2017).

2.3. Light Detection And Ranging System (LiDAR)

LiDAR (Light Detection And Ranging) is also one among active remote sensing technique using laser pulse beam (Drake et al., 2002). For vegetation studies, the pulse travelling between the object and the LiDAR sensor uses the near-infrared wavelength (Drake et al., 2002). The distance between the object and the sensor is measured by calculating travelling time between the moment the pulse left the sensor, the return time of the reflected radiation and the sensor distance (Drake et al., 2002). There are two types of LiDAR systems: Terrestrial Laser Scanner and Airborne Laser Scanner.

Terrestrial Laser Scanner (TLS)

TLS is a terrestrial type LiDAR which is mounted on a tripod see Figure 2.1 and scans surrounding objects by a laser pulse in a certain angular measurement (Liang et al., 2016). TLS uses Phase Shift (PS) and Time-off Light (ToF)techniques. According to Liang et al., (2016) PS ranging makes use of continuous laser illumination and amplitude modulation of the beam to discern the range at high frequency and ToF utilizes precise timing to determine the range from the pulse time of flight and the speed of light. TLS scans many points in a short time using vertical and horizontal rotation (Liang et al., 2016). The result is a very dense 3D point cloud of the scanned area.

Figure 2.1. Riegl VZ - 400 Terrestrial Laser Scanner (Fieldwork Berkelah forest, Malaysia 2017)

Airborne Laser Scanner (ALS)

Airborne laser scanning (ALS) is a LiDAR technology which is based in from an aircraft (see Figure 2.2) during measurement taking (Hyyppä et al., 2008). The system comprises of inertia measurement units (IMU) and differential global positioning system (GPS) along the flight path, so it collects locations and correct them at the same time. The ALS gives a geo-referenced 3D point cloud, from which can be used to generate digital terrain models (DTM), digital surface models (DSM) and three-dimensional models (e.g. the canopy height model) (Hyyppä et al., 2008). Airborne LiDAR is a remote sensing technology which can provide three-dimensional information about forest canopy structure and shows a lower sensitivity to signal saturation (Nie, et al., 2017).

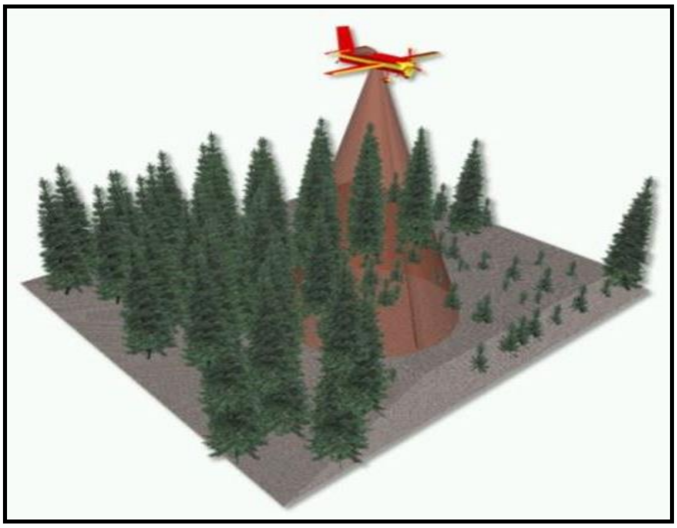

Figure 2.2. Airborne Laser Scanning System for Mapping forest. Source: (OSU, 2017)

2.4. Forest Canopy Density Mapper and Forest Canopy Density

A Forest canopy density mapper is also known as Rikimaru's model. Mapping and monitoring forest canopy density (FCD) combines four indices to express canopy density in percentages (Rikimaru et al., 2002). The indices behave differently with increasing vegetation cover and forest density (see Figure 2.3)

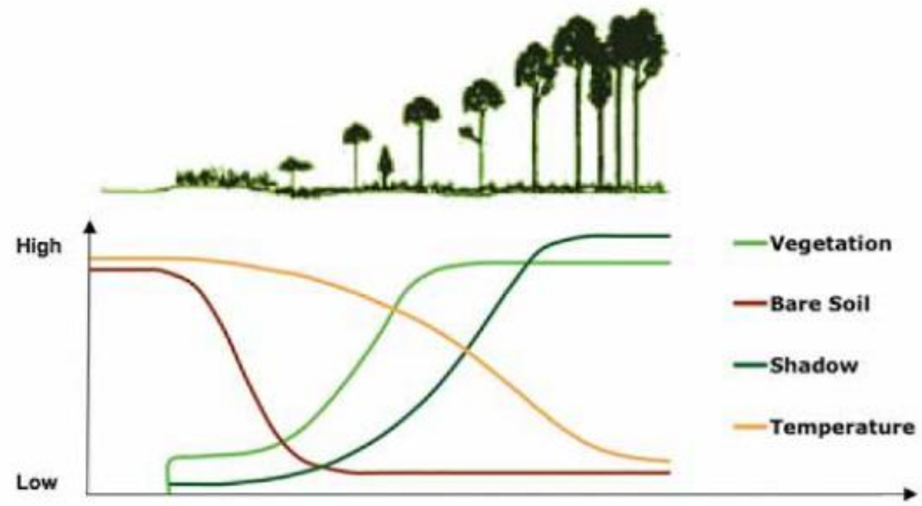

	Hi-FCD	Low-FCD	Grassland	Bare Land
AVI	Hi	Mid	Hi	Low
BI	Low	Low	Low	Hi
SI	Hi	Mid	Low	Low
TI	Low	Mid	Mid	Hi

Figure 2.3. Characteristics of four indices for forest condition. Source (Rikimaru et al., 2002)

Forest canopy density can be used assess the dynamics of the forest. FCD mapper assesses the forest condition by checking on the gaps in the forest canopy and this information can be used to predict/assess forest degradation (Neba et al., 2014). The FCD mapper uses four biophysical indices: advanced vegetation index (AVI), bare soil index (BI), canopy shadow index (SI) and thermal index (TI) (Hadi et al., 2004). The four indices have different calculation equations:

$$\mathrm{AVI} = ((\mathrm{B5} + 1)(255 - \mathrm{B4})(\mathrm{B5} - \mathrm{B4})^{\frac{1}{3}}$$

$$\mathrm{AVI} = 0 \text{ If } \mathrm{B5} < \mathrm{B4} \text{ after normalization}$$

Equation 2.1. Advanced Vegetation Index based on Landsat 8 bands

Whereby: AVI = Advanced Vegetation Index

B4 = Red (wavelenght - 0.45-0.52 micrometres)

B5 = Near Infrared (NIR) (wavelenght - 0.77-0.90 micrometres)

$$BI = BIO \times 100 + 100$$

$$BIO = (B6 + B4) - (B5 + B2)/(B6 + B4) + (B5 + B1)$$

Equation 2.2. Bare Soil Index based on Landsat 8 bands.

Whereby: BI = Bare soil Index

BIO = Normalize Vegetation Different Backgrounds

B2 = Blue (wavelenght - 0.45-0.52 micrometres)

B4 = Red (wavelenght - 0.45-0.52 micrometres)

B5 = Near Infrared (NIR) (wavelenght - 0.77-0.90 micrometres)

B6 = Shortwave Infrared (SWIR) 1 (wavelenght - 1.55-1.75 micrometres)

$$SI = \sqrt[3]{(255 - B2)(255 - B3)(255 - B4)}$$

Equation 2.3. Shadow Index based on Landsat 8 bands.

Whereby: SI = Shadow Index

B2 = Blue(wavelenght - 0.45-0.52 micrometres)

B3 = Green (wavelenght - 0.52-0.60micrometres)

B4 = Red (wavelenght - 0.63-0.69 micrometres)

$$T = K2/(ln(K1/L + 1))$$

$$L = Lmin + ((Lmax - Lmin)/255) \times Q$$

Equation 2.4. Ground Temperature

Whereby: T = Ground Temperature

Q = Digital Record

K1, K2 = Calibration Coefficients

K1=666.09 watts / (meter squared * ster* µm)

K2=1282.71 Kelvin

Lmin= 0.1238 watts / (meter squared * ster* µm)

Lmax= 1.500 watts / (meter squared * ster* µm)

$$FCD = \sqrt{VD \times SSI + 1} - 1$$

Equation 2.5. Forest Canopy Density Analysis

Whereby: VD = Vegetation Density

SSI = Normalized Shadow Index from other Indices

2.5. Forest Canopy Volume

Forest canopy volume is considered as stand volume or tree volume which is an estimate of the whole canopy volume, stem, branches and foliage, expressed in cubic meters. Forest volume/stand volume can be measured directly from the field or by estimating it through different linear and regression tree analysis such as generalized additive models and artificial neural networks (Mohammadi et al., 2011). Forest volume or tree volume can be derived from LiDAR, ALS and TLS point clouds.

Airborne LIDAR data can estimate the total forest volume or, if a threshold is used, forest canopy or foliage volume. However, since airborne LIDAR point clouds are taken from above, this data does not allow volume estimation of the stems. Cell grids are used to estimate the volume of the forest canopy and volume of foliage within the canopy. Forest canopy volume in combination with forest canopy density, derived from the FCD mapper, allows for the calculation of an adjusted forest canopy volume since forest canopy density is expressed in percentages.

2.6. Allometric Equation for ABG and Carbon estimates

An allometric equation is a statistical regression model that has been developed for estimating vegetation biomass using different vegetation parameters: vegetation indices, tree height, tree volume, diameter at breast height (DBH) and spectral reflectance (Basuki et al., 2009). Specific allometric equations have been developed for different forest types like tropical rainforest, savannah woodlands, and temperate forests (Araújo et al., 1999), or for different vegetation species such as grasses, pine trees, deciduous and evergreen. The development of allometric equations are widely used and replace destructive method of clear-cutting, oven drying and weighing, even though the latter, however, is more accurate (Basuki et al., 2009). AGB can be converted into Carbon stock by multiplying it by a fraction (Goslee et al., 2012; Petersson et al., 2012) (see Equation 4.5).

3. STUDY AREA, AND DATA COLLECTION

3.1. Study Area

Berkelah forest reserve is a tropical rainforest in the Eastern part of Pahang province, Malaysia. It is located some 235 km North East of Kuala Lumpur, between latitude 30^0 43' 06.57" - 30^0 45' 35.72" and longitude 102^0 056' 39.03" – 102^0 058' 47.33" and covers about 1,575 ha (see Figure 3.1).

The forest is comprised of multiple layers, has complex forest canopy structures and has two parts: North-Eastern and South-Western. The former has been logged for over 15 years and the latter has never been logged and remains a primary forest. The lower south part the forest has been converted into oil palm and rubber plantations. Within the study areas, there are several water streams and lakes in the lower parts. The study area has a hilly topography with steep slopes in the upper Northern part and more gentle slopes towards the lower Southern regions.

The climate of the study area is tropical rainforest which is has a rainfall of about 1900 mm to 2200 mm per year and temperature of 22^0 Celsius to 32^0 Celsius. The forest is in the lower part of the hill forest with an altitude between 204 meters to 236 meters (Barizan, 1997).The forest is encompassed of different vegetation species but mainly dominated by *Shorea* species which are large trees in size, *Eugeisonna tristis* and *Oncosperma horridum* (Rajpar & Zakaria, 2014). Figure 3.1 shows study area map.

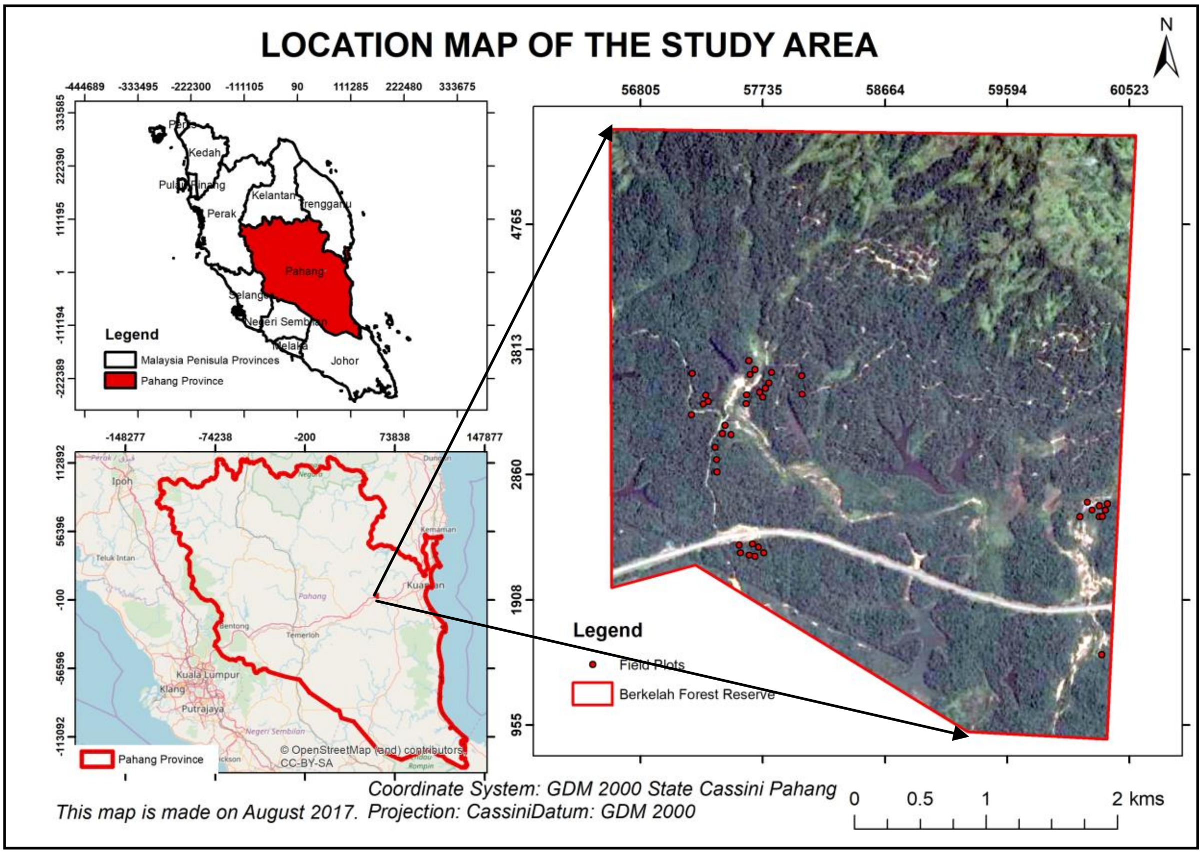

Figure 3.1. Berkelah Forest Reserve Map, In Kuantan, Pahang – Malaysia

3.2. Field Data

Fieldwork was conducted from 23rd September to 11th October 2017 in Berkelah forest reserve, Kuantan Malaysia. In total, 39 circular plots were sampled from which 34 plots were fully sampled (TLS scan and biometric data) and from the remaining 5 plots, only biometric data were recorded.

3.2.1. Pre – Fieldwork

Pre-fieldwork activities were organized to get familiar with fieldwork equipment, field measurements and prepare the materials and equipment that were used during the fieldwork data collection process. These steps involved:

i. Becoming familiar with the navigation in the forest towards sampling plots and point location recording: Garmin GPS, tablet with navigation Locust software.

ii. Training how to operate Riegl VZ - 400 Terrestrial Laser Scanner (TLS).

iii. Preparing field data sheets for recording information from sample plots: tree location and tree species, tree DBH and tree stem height below the canopy (see Appendix 1).

3.2.2. Plot size

For ground-based measurements, different types of sample plots shapes can be developed: circular, square, or rectangular. In a natural forest, circular sample plots are preferred. They have fewer trees along the borders compared to square or rectangular plots and the plot boundaries can easily be established by using a measuring tape (Hamilton G, 1988). Following on Van Laar (2007), a radius of 12.6 m was used, resulting in a plot of 500 m^2. Concerning the plot size, there is a practical issue at hand, since an increase in size will negatively influence the TLS results because of increased inclusion. Secondly the length and width of the slopes in the study area does not always allow larger plots. This is shown in Figure 3.2.

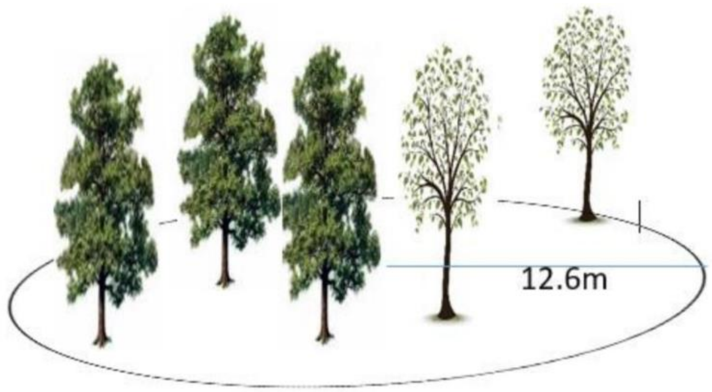

Figure 3.2. Circular plot with 500 m^2 area and radius of 12.6 m, Source (Adan, 2017)

3.2.3. Sampling Design and Intensity

In this research, a purposive sampling design was applied in order to acquire a data set representative for the variation in forest cover in the study area. Although random sampling does the same, due to time constraints, a random sampling scheme was not feasible.

The literature suggests that for an area of 0.75 ha, the sampling intensity can be 5%, taking into consideration that if the plot size is too small, it is not representative of the variation in the sample size and if the intensity is too low, the data set does not cover all variation in forest cover in the area (Van

Laar, 2007). Due to time constraints based on the length of the fieldwork period and duration of a TLS scan, the sampling intensity in this study was 0.12%. Equation 3.1 shows how sampling intensity is calculated.

$$NS = A \times \frac{SI}{SZ}$$

Equation 3.1. Sampling Intensity formula

Where: NS = Number of samples
A = Total area of study area
SI = Sampling Intensity
SZ = Sample size

3.2.4. Site selection

Since the time for fieldwork was limited to 20 days, the carried equipment was heavy and weighed for instance TLS weighted 30 kg, the selection of the actual sites was determined by the accessibility conditions in the field based on slope steepness, slope length and width, distance to the road, presence of rivers and lakes and other considerations.

Potentially suitable plots, with different forest cover conditions and taking the accessibility limitations into consideration, Google Earth aerial photographs and slope map that was made from elevation data downloaded from USGS website helped to identify.

3.2.5. Biometric Data Collection

Biometric measurements include diameter at breast height (DBH), tree and crown height, and tree location of every tree and relative to the plot location centre (Babst et al., 2014). The biometric data collected for this study included: DBH, height of the stem (indicating the lower boundary of the canopy) and coordinates of the plot centre and all individual trees.

After clearing the undergrowth of the plot, all trees were numbered. Trees with a DBH less than 10cm were left out because they have a neglectable contribution to the AGB calculations (Laurance et al., 1997; Cummings et al., 2002; Kauffman et al., 2002; Nascimento et al., 2007). The DBH of all other trees was measured using diameter measuring tape.

The coordinates of the individual trees were recorded with the GPS of smartphone and tablet. These data are required to later identify individual trees on the remote sensing images. The centre of the plot was recorded by the GPS of a smartphone or tablet, and by the GPS of the TLS. The reason for the use of smartphone or tablet was that the Garmin GPS did not work properly underneath forest canopy.

All the information was recorded in the field data sheet which has been prepared for data recording. After the fieldwork, all data were transferred to Microsoft office excel sheet for further analysis. Figure 3.3 presents biometric data collection process.

Figure 3.3. Field photo, a collection of biometric data.

3.2.6. TLS Data Collection

TLS data collection process involves two steps. The first step is to tag all trees within the circular plot with a number and place cylindrical and circular reflectors. The tags or markers were used for identifying individual trees from different scans. Cylindrical and circular reflectors were used for registration of point clouds (Wilkes et al., 2017). All of them were placed in a way that can be observed by TLS during the centre location scan, though but for other scans, only part of the reflectors and markers could be seen (Wilkes et al., 2017). Before starting to scan, the undergrowth in the plot was cleared in order to avoid unnecessary occlusion of the stems of trees.

The second step was carrying out four scans in each sample plot: one scan from the centre of the plot and the other three scans from different viewpoints to reduce signal occlusion (Grau et al., 2017). Figure 3.4 shows the nature of field plot it was during TLS scans.

Figure 3.4. Field photo: TLS plot scan

3.3. Remote Sensing Data

3.3.1. Airborne Laser Scanner (ALS) Data

Airborne Lidar data was collected on 12th November 2014 by Airborne Research and Survey Facility (ARSF) and made available for this research by courtesy of University Technology Mara Malaysia (UiTM). The ALS data consists of 22 flight lines. Flight line 21 and 22 were not included in the analysis because the former was outside the study area and the latter cut across other flights. The data were projected in WGS84, UTM48 North. The ALS data has a point cloud density of approximately 6-point per meter square. The difference in return time of the laser pulse to the sensor allows for the the construction of a 3D point cloud, whereby the first return reflects the highest part of the surface (canopy surface in this case) and the last return the lowest part (forest floor in this case). Figure 3.5 shows part of Berkelah forest ALS data digital surface model in 3D view.

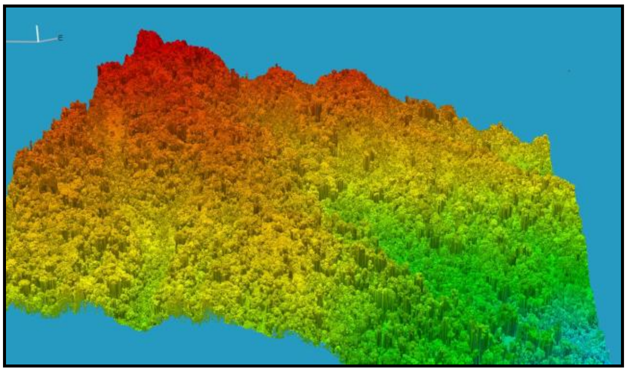

Figure 3.5. Part of digital surface model of ALS data in 3D view of the study area

3.3.2. Landsat 8 Satellite Image

Landsat 8 satellite image of 26th June 2016 with nadir viewing position and UT / WGS84, Zone 48 projection system was downloaded from www.earthexplorer.usgs.gov website on 8th August 2017. The image scene had 9.58% of land cloud cover and 9.62% scene cloud cover, but the study area was nearly clouds free. The image required pre-processing, like radiometric corrections and atmospheric corrections, for removing haze and masking clouds that were present in parts of the image.

Landsat 8 satellite image of 26th June 2016 was considered the most suitable since it had less cloud cover than other recent Landsat 8 images, even compared to other satellite images like Sentinel 2 images. Furthermore, the selection of Landsat 8 image considered presences of short-wave infrared (SWIR) band which is required for forest canopy density analysis. Together with that Landsat 8 image is a freely and globally coverage satellite. Also, Landsat 8 has 16 bits data with digital number (DN) 1 - 65536. Table 3.1 shows Landsat 8 bands, spectral reflectance and pixel size.

Table 3.1. Landsat 8 Band Spectral Reflectance values and resolution

Band	Wavelength (micrometers)	Resolution (meters)
Band 1 – Coastal Aerosol	0.43 – 0.45	30
Band 2 – Blue	0.45 – 0.51	30
Band 3 – Green	0.53 – 0.59	30
Band 4 – Red	0.64 – 0.67	30
Band 5 – Near Infrared (NIR)	0.85 – 0.88	30
Band 6 – SWIR 1	1.57 – 1.65	30
Band 7 – SWIR 2	2.11 – 2.29	30
Band 8 – Panchromatic	0.50 – 0.68	15
Band 9 – Cirrus	1.36 – 1.38	30
Band 10 – Thermal Infrared (TIRS) 1	10.60 – 11.19	100
Band 11 – Thermal Infrared (TIRS) 2	11.50 – 12.51	100

4. METHODS

The method of this study is divided into six steps, as shown in Figure 4.1.

1. Preparing the forest canopy density map (FCD)
2. Calculating forest volume, based on airborne Lidar 3D point cloud and field data (VOL_{ALS})
3. Combining the FCD map with forest volume derived from ALS point clouds ($VOL_{ALS/FCD}$) (adjusted forest volume)
4. Estimating aboveground forest biomass (AGB), using DBH from field measurements and tree heights derived from ALS
5. Assessing the relationship between forest volume (viz. VOL_{ALS} and $VOL_{ALS/FCD}$) and forest biomass (AGB)
6. Preparing a forest biomass map using the relation from step 5 (AGB_{MAP})

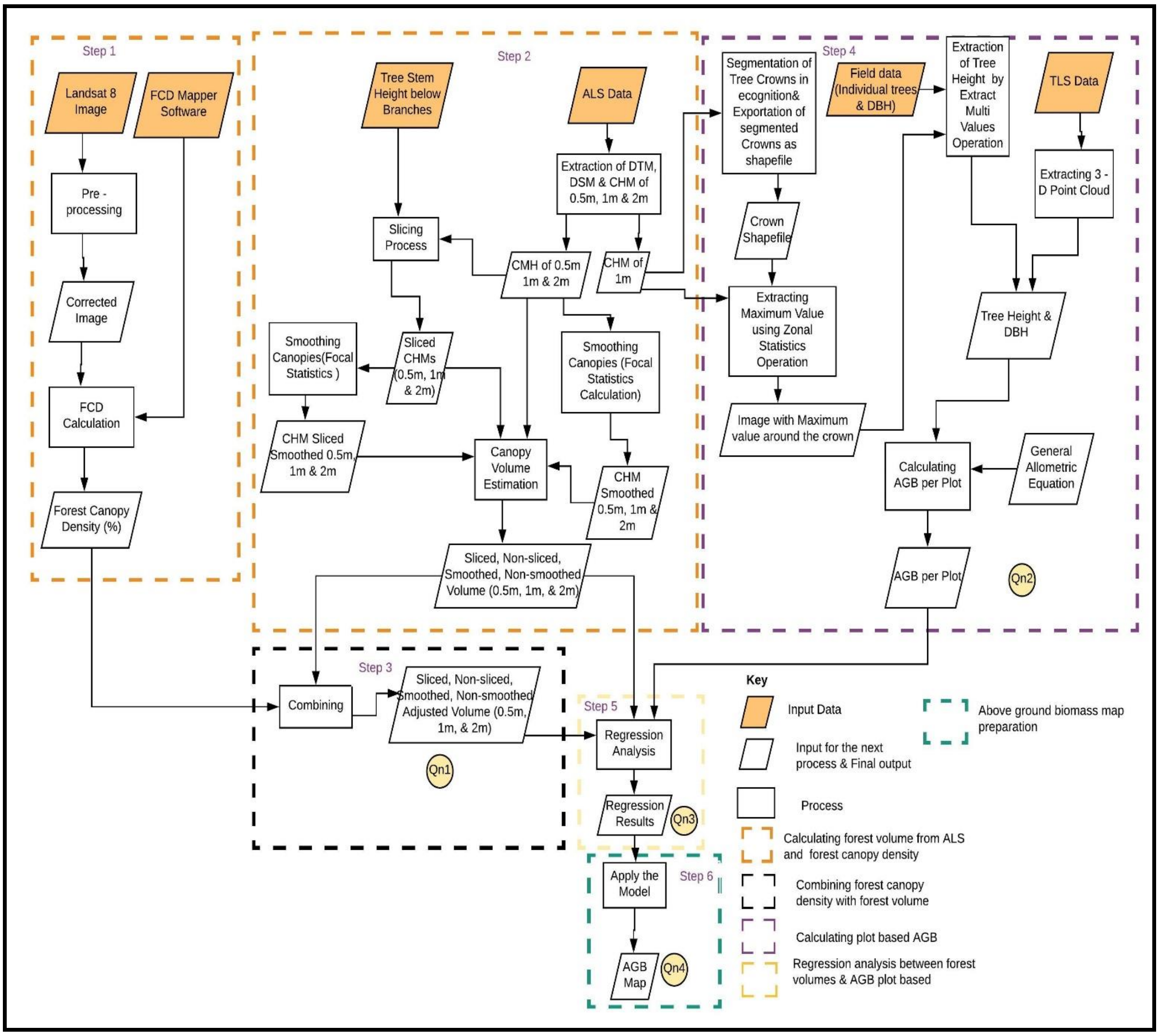

Figure 4.1. Study flow chart of research methods.

4.1. Forest Canopy Density Map.

4.1.1. Acquisition and pre-processing

A recent Landsat 8 image (26th June 2016, UT / WGS84, Zone 48) with a nearly cloud-free view of the study area, was downloaded from the website of the United States Geological Survey (www.earthexplorer.usgs.gov).

4.1.1.1. Image conversion

Since Landsat 8 is delivered as 16 bits images and the FCD mapper software requires 8 bits date, the images must be converted to 8 bits signed data. Converting Landsat 8 images involves two stages. The first stage involves converting Landsat 8 raw data reflectance in 0 – 255 values. The second stage is to convert reflectance images from 16 bits to 8 bits signed. This image conversion was performed using ENVI 5.3 + IDL 8.5 (64 bit) software.

4.1.1.2. Sub-setting

A subset of the study area from each band was created, using ERDAS imagine 2017.

4.1.1.3. Forest Canopy Density Map

The FCD mapper combines a number of indices (Bare Soil Index, Advanced Vegetation Index, Shadow Index and Thermal Index) and uses spectral information from 7 bands: blue, green, red, near infrared, short wave infrared 1 & 2 and thermal infrared 1. The final output is a classified image expressing forest canopy cover from 0 – 100% in steps of 10%. Because FCD of this study used Landsat 8 images, bands were switched to match with Landsat 7 as Figure 4.2.

Landsat-7 ETM+ Bands (μm)			Landsat-8 OLI and *TIRS* Bands (μm)		
			30 m Coastal/Aerosol	0.435 - 0.451	Band 1
Band 1	30 m Blue	0.441 - 0.514	30 m Blue	0.452 - 0.512	Band 2
Band 2	30 m Green	0.519 - 0.601	30 m Green	0.533 - 0.590	Band 3
Band 3	30 m Red	0.631 - 0.692	30 m Red	0.636 - 0.673	Band 4
Band 4	30 m NIR	0.772 - 0.898	30 m NIR	0.851 - 0.879	Band 5
Band 5	30 m SWIR-1	1.547 - 1.749	30 m SWIR-1	1.566 - 1.651	Band 6
Band 6	60 m TIR	10.31 - 12.36	*100 m TIR-1*	*10.60 – 11.19*	Band 10
			100 m TIR-2	*11.50 – 12.51*	Band 11
Band 7	30 m SWIR-2	2.064 - 2.345	30 m SWIR-2	2.107 - 2.294	Band 7
Band 8	15 m Pan	0.515 - 0.896	15 m Pan	0.503 - 0.676	Band 8
			30 m Cirrus	1.363 - 1.384	Band 9

Figure 4.2. Landsat 7 and Landsat 8 bands switch. Source: (www.earthexplorer.usgs.gov)

There was no need to perform an atmospheric correction because within the FCD software there was a stage where different atmospheric corrections could be done such as removing clouds, removing cloud shadows and haze. Moreover, performing an atmospheric correction prior to uploading the images in the FCD software affected the spectral reflectance of the bands and caused the software to crash.

During the process of forest canopy density calculations, there were different conditions set on the model. Those conditions were: water masking value was 25, cloud masking – 25, vegetation index the selection was NDVI because it had a correlation coefficient of 0.869 which was higher than AVI and ANVI. Also, the threshold for GAP detection was 55, vegetation density was 60, bare soil – 140, vegetation range set; minimum – 80 and maximum – 120. Then clustering of vegetation indexes, bare index and soil index for identifying forest cluster was from 5 – 9 and threshold for shadow, soil index its minimum was 110 and maximum was 175. This process took place through normalization of data for each band as in FCD process flowchart in Figure 4.3.

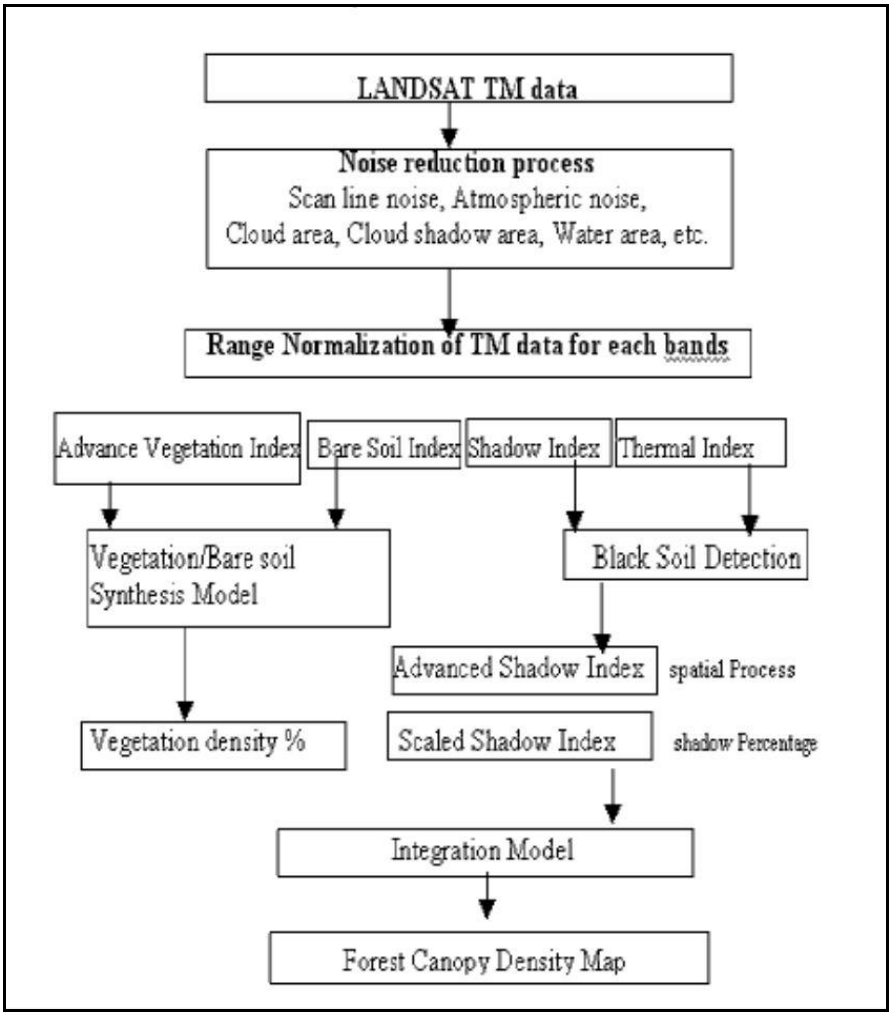

Figure 4.3. Forest canopy density analysis processes in FCD mapper. Source: (Godinho et al,. 2016)

4.2. Airborne Laser Scanner (ALS) Data Processing

Airborne Laser Scanner (ALS) data was used for tree height extraction and forest volume calculation (see figure 4.1.)

4.2.1. Extraction of Tree Height

The point density of ALS data in this study was 6 points per meter square. After the LiDAR scanner sent out the laser pulse it was reflected when it hit a surface and, depending on the properties of the object the multiple returned signals could be used to derive the height (see Figure 4.4).

Digital surface model (DSM) was extracted from first returns which is from the top surface of the forest and the last was extracted for the digital terrain model (DTM) of the study area. Both, first returns and last returns were converted to tiff raster files format, with a pixel size of 1m*1m. The reason for this was because when using pixel 1x1, every pixel has a number of ALS points allowing for the estimation of height value for each pixel without interpolation. Then, DSM and DTM were subtracted to obtain the canopy height model (CHM) (see Figure 4.5), and tree heights were extracted within the study area.

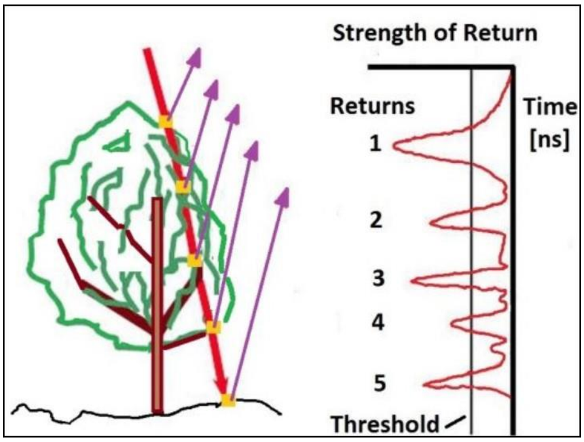

Figure 4.4. Multiple returns of the signal from Lidar scanner. Source; (Lemmens, 2017).

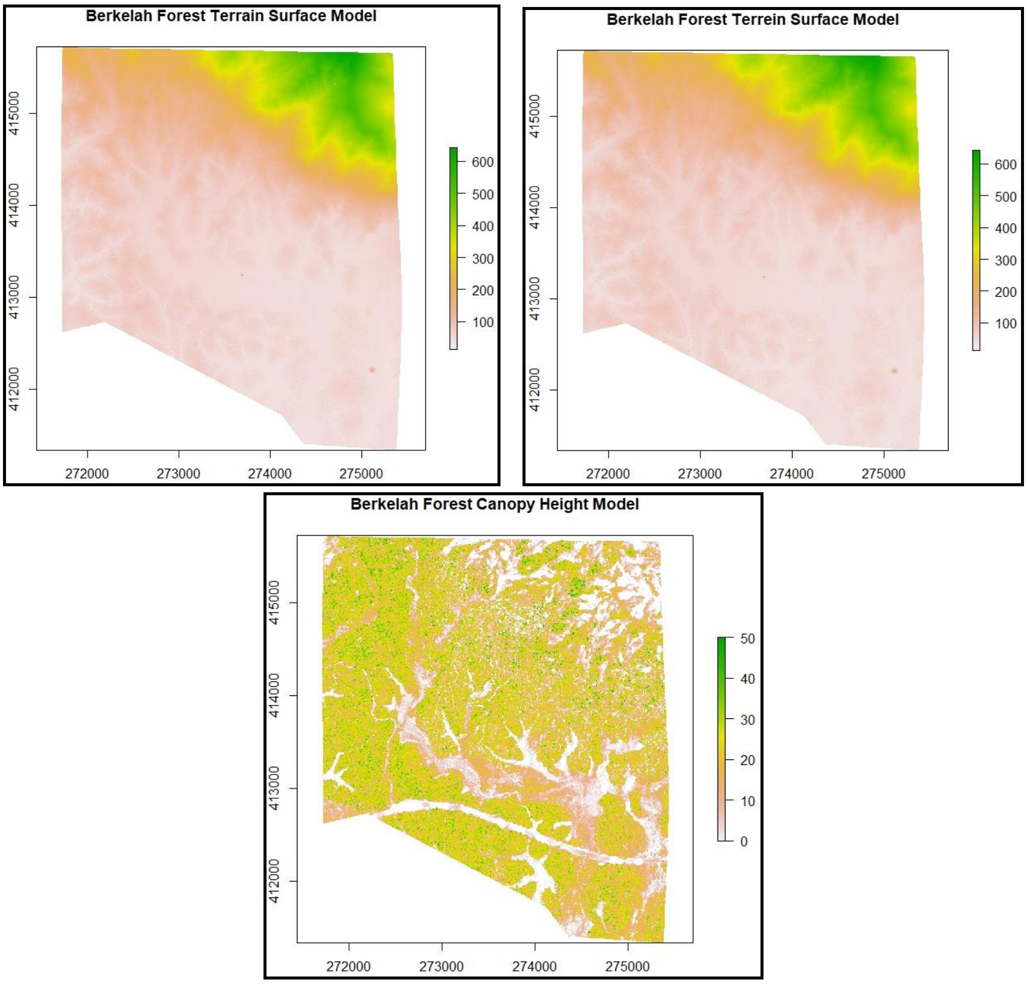

Figure 4.5. Forest digital surface model, digital terrain model and canopy height model that have been used to extract tree heights.

Next, the CHM was segmented by using ecognition software, applying multiresolution segmentation in a way that the obtained segments coincided with the individual tree crowns. The segments were exported as a shapefile to ArcGIS, in order to calculate tree crown maximum, using zonal statistics (see step 4 in Figure 4.1). Figure 4.6 shows part of segmentation of Berkelah forest CHM from eCogniton. This value represented the height of the tree top. Before tree crown maximum value calculation, the segmented crowns were assessed its accuracy by comparing manually (digitized) segmented individual trees and ecognition segmented trees. The following formula was applied in assessing the accuracy:

$$Under\ segmentation = 1 - (\frac{Aref \cap As}{Ar})$$

Equation 4.1. Under segmentation assessment.

$$Over\ segmentation = 1 - (\frac{Ar \cap As}{Aseg})$$

Equation 4.2. Over segmentation assessment.

$$Total\ Error = \sqrt{(OverSeg^2 + UnderSeg^2)/2}$$

Equation 4.3. Total error segmentation assessment.

Whereby:

Under segmentation = Several crowns have been grouped together into one segment
Over segmentation = One crown has been segmented several times
Total error = errors that have been caused by over segmentation and under segmentation
Aref = Area of reference (manually digitized crowns)
Arseg = Area of Segmented crowns

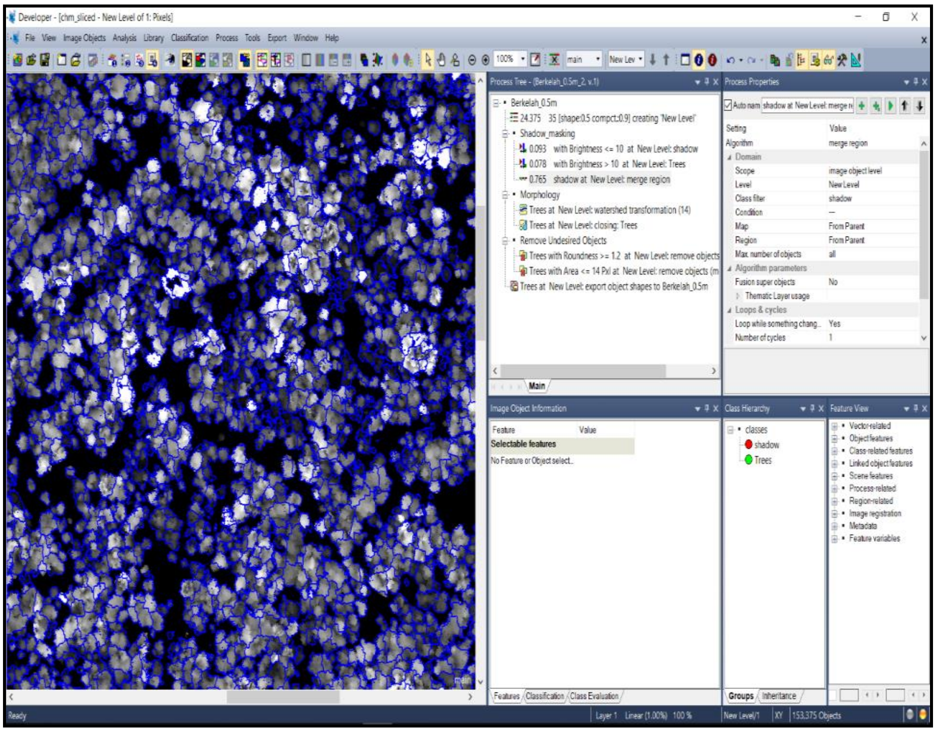

Figure 4.6. Part of CHM segmented image in ecognition software that used calculation of tree height.

4.2.2. Estimation Forest Canopy Volume

Forest volume is considered as stand volume or tree volume, which is an estimate of the whole canopy volume, stem, branches and foliage, expressed in cubic meters. Forest foliage volume is the volume of the forest canopy that has remained after a cut-off level of removing tree trunk has been applied, it consists tree leaves and branches. Different pixel sizes (0.5m, 1m and 2m) were used in developing canopy height model of the forest in order to analyse if pixel size had an effect on the estimation of forest canopy volume or forest canopy foliage volume. The ALS data was delivered with a density of 6 pointss per square meter. The larger the pixel size of the CHM, the more ALS points it contained. Figure 4.7 shows the distribution of ALS points for different pixel sizes. Pixels of 2mx2m and 1mx1m contained multiple ALS points.

It should be noted that when applying 0.5mx0.5m pixels, not all pixels had ALS points. This affected the development of forest canopy height model, as they were assigned zero values. Figure 4.8 shows a circular field plot with different pixel sizes.

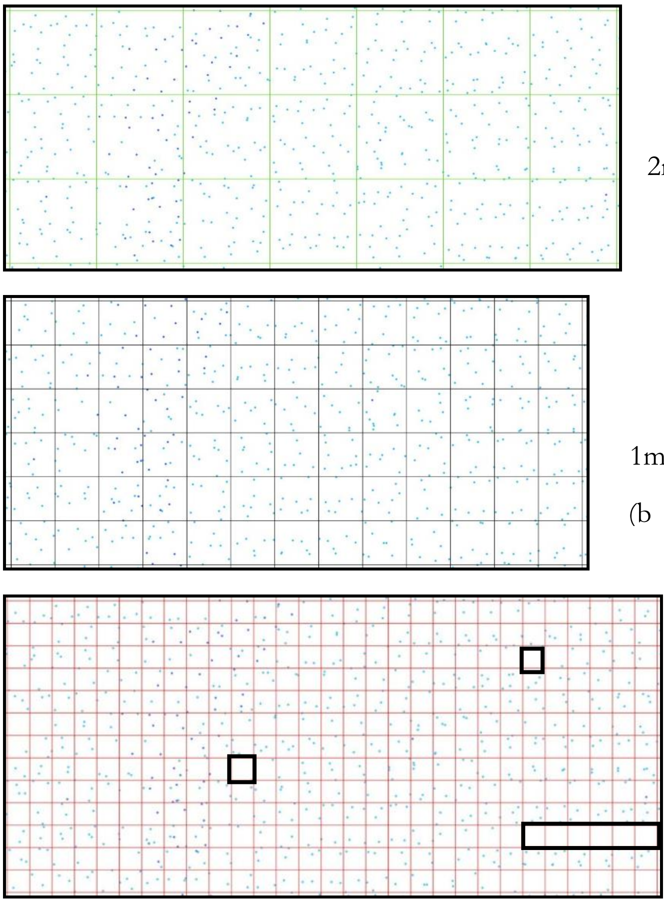

2m pixel size

(a)

1m pixel size

(b

0.5m pixel size

(c)

Figure 4.7. Spatial distribution of point clouds first returns and number of points in different pixel sizes.

4.2.2.1. Calculation of Forest Canopy volume

In this study, two forest volume measures were calculated: sliced volume (the volume of branches and leaves) and non-sliced volume (total volume of the forest). In order to estimate the sliced foliage volume a cut off level or threshold in meters above the forest floor was determined, separating the tree trunks from the lower boundary of the canopy. In each field plot, for most of the individual trees, the trunk height (lower boundary of the canopy) was measured by laser ranger. This resulted in a threshold (cut off level) of 9 m.

Before estimating the sliced and non-sliced volume of the canopy, the canopy height models (pixel size 0.5, 1 and 2-metre square) were smoothed by running the focal statistics mean tool in ArcGIS two times. Koukoulas & Blackburn (2005) have suggested that smoothing two times removes the effects and errors that smoothing can create in the first round. Smoothing the canopy averages neighbouring pixel sizes within the canopy in order to regulate differences that are in pixel values within the forest canopy.

These operations resulted in twelve different CHM's:

- Non-sliced and non-smoothed, pixel size 0.5, 1 and 2 m^2
- Non-sliced and smoothed, pixel size 0.5, 1 and 2 m^2
- Sliced and non-smoothed, pixel size 0.5, 1 and 2 m^2
- Sliced and smoothed, pixel size 0.5, 1 and 2 m^2

Subsequently, the central point of the field plot was overlaid on all twelve CHM's in ArcGIS and around it a circular buffer of 500m^2 (the size of the plots) was created and clipped, resulting in 38 clipped plots for all twelve CHM types. Figure 4.9 shows an example of a CHM and a clipped CHM of one of the field plots.

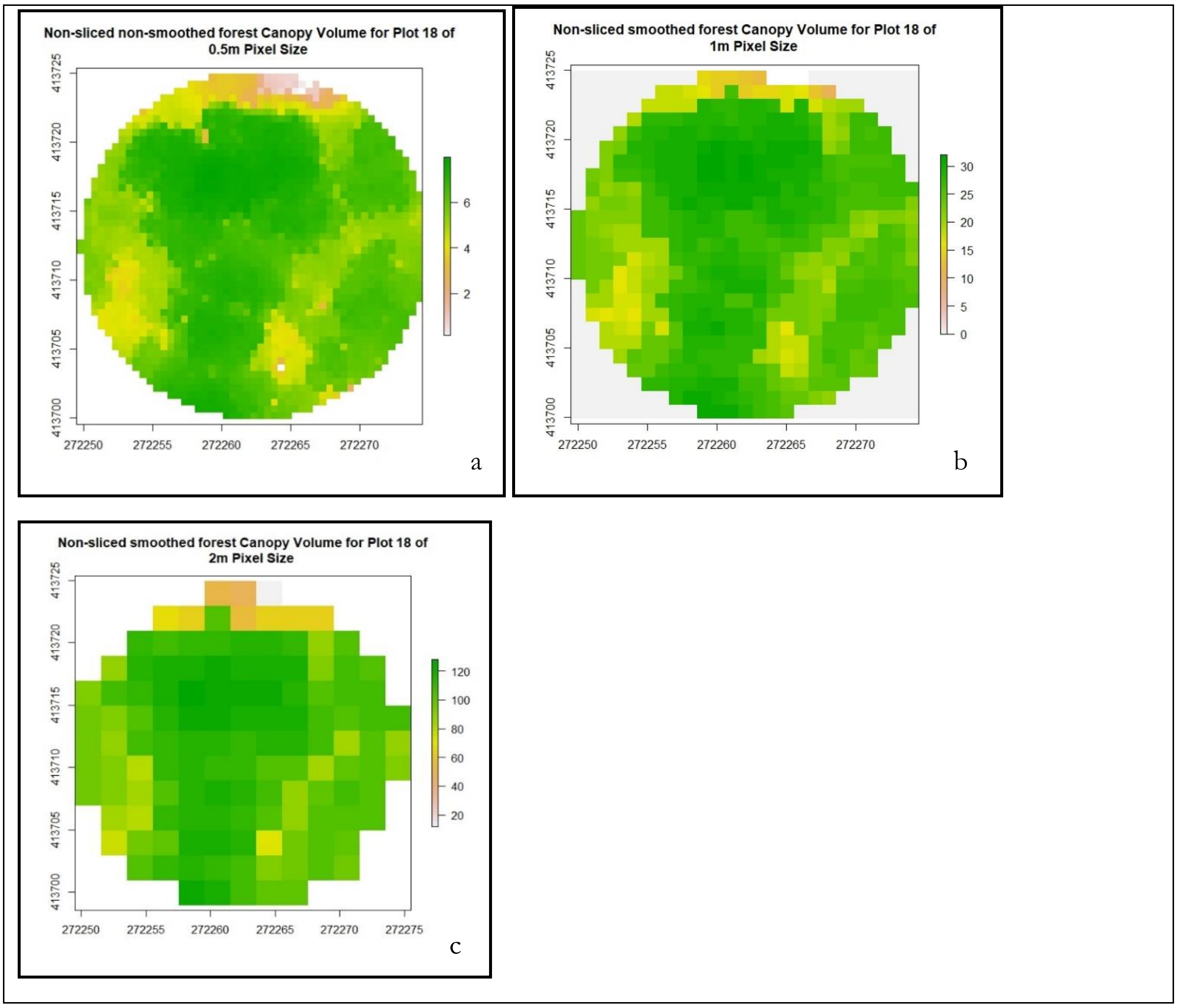

Figure 4.8. Three different pixel sizes that have been used to estimate forest canopy volume:(a) is 0.5m, (b) is 1m and (c) is 2m pixel size.

From all clipped CHM's, the forest volume was calculated in R-statistics package, by using grid cell technique. For every pixel in the clipped CHM, the pixel size was multiplied by the pixel value and the value of all pixels was summed, resulting in a forest volume measure expressed in meter cubic. Figure 4.9 shows one of the plots with different conditions and part of R-statistics script that had been used to estimate volume and Figure 4.10 shows the R-script which had been used to estimate foliage volume.

The 38 clipped plots per CHM type were summed and summarized, resulting in a mean, minimum and maximum forest volume (see Table 5.2).

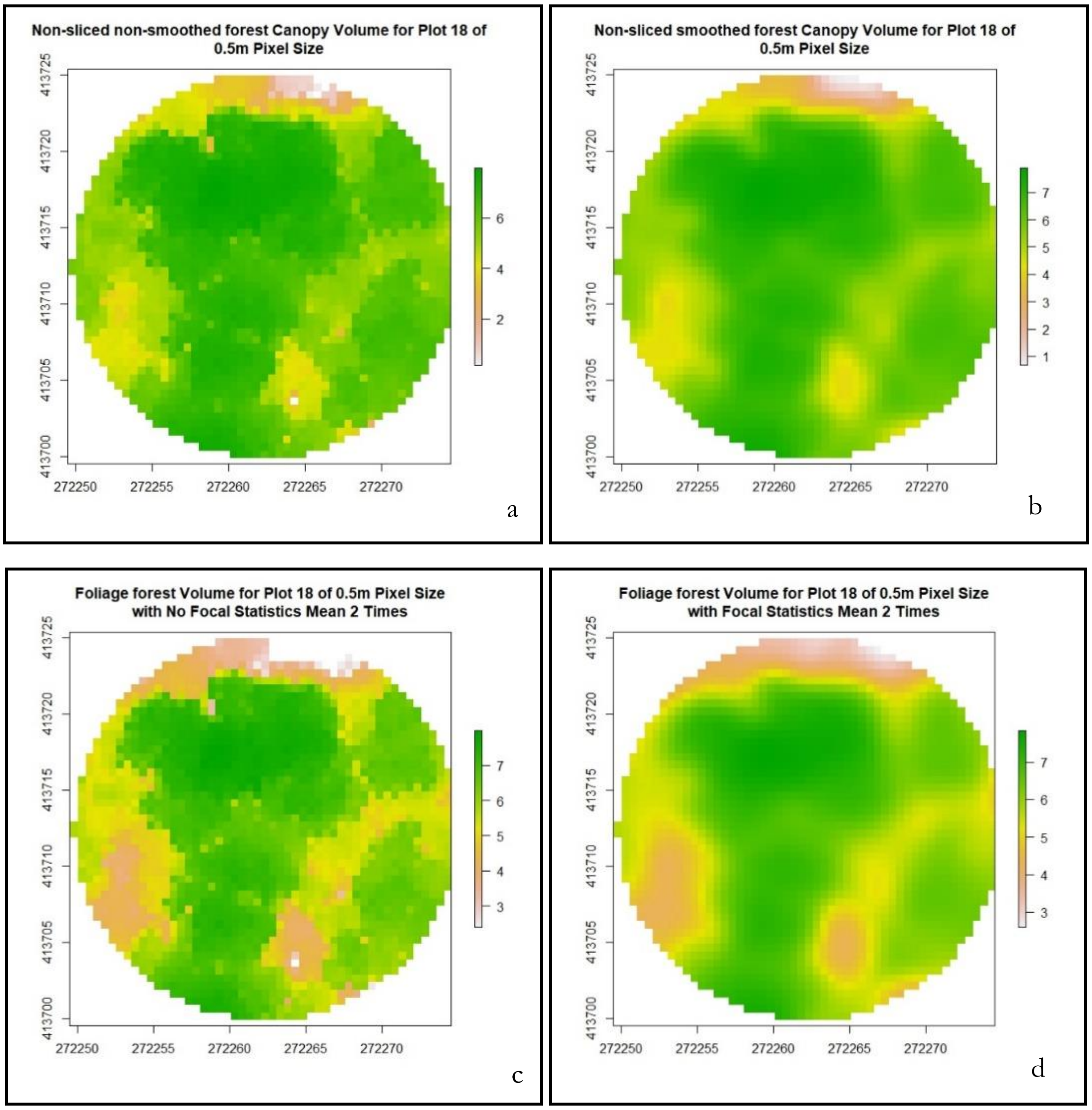

Figure 4.9. Example plot 18 forest canopy volume from different four conditions that have been applied in estimating foliage volume from all 38 plots ((a) is non-sliced non-smoothed, (b) is non-sliced smoothed, (c) is sliced non-smoothed and (d) is sliced smoothed forest canopy volume in cubic meter.

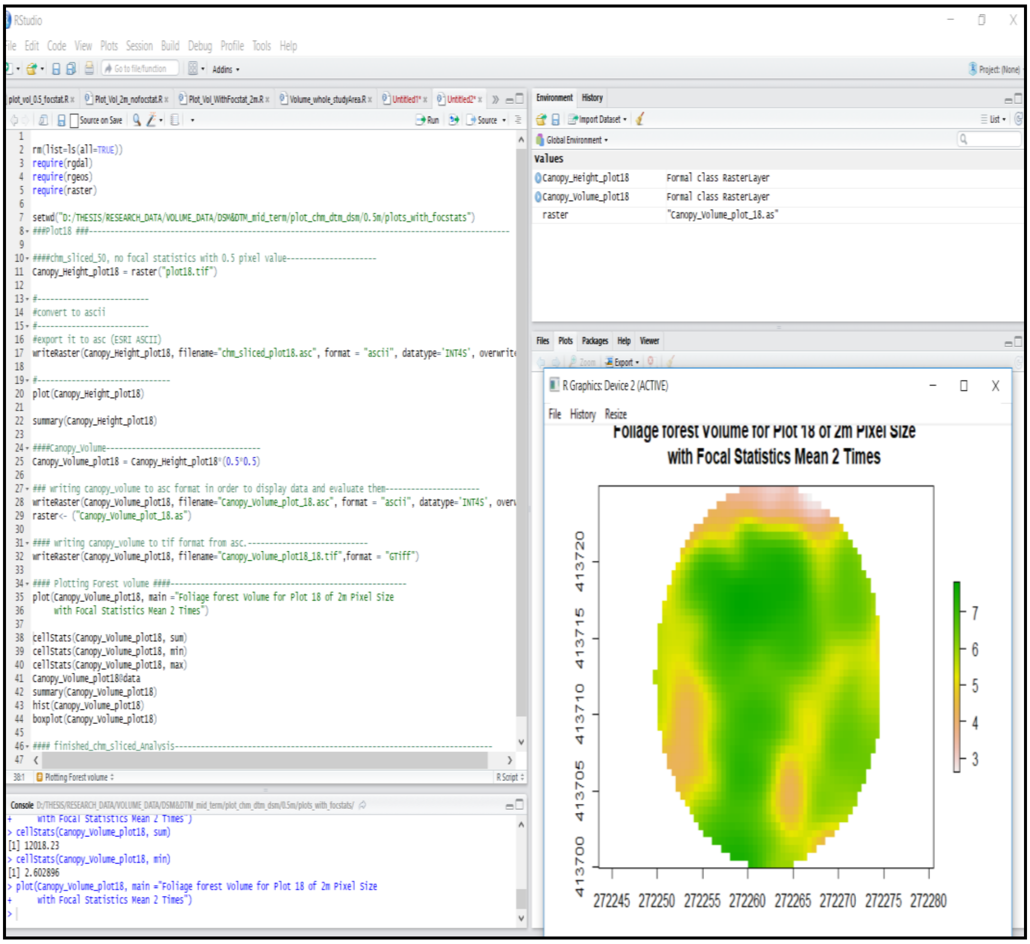

Figure 4.10. R script which has been used in estimating forest volume per field plot.

4.3. Adjusted Forest Volume

Since the volume measures described in the previous section were a kind of envelope draped over the outer boundary of the canopy or forest, it does not take canopy openness into consideration. Two forest sites with the same volume can have a different canopy density. In order to assess whether canopy density had an effect on AGB estimation of the forest, all volume measures, described in section 4.2.2. were multiplied by the canopy density, expressed in percent (see section 4.1.), resulting in the adjusted forest volume.

4.4. Calculation of Aboveground Biomass and Carbon Stock

Extracted tree height from ALS point cloud data for upper canopy trees, lower canopy tree heights were adopted from Maasa (2018) and Wassihun (2018) studies and the diameter at breast height (DBH) measured in the field were entered in the allometric equation in order to estimate the aboveground biomass (AGB) per tree. This was done for every tree within the plot and the obtained values were summed in order to arrive at the total ABG for that particular plot. Following this, all plot based AGB values were summed and divided by the total area covered by the field plots to obtain an approximation the aboveground biomass in the whole study area.

The allometric equation is a statistical regression model that has been developed for estimating vegetation biomass using different vegetation parameters such as vegetation indices, tree height, tree volume, diameter at breast height (DBH), and spectral reflectance (Basuki et al., 2009). An allometric equation is an empirical formula because it involves a number of parameters for estimating aboveground biomass. The development of allometric equations replace the time consuming and destructive, but more accurate method of clear-cutting trees, drying and weighing (Basuki et al., 2009). In this study, the allometric equation developed by Chave et al., (2014) was used (see Equation 4.4). Compared to other allometric equations, Chave's equation has the best goodness of fit (AIC=3130) when df=4002 and comprises wood density, DBH and tree height which are predictor variables (Chave et al., 2005).

General allometric equation developed by Chave et al. (2014):

$$AGB = 0.0673 \times (\rho D^2 H)^{0.976}$$

Equation 4.4. Aboveground biomass estimation equation.

Where: AGB = Aboveground Biomass
ϱ= Specific Wood Density (g/cm^3)
D^2 = Diameter at breast height (DBH) (cm)
H = Height (m)
0.0673 = Constant form factor

The carbon stock is the amount of carbon that is stored in the vegetation that will be emitted into the atmosphere when the vegetation is cut, burned, or decayed (Ribeiro et al., 2011). The carbon stock was converted from aboveground biomass using conversion factor 0.47 formulated by IPCC.

The conversion equation is:

$$C = AGB \times CF$$

Equation 4.5. Carbon stock estimation equation.

Where: C = Carbon stock (MgC)
AGB = Aboveground biomass
CF = Fraction of aboveground biomass (0.47)

4.5. Statistical Analysis

In the final step of the study, a regression analyses were used to test the relation between the various forest volume measures (see section 4.2.2 and 4.3) and aboveground biomass of the field plots. Since the aim of the study is to estimate AGB, the (adjusted) forest volume measure is the independent variable(Quinn, 2002). A linear and exponential trend line was fit through the points in the scatter diagram. The exponential model was adopted, since at some point in time the forest canopy might have reach a maximum, while carbon sequestration might continue because of the growth of the stem of the tree.

The goodness of relationship was assessed by using r^2 whereby the best model was expressed by the highest value of r^2. The significances of the models were assessed by using alfa value (p-value) smaller than 0.05 (95% confidence level).

5. RESULTS

5.1. Descriptive Statistics

5.1.1. Forest Canopy Density

Forest canopy density analysis from FCD mapper model has been taken through section 4.1. Analysis is represented in terms of percentages and ranges within 10 classes: class 0 is bare soil or non-forest vegetation (e.g. grass), class 1 is 10% canopy cover and class 10 is very dense forest (i.e., 100% canopy cover). The study area vegetation (i.e., trees) have started being recognised in class number 5 up to 10, meaning that according to the FCD output the forest canopy density in the area does not drop below 30%. Figure 5.1 (a) shows the legend of the FCD mapper and Figure 5.1(b) left shows spatial distribution of forest canopy density in the study area and the right side is the study area canopy height model with field sample plots. The value of canopy density of the plot was assigned in relation to the dominance of colour in the plot and expressed as the middle value of the class. If the dominant colour of the plot was red (31 – 40%) the value assigned to the plot was 35%. Table 5.1 presents canopy density values of the plots after assigning forest canopy density values.

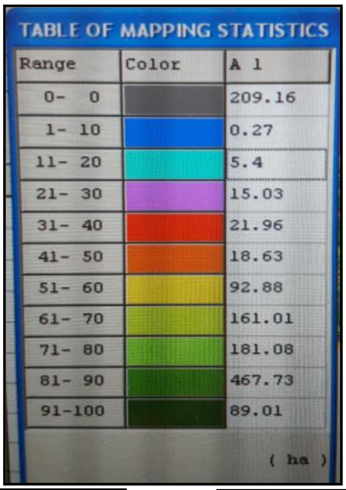
TABLE OF MAPPING STATISTICS

Range	Color	A 1
0- 0		209.16
1- 10		0.27
11- 20		5.4
21- 30		15.03
31- 40		21.96
41- 50		18.63
51- 60		92.88
61- 70		161.01
71- 80		181.08
81- 90		467.73
91-100		89.01

(ha)

(a)

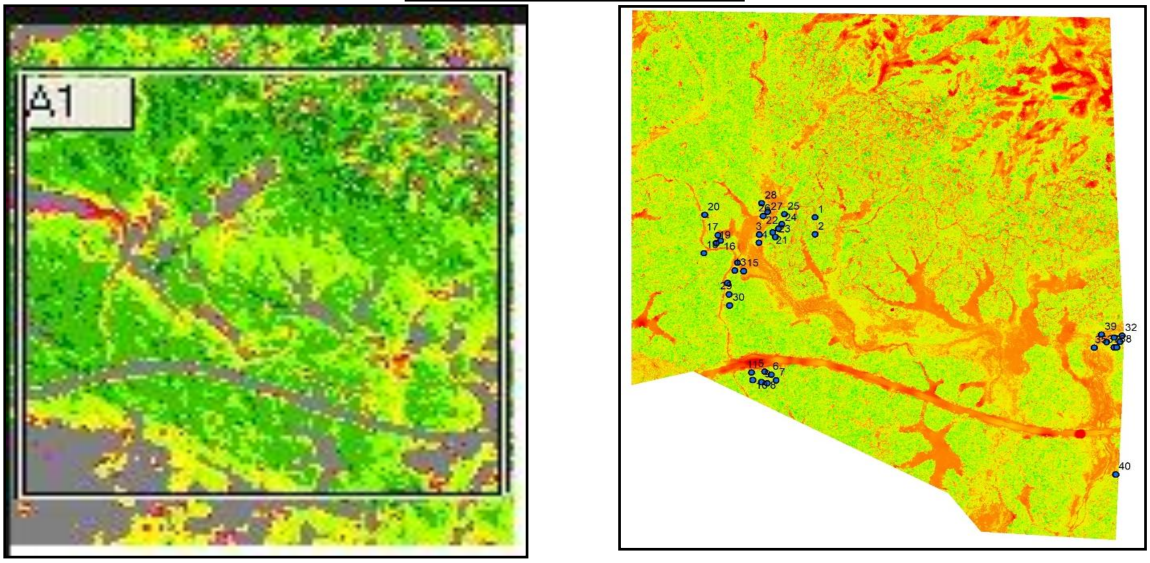

(b)

Figure 5.1. Forest Canopy Density Map statistics and forest canopy density map derived from FCD mapper and forest canopy model with field sample plots.

Table 5.1. The plots of canopy density values derived from map statistics table.

Plots	Plot Percentages	Average %	Canopy Density	Plots	Plot Percentages	Average %	Canopy Density
1	81-90	85	0.85	**21**	81-90	85	0.85
2	81-90	85	0.85	**22**	81-90	85	0.85
3	61-70	65	0.65	**23**	81-90	85	0.85
4	61-70	65	0.65	**24**	81-90	85	0.85
5	71-80	75	0.75	**25**	81-90	85	0.85
6	81-90	85	0.85	**26**	71-80	75	0.75
7	81-90	85	0.85	**27**	71-80	75	0.75
8	81-90	85	0.85	**28**	71-80	75	0.75
9	81-90	85	0.85	**29**	71-80	75	0.75
10	71-80	75	0.75	**30**	71-80	75	0.75
11	71-80	75	0.75	**31**	61-70	65	0.65
12	61-70	65	0.65	**32**	61-70	65	0.65
13	61-70	65	0.65	**33**	61-70	65	0.65
14	71-80	75	0.75	**34**	61-70	65	0.65
16	81-90	85	0.85	**35**	61-70	65	0.65
17	81-90	85	0.85	**37**	61-70	65	0.65
18	61-70	65	0.65	**38**	61-70	65	0.65
19	81-90	85	0.85	**39**	61-70	65	0.65
20	91-100	95	0.95	**40**	61-70	65	0.65

5.1.2. Forest Canopy Volume

Forest canopy volume was estimated through the Canopy Height Model (CHM) four different conditions (viz. smoothed, non-smoothed, sliced, non-sliced) and with three different pixel sizes (viz. 05, 1 and 2m.) (see section 4.2.2.1). Figure 5.2, Table 5.2 and Appendix 2 present the summary of descriptive statistics of forest canopy volume that has been estimated from different conditions.

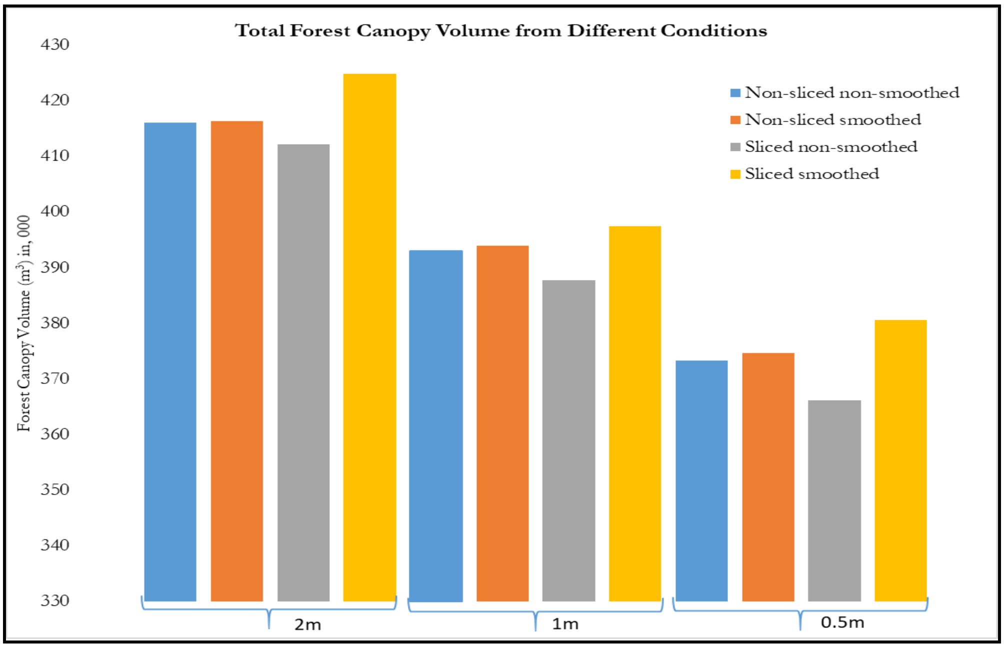

Figure 5.2. Descriptive statistics summary of forest canopy volume in meter cubic plot based.

Table 5.2. Descriptive statistics summary of forest canopy volume in meter cubic plot based.

Variable	Minimum	Maximum	Mean	Standard Deviation	Total
Non-sliced non-smoothed forest canopy volume (m3) 2m	3348	15024	10947.5	2981.3	416004
Non-sliced smoothed forest canopy volume (m3) 2m	3244.4	14878.9	10955.9	2902.1	416323.8
Sliced non-smoothed forest canopy volume (m3) 2m	1320	15024	10844.3	3217.1	412084
Sliced smoothed forest canopy volume (m3) 2m	4132.8	14878.9	11181.1	2619.5	424883.1
Non-sliced non-smoothed forest canopy volume (m3) 1m	2723	14482	10341.1	2972.2	392962
Non-sliced smoothed forest canopy volume (m3) 1m	2706.2	14439.9	10365	2950.8	393868.3
Sliced non-smoothed forest canopy volume (m3) 1m	962	14482	10204.8	3225.7	387782
Sliced smoothed forest canopy volume (m3) 1m	2464	14439.9	10460.1	2878.7	397483.3
Non-sliced non-smoothed forest canopy volume (m3) 0.5m	2151.7	14248.7	9823.1	2995.5	373277.6
Non-sliced smoothed forest canopy volume (m3) 0.5m	2356.7	14238.9	9859.6	2960.5	374666
Sliced non-smoothed forest canopy volume (m3) 0.5m	490.3	14248.7	9635.5	3299.6	366148
Sliced smoothed forest canopy volume (m3) 0.5m	1920.6	14224	10014	2867.3	380530.1

5.1.3. Adjusted Forest Canopy Volume and Adjusted Forest Canopy Foliage Volume

The sum of forest canopy volume in each plot was multiplied with its respective forest canopy density. The result of this combination is considered as adjusted forest canopy volume. This was applied to all conditions in all canopy types. Figure 5.3 presents sum of adjusted forest canopy volume in every condition in every forest canopy..

Table 5.3 and Appendix 3 present four adjusted forest canopy volume in meter cubic.

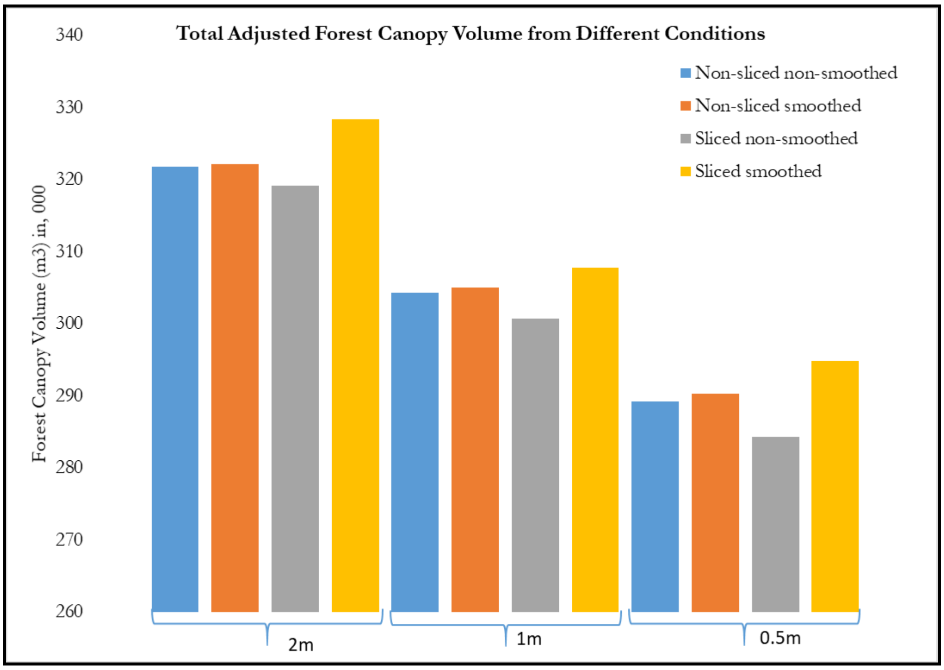

Figure 5.3. Descriptive statistics summary of adjusted forest canopy volume in meter cubic plot based.

Table 5.3. Descriptive statistics summary of adjusted forest canopy volume in meter cubic plot based.

Variable	Minimum	Maximum	Mean	Standard Deviation	Total
Non-sliced non-smoothed forest canopy volume (m3) 2m	2192.9	12845.5	8466.9	2891.3	321743.4
Non-sliced smoothed forest canopy volume (m3) 2m	2125.1	12721.4	8477.7	2848.7	322151.0
Sliced non-smoothed forest canopy volume (m3) 2m	864.6	12845.5	8398.6	3026.7	319148.6
Sliced smoothed forest canopy volume (m3) 2m	2707.0	12721.4	8642.0	2683.0	328394.7
Non-sliced non-smoothed forest canopy volume (m3) 1m	1783.6	12382.1	8006.5	2837.8	304247.7
Non-sliced smoothed forest canopy volume (m3) 1m	1772.6	12346.1	8026.5	2830.0	305005.6
Sliced non-smoothed forest canopy volume (m3) 1m	630.1	12382.1	7912.1	2987.3	300661.2
Sliced smoothed forest canopy volume (m3) 1m	1613.9	12346.1	8100.4	2785.3	307815.4
Non-sliced non-smoothed forest canopy volume (m3) 0.5m	1409.4	12182.7	7609.8	2811.8	289171.5
Non-sliced smoothed forest canopy volume (m3) 0.5m	1543.6	12174.2	7637.7	2794.0	290232.8
Sliced non-smoothed forest canopy volume (m3) 0.5m	321.1	12182.7	7480.2	3001.5	284246.4
Sliced smoothed forest canopy volume (m3) 0.5m	1258.0	12161.5	7757.2	2736.6	294772.9

5.2. Aboveground Biomass

Field plot based above ground biomass has been estimated by using diameter at breast height (DBH) field measured and tree height extracted from the airborne laser scanner (ALS) for upper canopies (see Section 4.2.1) and terrestrial laser scanner (TLS) for lower canopies (TLS tree height was made available for this study by from (Maasa, 2018 and Wassihun, 2018). These parameters were input for the general allometric equation for aboveground biomass estimation at plot level (see Section 4.4). The extraction of tree heights from ALS data was based on the segmented ALS-CHM using eCognition. The segmentation resulted in crown over segmentation of 80%, under segmentation of 0.01% and total error of 5%.

Aboveground biomass was estimated from 38 field plots of 500m² each which is equivalent to 0.76 hectares. There was 1262 number of trees with maximum DHB of 38 cm and minimum of 10 cm. Height of trees was 49 meters maximum and 10 meters minimum. Total aboveground biomass in all plots was 15,026 (tons/ha), the minimum 64.6 ton/ha and the maximum was 745 ton/ha. Table 5.4 is the summary of variables and results obtained for aboveground biomass. Figure 5.4 shows the frequency distribution of the AGB at plot level.

Table 5.4. Summary of AGB in tonnes ha^{-1}

Variable	Plots	Min	Max	Average	Total
Number of Trees	38	16	60	33	1262
Tree Height (m)	38	10	49	27.7	
Tree Diameter at Breast Height (DBH) (cm)	38	10	104.5	22.3	
AGB (ton/ha)	38	64.6	745	395.4	15026

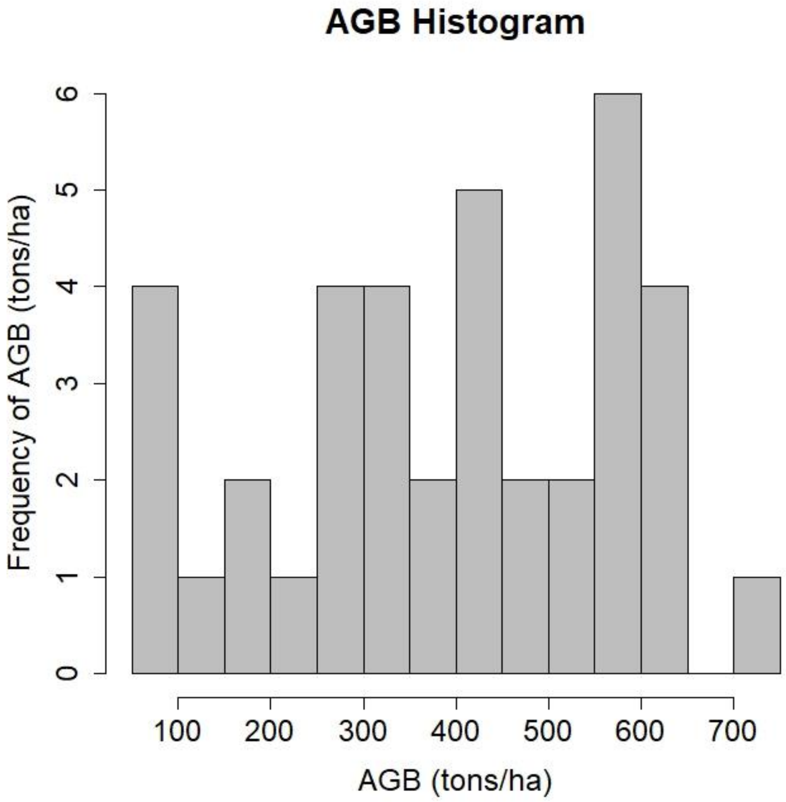

Figure 5.4. AGB histograms in tonnes ha^{-1}.

Table 5.5. Summary of AGB field measured.

Plot No	Tree No	Mean DBH (cm)	Mean Tree Height (m)	Mean Plot AGB (kg)	Total AGB (Plot/kg)	Total AGB (ha/kg)	ABG tones/ha
1	30	22.3	28.6	681.6	14701.1	294022	294.0
2	44	18.4	25.3	429.9	15138.1	302762	302.8
3	31	16.7	15.8	183.9	4798.8	95976	96.0
4	36	17.3	24.8	538.7	15493.5	309870	309.9
5	33	24.4	33.4	1089.0	27874.1	557482	557.5
6	36	22.8	32.3	735.1	21504.6	430092	430.1
7	30	20.8	34.5	814.3	18995.2	379904	379.9
8	35	22.4	29.0	834.1	22700.0	454000	454.0
9	24	26.1	33.9	1314.3	25018.5	500370	500.4
10	35	20.0	31.8	559.4	16009.7	320194	320.2
11	38	22.0	26.3	698.0	21362.0	427240	427.2
12	37	18.2	19.2	279.4	8800.4	176008	176.0
13	24	22.6	27.8	701.9	13240.4	264808	264.8
14	44	22.5	28.2	698.6	24895.4	497908	497.9
16	33	23.8	28.6	838.7	22267.9	445358	445.4
17	33	23.0	29.2	713.0	19090.2	381804	381.8
18	38	26.7	27.3	919.7	28156.1	563122	563.1
19	45	23.0	30.0	783.3	28482.2	569644	569.6
Plot No	**Tree**	**Mean DBH**	**Mean Tree**	**Mean Plot**	**Total AGB**	**Total AGB**	**ABG**

	No	**(cm)**	**Height (m)**	**AGB (kg)**	**(Plot/kg)**	**(ha/kg)**	**tones/ha**
20	33	25.9	28.6	981.1	25947.4	518948	518.9
21	32	25.0	38.5	1254.9	31974.8	639496	639.5
22	42	23.9	33.0	942.5	31842.9	636858	636.9
23	41	22.8	35.9	962.3	32380.5	647610	647.6
24	23	29.7	34.2	1622.1	37248.7	744974	745.0
25	43	21.4	33.7	849.6	29296.7	585934	585.9
26	22	33.2	29.8	1844.0	31913.8	638276	638.3
27	22	17.8	18.8	238.0	4186.8	83736	83.7
28	24	26.6	32.3	1170.3	22420.0	448400	448.4
29	28	18.1	23.7	360.3	8318.9	166378	166.4
30	29	23.6	33.4	943.3	21949.9	438998	439.0
31	16	20.9	18.5	336.3	4471.8	89436	89.4
32	35	20.0	31.8	559.4	16009.7	320194	320.2
33	27	27.8	31.7	1349.5	28929.4	578588	578.6
34	41	18.7	18.7	462.8	13471.4	269428	269.4
35	60	17.4	21.7	284.7	14218.1	284362	284.4
37	23	17.8	19.3	278.9	5327.1	106542	106.5
38	33	26.5	30.3	1041.2	27596.5	551930	551.9
39	25	16.5	11.4	153.6	3228.4	64568	64.6
40	37	20.8	21.0	394.2	12038.5	240770	240.8
Average		**22.3**	**27.7**	**759.0**	**19771**	395420.8	**395.4**
Total	**1262**			**20684.3**	**751299.2**	**15025990**	**15026.0**

5.3. Regression Statistical Analysis

Two regression analyses (linear and exponential) were used to assess the relationship between forest canopy volume, adjusted forest canopy volume and aboveground biomass from all four conditions in all canopy types. The coefficient determination (r^2), standard error and alfa value (p-value) were used to assess performance of relationship between forest canopy volume and AGB. Best model was used to predict aboveground biomass over the whole study area.

5.3.1. Regression analysis between Canopy forest volume and aboveground

Volume from 0.5m*0.5m pixel size value

Referring to section 4.2.2.1 four different conditions were used to assess relationship between forest canopy volume and aboveground biomass. Coefficient of determination (r2) of linear and exponential regression, Root Mean Square Error (RMSE), and alfa value (P-Value) of each regression analysis value were used to assess the relationship between forest canopy volume and aboveground biomass at confidence interval of 95%.

As can be seen in Table 5.6 below, all linear and exponential models were significant ($p<0.05$). All exponential models explained more than 70% of variation in forest canopy volume. While, linear models explained less than 70%. However, the RMSE of all linear models are higher than their corresponding exponential models. Appendix 4, Appendix 5, Appendix 6 and Appendix 7 are ANOVA results of linear regression of 0.5m.

Table 5.6. Comparison of linear and exponential regressions of forest canopy volume and aboveground biomass from four different conditions: non-sliced smoothed and non-smoothed, sliced smoothed and non-smoothed.

Relation Type		(R2)	RMSE	P - Value
Non-sliced smoothed Forest Canopy Volume of 0.5m	Linear	0.6975	32133.7	7.01E-11
	Exponential	0.744	29560.9	2.005E-18
Non-sliced Non-smoothed Forest Canopy Volume of 0.5m	Linear	0.6955	32620.9	7.94E-11
	Exponential	0.7459	29799.2	2.611E-18
Sliced smoothed Forest Canopy Volume of 0.5m	Linear	0. 6963	31184.3	7.56E-11
	Exponential	0.7597	27738.9	2.35E-18
Sliced Non-smoothed Forest Canopy Volume of 0.5m	Linear	0.6921	36133.3	7.94E-11
	Exponential	0.761	31834.8	4.005E-18

Figure 5.5 presents the trend of relationship between forest canopy volume and aboveground biomass in linear and exponential lines. Generally, increase in canopy volume shows increase in AGB.

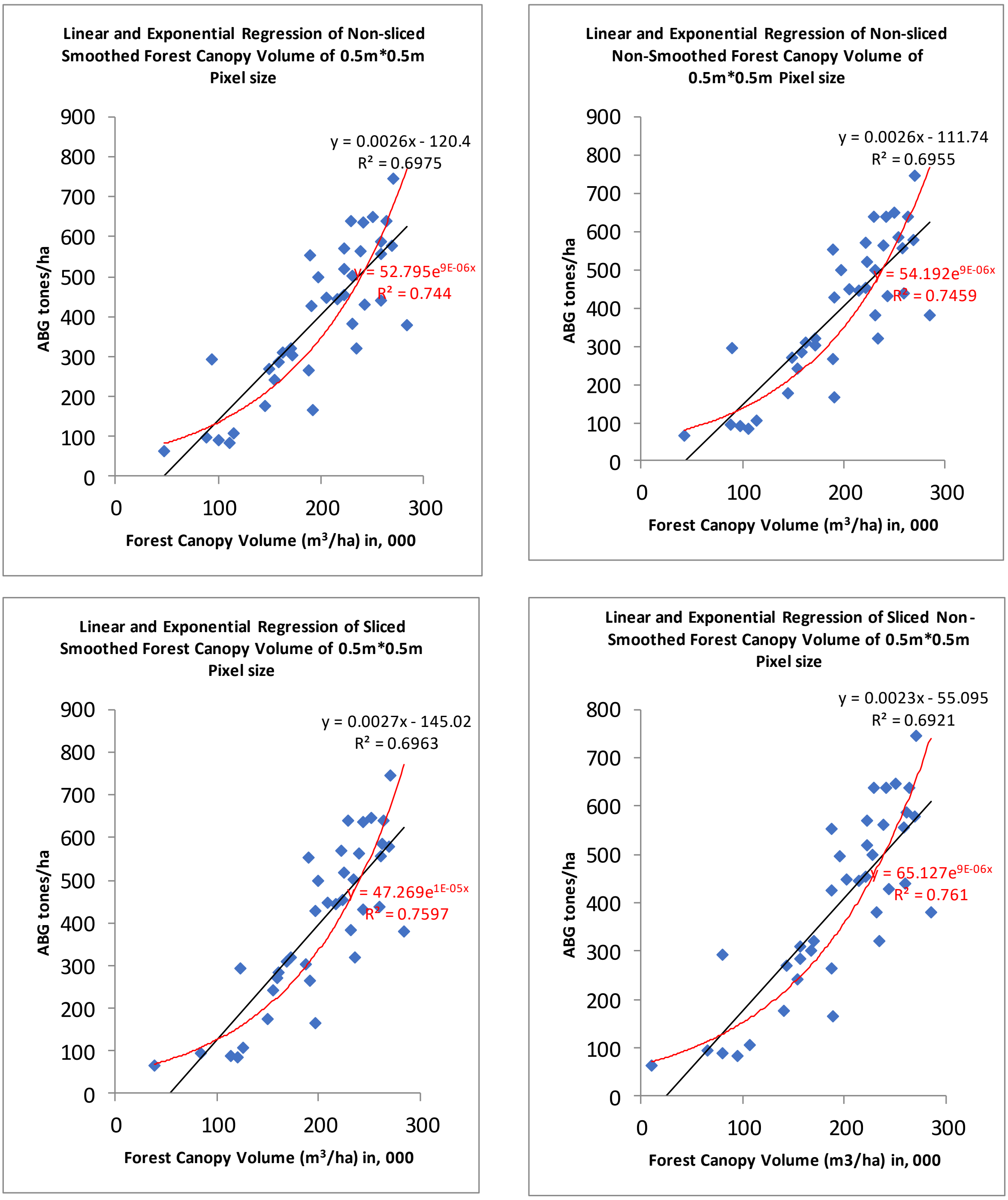

Figure 5.5. Linear and exponential regression between forest canopy volume in 0.5m*0.5m pixel and aboveground biomass.

Volume from 1m*1m pixel size value

Linear and exponential regression analysis were used to predict aboveground biomass by using forest canopy volume from 1m*1m canopy pixel size in four different conditions as described in section 4.2.2.1. Coefficient of determination (r2), Root Mean Square Error (RMSE), and alfa value (P-Value) of each regression analysis value were evaluated to assess the relationship of models at confidence interval of 95%.

Table 5.7 provides results obtained from regression analysis. All linear and exponential models were significant ($p<0.05$). Both linear and exponential models explained more than 70% of variation in forest canopy volume, except linear model from sliced non-smoothed. However, the RMSE of smoothed forest canopy volumes were higher than their corresponding non-smoothed canopies in all models. Appendix 8, Appendix 9 Appendix 10 and Appendix 11 containts other parts of linear regression analysis of 1m.

Table 5.7. Comparison of linear and exponential regressions of forest canopy volume and aboveground biomass from four different conditions: non-sliced smoothed and non-smoothed, sliced smoothed and non-smoothed.

Relation Type		**(R2)**	**RMSE**	**P - Value**
Non-sliced smoothed Forest Canopy Volume of 1m	Linear	0.7055	31602.1	4.32E-11
	Exponential	0.761	28391.5	7.1E-19
Non-sliced Non-smoothed Forest Canopy Volume of 1m	Linear	0.7025	31993.4	5.19E-11
	Exponential	0.762	28687.5	1.05E-18
Sliced smoothed Forest Canopy Volume of 1m	Linear	0.7049	30861.9	4.47E-11
	Exponential	0.773	27049.8	7.66E-19
Sliced Non-smoothed Forest Canopy Volume of 1m	Linear	0.6925	35300.4	5.19E-11
	Exponential	0.773	30363.3	3.84E-18

Figure 5.6 presents the trend of relationship between forest canopy volume and aboveground biomass in linear and exponential lines. Generally, increase in canopy volume shows increase in AGB.

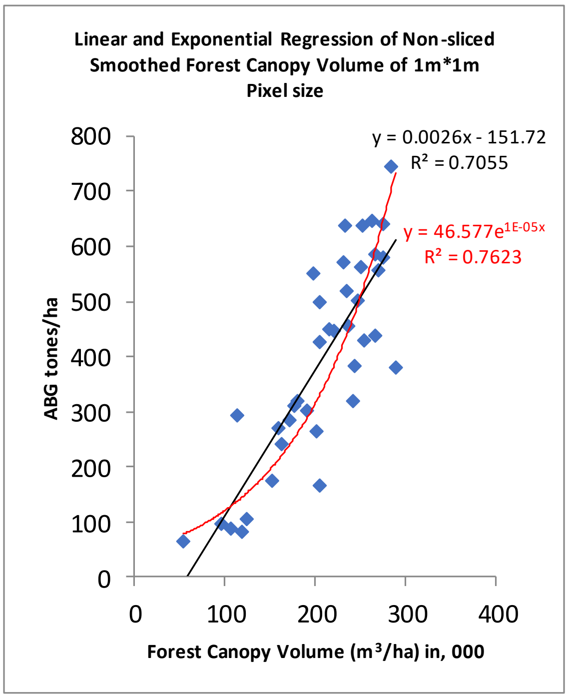

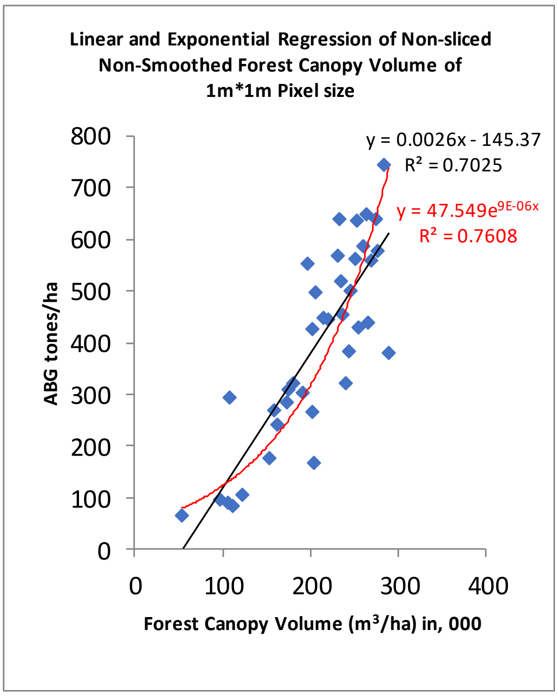

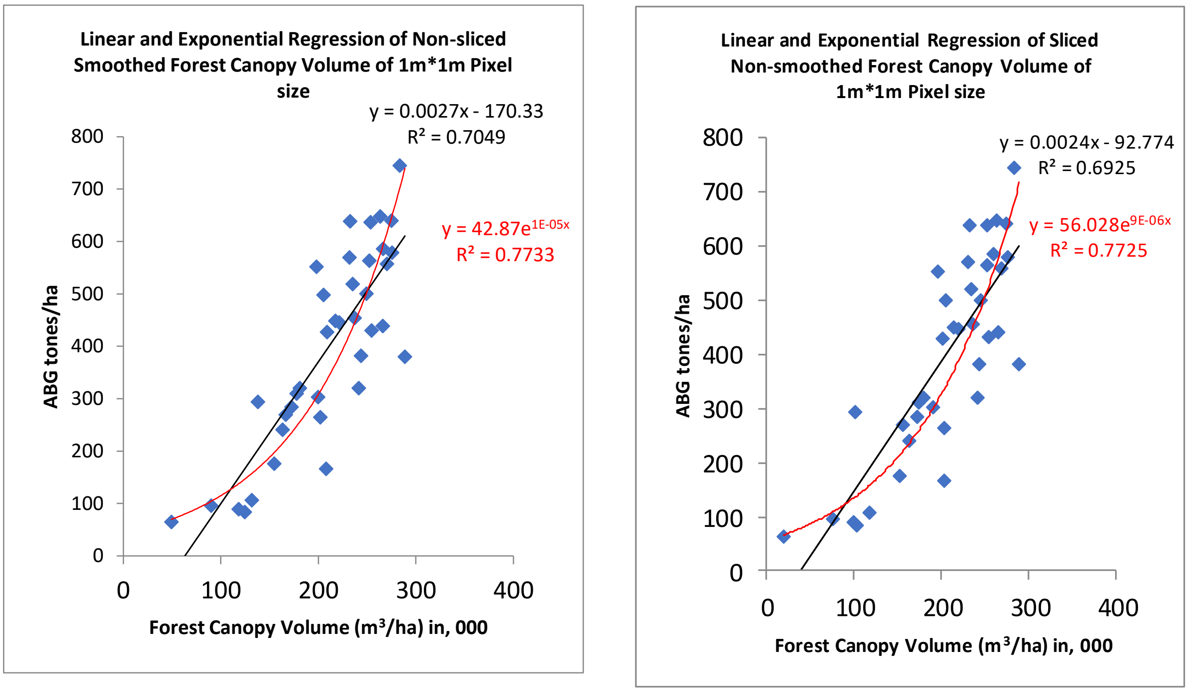

Figure 5.6. Linear and exponential regression between forest canopy volume of 1m*1m pixel and AGB.

Volume from 2m*2m pixel size value

Comparing the effects of pixel size in estimating forest canopy volume and its relationship with aboveground biomass, forest canopy of pixel size 2m*2m was used to estimate forest canopy volume. Four conditions from the canopy were used to estimate forest canopy volume and assess the relationship with aboveground biomass. Coefficient of determination (r2) of linear and exponential regression, Root Mean Square Error (RMSE), and alfa value (P-Value) of each regression analysis value were used to assess the relationship between forest canopy volume and aboveground biomass at confidence interval of 95%.

Regression analysis results are set in Table 5.8, all linear and exponential models were significant ($p<0.05$). All exponential models explained more than 75% of variation in forest canopy volume. While, linear models explained less than 74%. However, the RMSE of all linear models are higher than their corresponding exponential models. Appendix 12, Appendix 13 Appendix 14 and Appendix 15 are containts other parts of linear regression analysis from 2m*2m.

Table 5.8. Comparison of linear and exponential regressions of forest canopy volume and aboveground biomass from four different conditions: non-sliced smoothed and non-smoothed, sliced smoothed and non-smoothed.

Relation Type		(R2)	RMSE	P - Value
Non-sliced smoothed Forest Canopy Volume of 2m	Linear	0.7156	30543.7	2.29E-11
	Exponential	0.7807	26814.9	1.83E-19
Non-sliced Non-smoothed Forest Canopy Volume of 2m	Linear	0.6994	32257.7	6.28E-11
	Exponential	0.7573	28985.0	1.58E-18
Sliced smoothed Forest Canopy Volume of 2m	Linear	0.6988	28371.1	6.50E-11
	Exponential	0.7481	25945.6	1.71E-18
Sliced Non-smoothed Forest Canopy Volume of 2m	Linear	0.6877	35480.7	1.26E-10
	Exponential	0.7722	30302.9	6.97E-18

Figure 5.7 presents the trend of relationship between forest canopy volume and aboveground biomass in linear and exponential lines. Generally, increase in canopy volume shows increase in AGB.

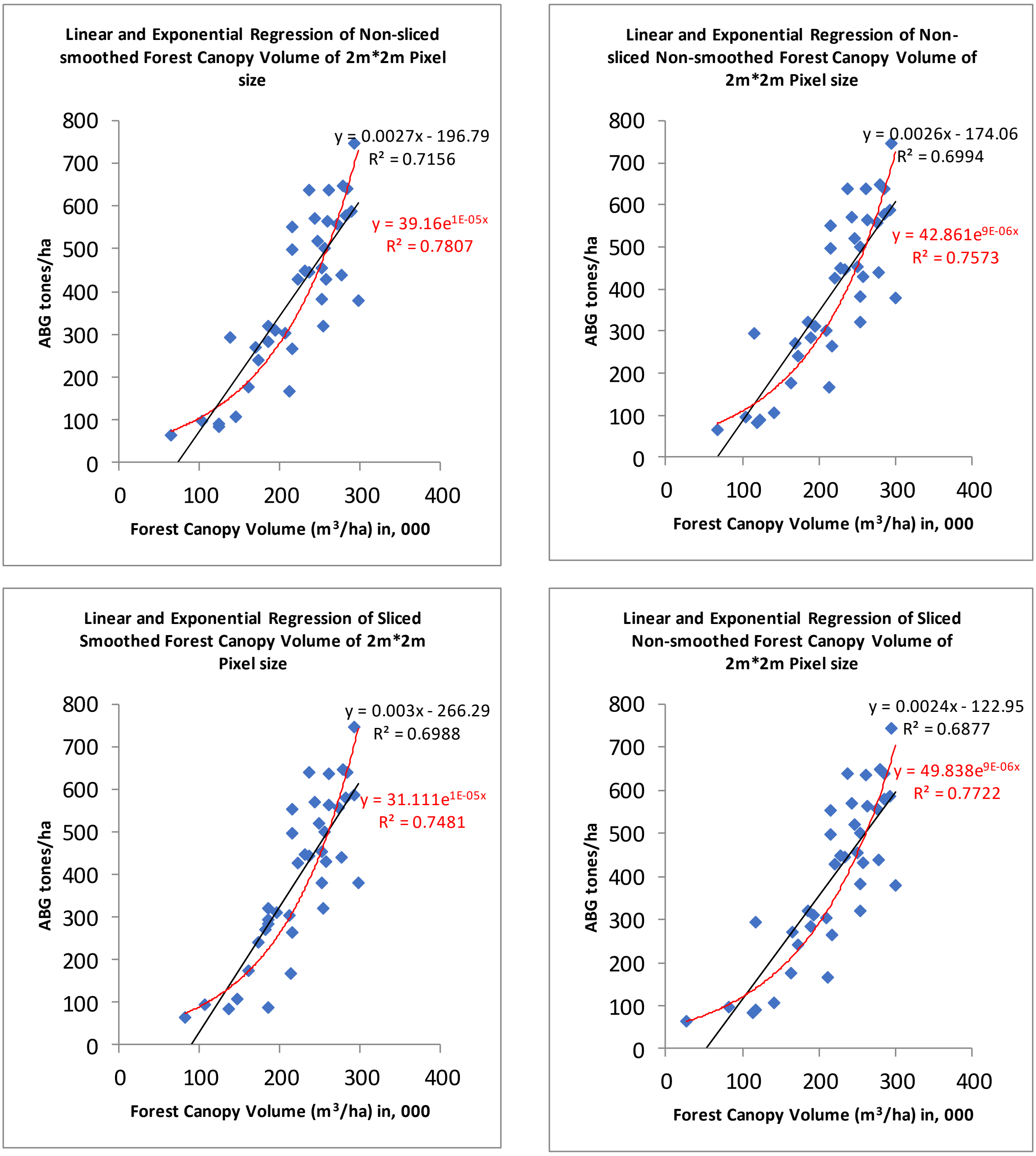

Figure 5.7. Linear and exponential regression between forest canopy volume of 2m*2m pixel and aboveground biomass.

5.3.2. Regression analysis between Adjusted Forest Canopy volume and aboveground

Referring to specific objective three of the study aimed to assess the relationship between adjusted forest canopy volume and aboveground biomass. Adjusted forest canopy volume is the function of combining forest canopy volume and forest canopy density (see 4.3). All three forest canopy volume types and their corresponding conditions were applied to assess the relationship.

Adjusted Volume from 0.5m*0.5m pixel size

Based on regression analysis, linear and exponential analysis were performed and coefficient of determination (r2), RMSE and p-value from regression were used to assess the performance of the models. It can be seen from Table 5.9, alfa value (p-value) showed that all models are significant ($p<0.05$) to 95% confidence interval. Linear and exponential models presented degrees of variation more than 65%. Furthermore, exponential models had less RMSE compared to their respective linear models. Appendix 17, Appendix 18 and Appendix 19 present other values of linear regression analysis.

Table 5.9. Comparison of linear and exponential regressions of adjusted forest canopy volume and aboveground biomass from four different conditions: non-sliced smoothed and non-smoothed, sliced smoothed and non-smoothed.

Relation Type		(R2)	RMSE	P - Value
Adjusted Non-sliced smoothed Forest Canopy Volume of 0.5m	Linear	0.6708	31637.2	3.28E-10
	Exponential	0.6843	30981.7	5.368E-17
Adjusted Non-Sliced Non-smoothed Forest Canopy Volume of 0.5m	Linear	0.6721	31775.2	3.06E-10
	Exponential	0.6887	30960.5	4.6392E-17
Adjusted Sliced smoothed Forest Canopy Volume of 0.5m	Linear	0.6643	31291.1	4.70E-10
	Exponential	0.6901	30064.7	1.15E-16
Adjusted Sliced Non-smoothed Forest Canopy Volume of 0.5m	Linear	0.6786	33581.2	2.12E-10
	Exponential	0.7098	31909.7	2.113E-17

Also, Figure 5.8 present trendlines of linear and exponential regression results. The graphs showed that, the increase of forest canopy volume, lead to increase of AGB. But, it reaches a stage where forest canopy volume did not increase further but AGB increased.

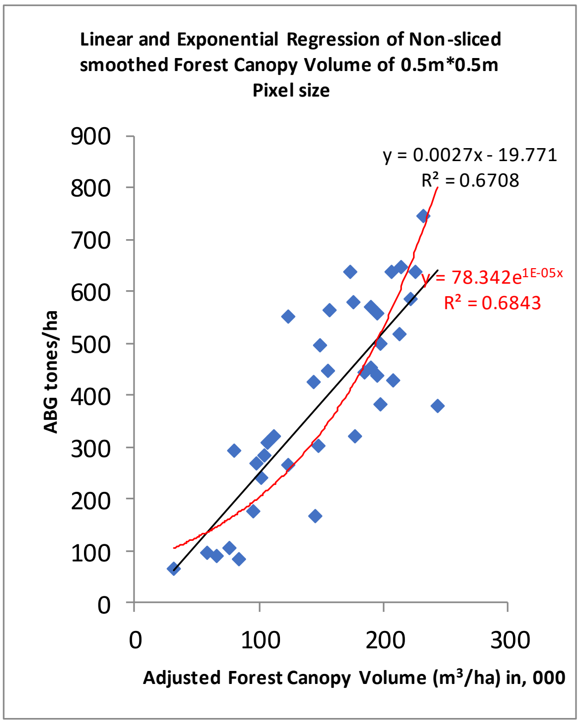

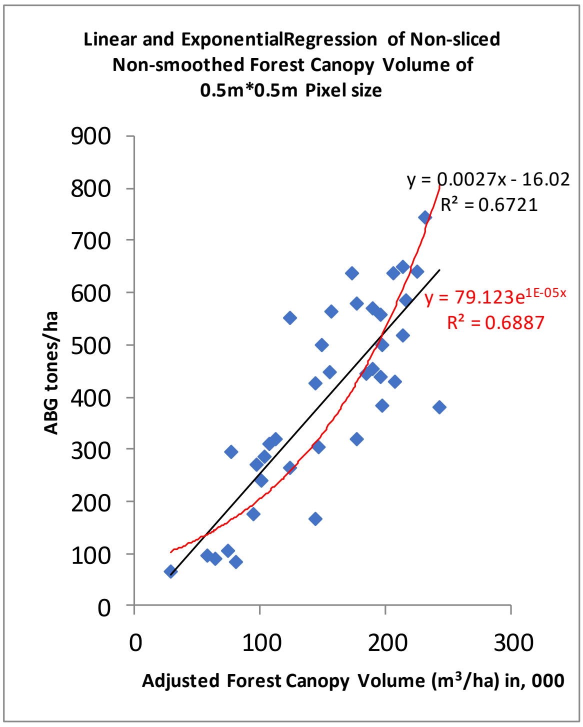

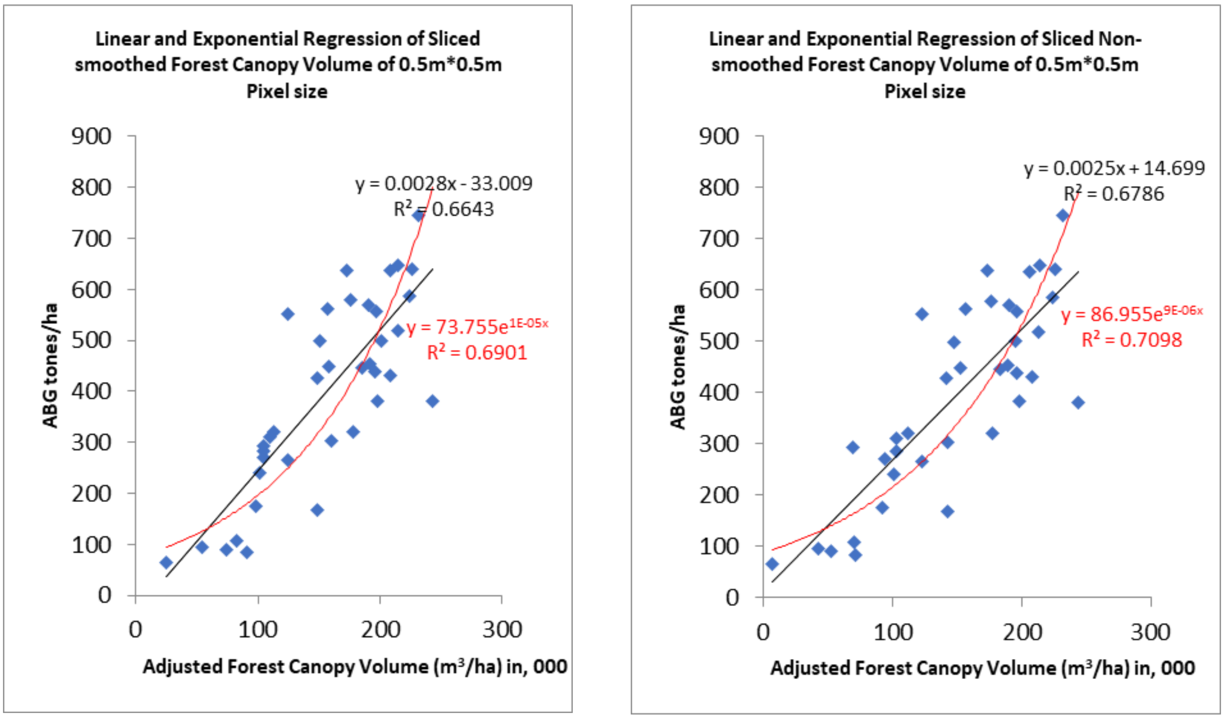

Figure 5.8. Linear and exponential regressions between adjusted forest canopy volume in 0.5m*0.5m pixel and aboveground biomass.

Adjusted Volume from 1m pixel size

From Table 5.10 linear and exponential regression explained that adjusted forest canopy volume of 1m*1m pixel size has presented degree of variation more than 65% under confidence interval of 95% with $p<0.05$. However, RMSE from linear models is higher compared to its corresponding exponential models. Appendix 20, Appendix 21, Appendix 22 and Appendix 23 present other values of linear regression analysis.

Table 5.10. Comparison of linear and exponential regressions of adjusted forest canopy volume and aboveground biomass from four different conditions: non-sliced smoothed and non-smoothed, sliced smoothed and non-smoothed.

Relation Type		(R2)	RMSE	P - Value
Adjusted Non-sliced smoothed Forest Canopy Volume of 1m	Linear	0.6699	32088.5	3.45E-10
	Exponential	0.6901	31091.2	5.983E-17
Adjusted Non-Sliced Non-smoothed Forest Canopy Volume of 1m	Linear	0.671	32122.7	3.25E-10
	Exponential	0.6927	31045.3	5.265E-17
Adjusted Sliced smoothed Forest Canopy Volume of 1m	Linear	0.6643	31848.7	4.69E-10
	Exponential	0.6929	30461.8	1.149E-16
Adjusted Sliced Non-smoothed Forest Canopy Volume of 1m	Linear	0.6749	33614.6	2.61E-10
	Exponential	0.7136	31550.5	3.297E-17

Figure 5.9 explains trend of forest canopy volume against AGB. The trendlines show that increase of forest canopy volume lead to increase of AGB. However, the trendlines show that AGB keep increasing even though there is no more forest canopy increase.

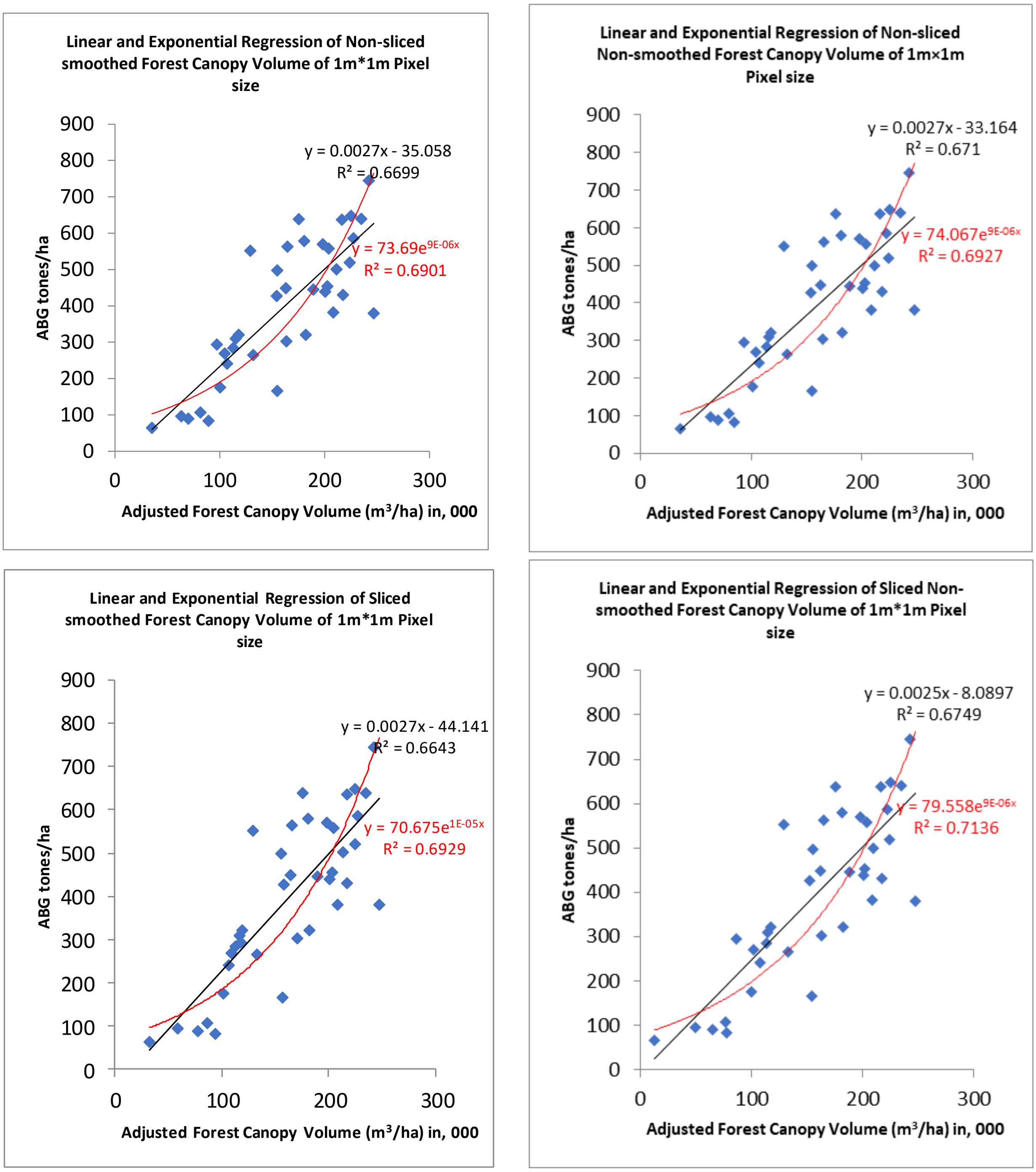

Figure 5.9. Linear and exponential regression between adjusted forest canopy volume in 1m*1m pixel and aboveground biomass.

Adjusted Volume from 2m pixel size

Linear and exponential regression results in Table 5.11 show that all linear and exponential models were significant ($p<0.05$). The results of all two models explained more than 60% of variation in forest canopy volume. However, the RMSE of all linear models are higher than their corresponding exponential models. Appendix 24, Appendix 25, Appendix 26 and Appendix 27 present other values of linear regression analysis.

Table 5.11. Comparison of linear and exponential regressions of adjusted forest canopy volume and aboveground biomass from four different conditions: non-sliced smoothed and non-smoothed, sliced smoothed and non-smoothed.

Relation Type		**(R2)**	**RMSE**	**P - Value**
Adjusted Non-sliced smoothed Forest Canopy Volume of 2m	Linear	0.6683	32378.5	3.77E-10
	Exponential	0.6935	31124.3	7.19E-17
Adjusted Non-Sliced Non-smoothed Forest Canopy Volume of 2m	Linear	0.6656	32996.0	4.37E-10
	Exponential	0.6863	31958.5	9.85E-17
Adjusted Sliced smoothed Forest Canopy Volume of 2m	Linear	0.6396	31787.6	1.71E-09
	Exponential	0.6549	31105.9	1.79E-15
Adjusted Sliced Non-smoothed Forest Canopy Volume of 2m	Linear	0.6684	34396.4	3.75E-10
	Exponential	0.7093	18545.4	7.13E-17

Figure 5.10 explains trend of forest canopy volume against AGB. The trendlines show that increase of forest canopy volume lead to increase of AGB. However, the trendlines show that AGB keep increasing even though there is no more forest canopy increase.

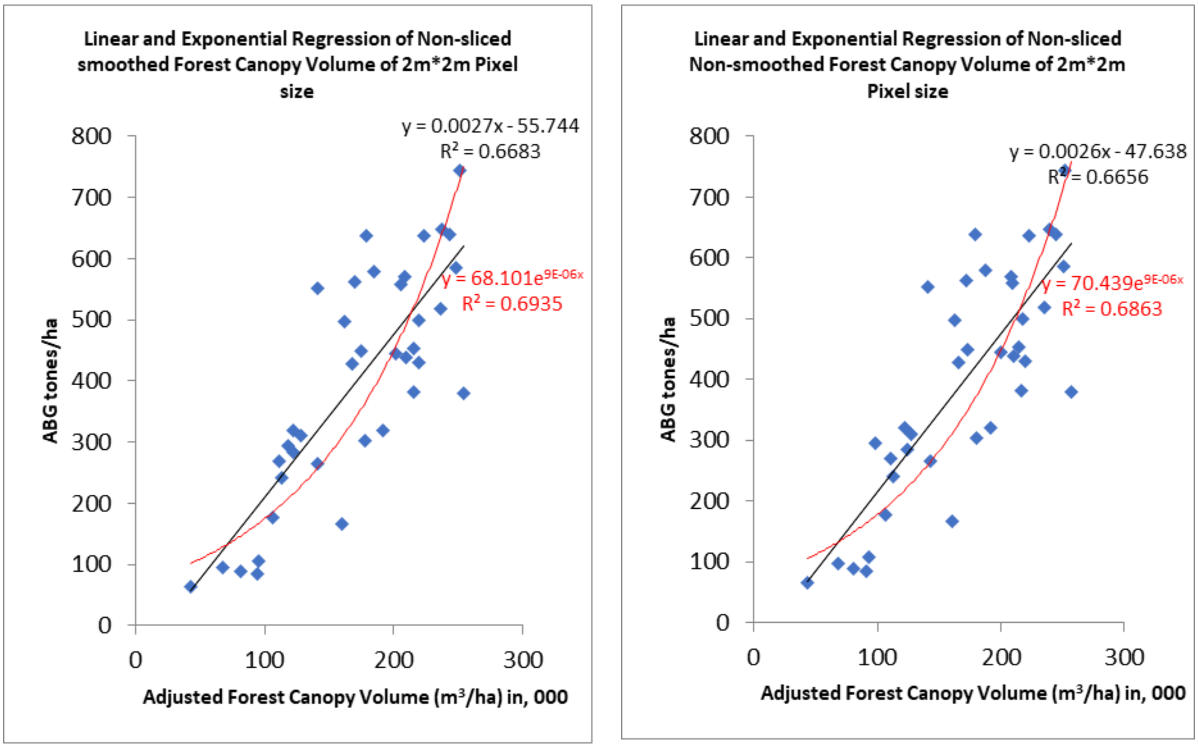

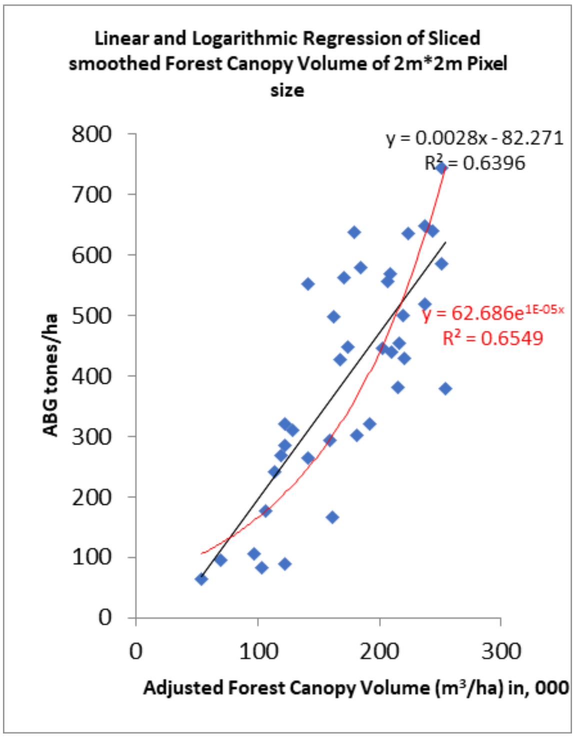

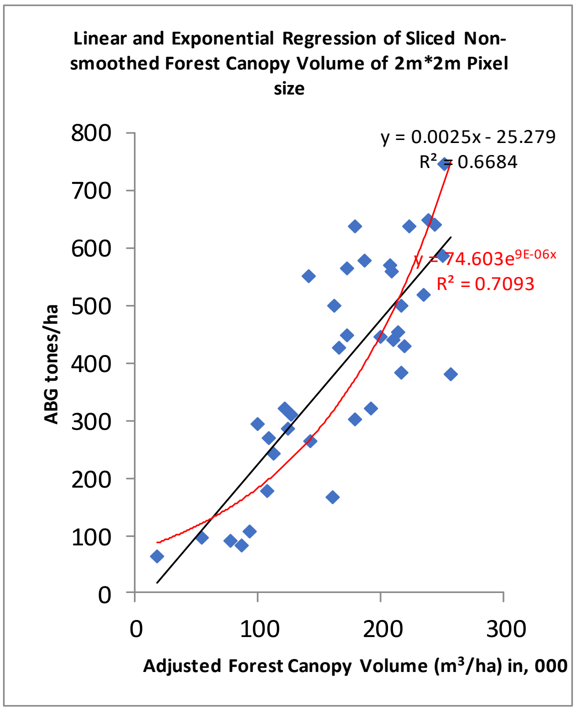

Figure 5.10. Linear and exponential regression between adjusted forest canopy volume in 2m*2m pixel and aboveground biomass.

5.4. Aboveground biomass throughout the study area

Answering specific research question four (4), exponential model from non-sliced smoothed forest canopy volume predicted more AGB than others. The model explained 78% variation of forest canopy volume with significance of 2.29E-11 under 95% confidence interval and RMSE of 29560.9. Total amount of 1,079,478 tons biomass in 1,575 ha, which is equivalent to 685.4 tons ha^{-1}. Figure 5.11 presents spatial distribution of aboveground biomass throughout the study area.

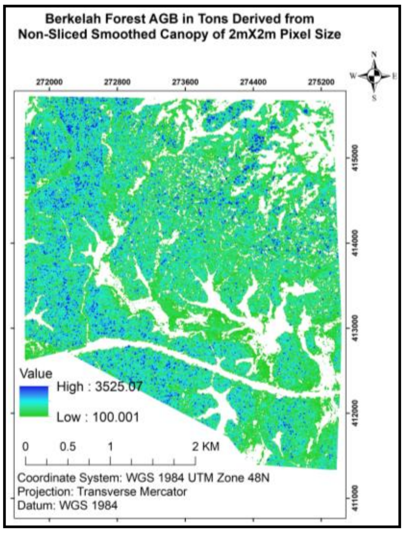

Figure 5.11. Above ground biomass of Berkelah forest derived from forest canopy volume of non-sliced smoothed 2m pixel size canopy.

6. DISCUSSION

The main goal of this research was to investigate the influence of forest canopy volume and forest canopy density in predict amount of AGB in the forest. There were four key research questions for the study:

1. What is the forest volume derived from ALS and FCD mapper in a tropical rainforest?
2. What is the above ground biomass of the field plots (AGB_{field}) used in this research?
3. What is the relation between forest canopy volume derived from ALS and FCD mapper and AGB_{field}?
4. How accurately does the AGB map from forest volume predict the actual AGB in the field?

Also, it was hypothesized that there is no significant relation between AGB_{field} and forest volume from ALS and FCD in a tropical rainforest. The findings of this research have critical implications in the assessing and influencing addressing the main objective of the study.

6.1. Sample Site Selection

The field sample plots for this study have dense and medium forest canopy cover according to the classification proposed by Mon et al. (2012). The selection of the sample plots was determined by accessibility, in particular distance to roads, slope impenetrability of the forest. In areas with steep and short slopes it is not possible to make a 3-D scan with the Terrestrial Laser Scanner (TLS) and areas far from the road were not feasible because of time constraints. It takes about 2 hours to make a TLS scan and clearing a plot from undergrowth in order to provide a clear view of all the trees for the TLS also takes a few hours and in order to do statistical analysis of the data a minimum of 30 plots is required.

6.2. Forest Canopy Density

Mon et al. (2012) forest canopy density mapper integrates biophysical indices derived from optical satellite images reflectance. The FCD mapper grouped the canopy into four: closed forest canopy are all classes ≥ 70%, medium canopy forest all classes between 40% ≥FCD< 70%), open canopy forest 10% ≥ FCD < 40%) and non-forest < 10%). The increase of bare soil degree lead to increase of bare soil index. Bare soil index is a function of the amount of bare soil, decrease in forest canopy lead to increase in bare soil index and exposure of the ground increases (Rikimaru et al., 2002).

In this study, the study area most of its part was dense forest (>70% of canopy cover) with multiple layers of forest canopies and some had medium forest canopy density. While on the other parts of the study area were <10% of forest canopy cover. These areas were those with roads, grasses, bare soils or patches of independent individual trees, looked not having vegetations and water bodies (ponds). Areas with dense canopy had high percentage of shadow index which means less bare soil exposure.

Assessing forest canopy density by using FCD mapper software were some of the challenges that can influenced over estimation or under estimation of forest canopy density of the forest. Some parts during analysis process decision on selecting parameters were subjective relating to the experience of whom will be analysing. But this does not guarantee best analysis of forest canopy density. Also, the process of converting Landsat 8 bands from 16 bits to 8 bits cause loss of some spectral information because it compresses spectral information from 16 bits to 8 bits in terms of brightness (Antunes, 2013).

Areas that had sample plots for this study analysis had dense and medium canopy cover with the forest according to Mon et al. (2012) four canopy groups. The selection of the areas was due to easy accessibility to the forest, less under store because there was other measurement needed to be taken, so needed to be taken and less sloppy areas. Areas with open canopy were not taken because either trees that were within those areas were less than 10 cm DBH (DBH for biomass estimation) or they had those factors that influenced plot selection.

6.3. Forest Canopy Volume

Filled and open is another technique that can be applied to assess and model canopy structure using LiDAR data by using full waveform data (Lefsky et al., 1999). Lefsky et al., (1999) developed a technique to examine and model three-dimensional canopy structure through forest canopy volume profiles. Lefsky et al., (1999) used filled canopy volume shape with full waveform to estimate forest canopy volume in six different conditions: filled space, Open gap space, euphotic zone, oligophotic zone and closed gap space. The method covered by matrix over the forest canopy composed of 10m * 10m square and 1m tall cells or voxels up to the level of the highest return. This technique is the same as grid cell technique which has been used to estimate forest volume for this study.

Forest canopy volume for this study applied four different conditions to estimate amount of volume within the forest canopy in three different canopy pixel sizes. 2m*2m pixel size forest canopy conditions estimated more amount of volume compared to others because of the effects of pixel size in volume estimation. Together with that, 2m*2m pixel size canopies had had possibilities of its pixel possessing high pixel value compared to 1m*1m or 0.5m*0.5m. Reasons behind that were high possibility of pixel value to gain the high maximum value because in 2m*2m pixel size there were more point clouds compared to 1m*1m and 0.5m*0.5m. Also, 2m*2m pixels had large area compared to other canopies from other pixel sizes.

Furthermore, canopies that were smoothed before estimating forest canopy volume had estimated more forest canopy volume compared to their corresponding canopies. Smoothing canopies yields high forest canopy volume compared to non-smoothed because it removes pits. That means there are some pixels within the canopy will gain and some loose pixel value during smoothing operations. Popescu & Kaiguang (2008), describe the effectiveness of applying smoothing through Fourier filtering to adjust individual trees crown architecture, the results obtained led to more yield compared to non-smoothed. Figure 6.1 presents the sketch of smoothed and non-smoothed canopy and forest canopy pixel the way they behave in two conditions.

Adjusted forest canopy volume is the function of forest canopy volume and forest canopy density. Forest canopy density was the multiplying factor to assessing if forest canopy openness has effects in estimating aboveground biomass. Combining two variables for assessing its effectives in modelling aboveground biomass has been done by several other studies too. Lu (2005) combined spectral reflectance and forest canopy texture to predict amount of biomass. Cutler et al., (2012) combined SAR backscatter and Landsat TM spectral reflectance to predict aboveground biomass for Malaysian, Thailand and Brazilian forests.

Results of this study and other studies are difficult to compare because different variable that have been applied for combination. The study has combined forest canopy volume and forest canopy density, Lu (2005) combined spectral reflectance and forest canopy texture and Cutler et al., (2012) combined SAR backscatter and Landsat TM spectral reflectance. Also, too little information about forest complexity. Spectral image texture and backscatter can be used to describe forest complexity but there is too little information on it.

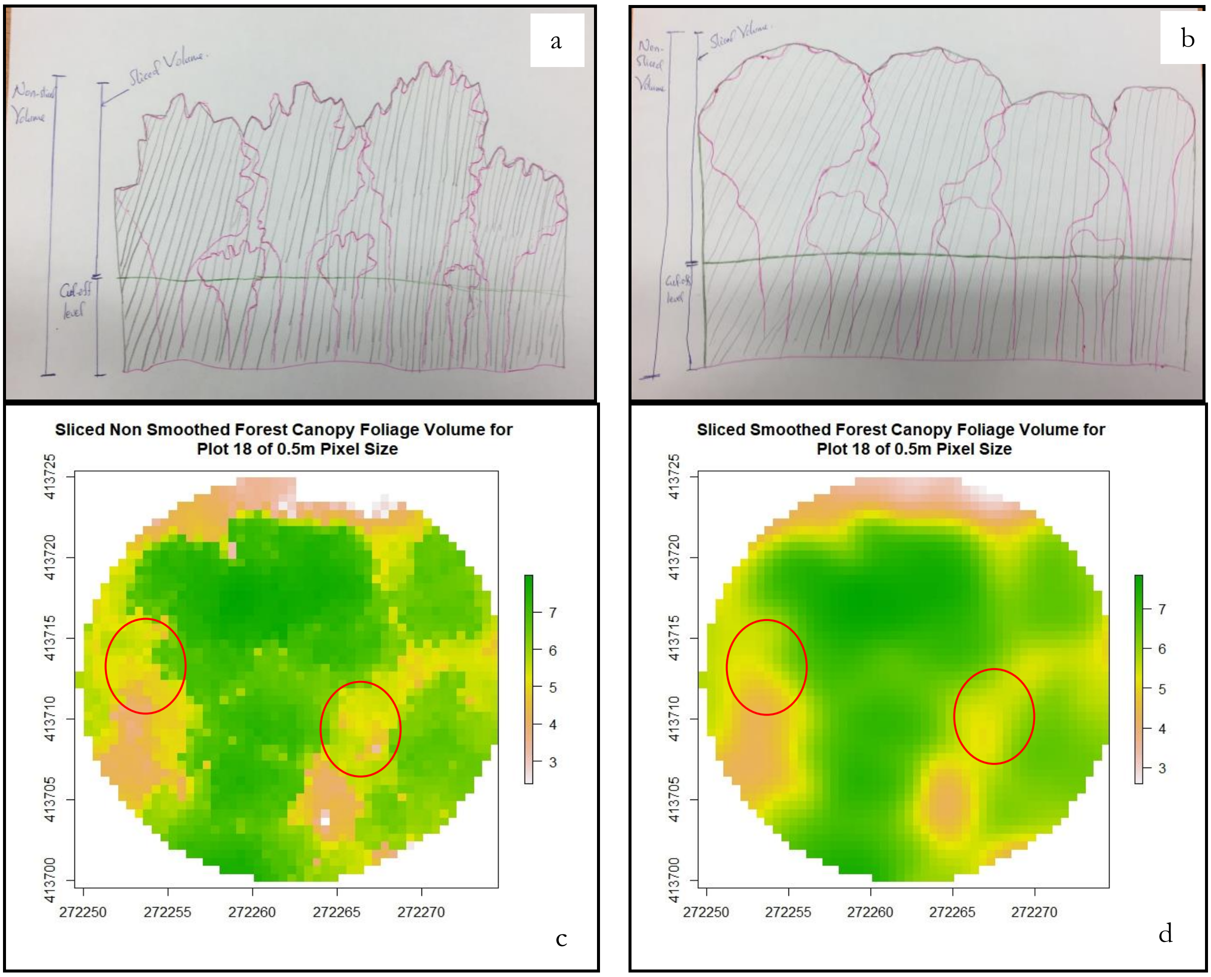

Figure 6.1. Picture (a) and (b) are sketches of non-smoothed and smoothed tree canopy and (c) and (d) are non-smoothed and smoothed forest canopy volume.

6.4. AGB Measured

Aboveground biomass was estimated by computing tree heights and diameter at breast height (DBH) to allometric equation for tropical rainforest developed by Chave et al., (2014). Brown (1997) describes the effects of size of DBH in estimating aboveground biomass. DBH <10 cm have no significant contribution to aboveground biomass. For this study DBH less than 10cm were excluded. Tree height also contributes to the aboveground biomass: the taller the tree the more will influence the amount of biomass. This resulted in an ABG estimate ranging from 64.6 to 745 tons/ha. Total AGB calculated was 15025.98 tons for 1.9 ha (38 plots of 500m^2 each. AGB estimated in this study can be described that those plots that had tree with higher heights compared to others have estimated more aboveground biomass. While, those plots with less DBH compared to others regardless of their tree height had estimated less AGB.

Tree heights and DBH were influenced by several environmental factors (Drake et al., 2000). Some were climate, soil and human influence. For tropical rainforests measuring tree height is a challenge because layers within a canopy. LiDAR remote sensing technology regardless of cost has overcome the challenge of estimating tree height (Muluken, 2017). For upper canopy trees ALS LiDAR is applied and lower canopy TLS LiDAR is applied (Muluken, 2017). Accurate collection of measurement for AGB estimation lead to accurate AGB estimation. Estimation of AGB for this study has been estimated by measuring tree heights using LiDAR technology and

DBH were measured directly to the field. Sadadi (2016) explained how ALS and TLS measured tree height in tropical forest in Figure 6.2. with multiple layers.

But, it was challenge to merge between DBH field measured and tree height that has been extracted from ALS LiDAR data. There was location shift on the individual tree locations which was caused by GPS shift errors. Even though segmentation of tree crown in CHM was applied still there was a challenge of over and under segmentation because of different spectral reflectance between trees in the forest. In tropical rainforests contained different tree species and multiple layers. That affected segmentation under multi resolution function in ecognition software. Also, that it was a challenge to determine which tree crown on the segmented image belongs to which tree in the field and that because of complexity of the forest canopy and subsequent occlusion, it is uncertain if the highest value in the segment really is the tree height. It is imaginable that the highest point of a particular tree in the lower canopy is not visible from above.

Aboveground biomass for most accurate estimation applies specific allometric equation for tree species and specific wood density. But for this study AGB estimation did not consider the use of allometric equation for species and wood density. Reason for not considering that was the study area is a tropical rainforest that has many tree species and some species have no specific allometric equation for estimating AGB. In addition to that but limitation and researcher had no knowledge on most of tropical rainforest tree species which could lead to wrong identification of specie names.

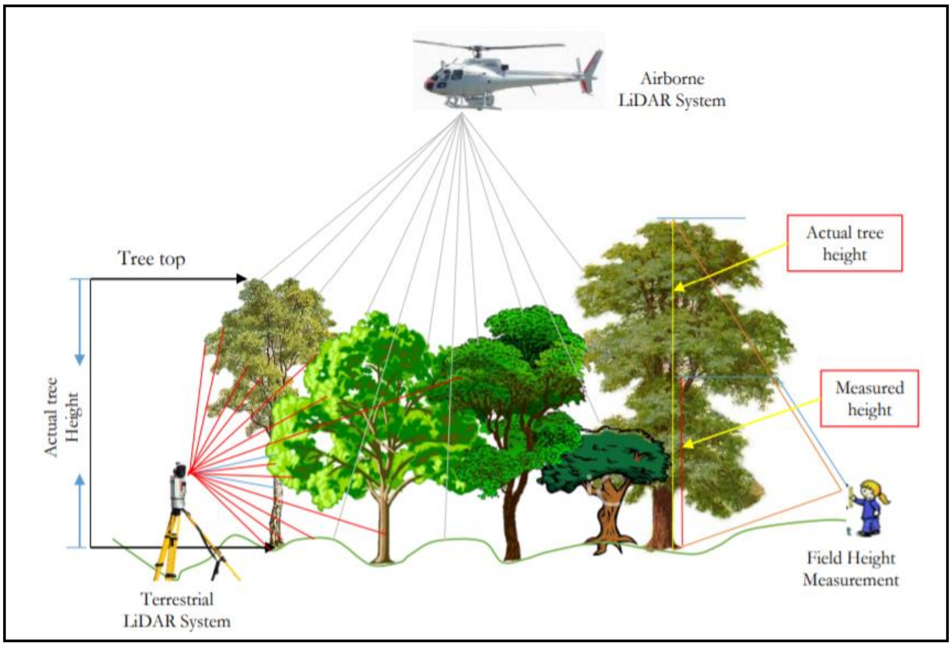

Figure 6.2. Trees height assessment in tropical forest using ALS and TLS sensors (Sadadi, 2016).

6.5. AGB Model

This study applied regression empirical models to assess relationship between forest canopy volume and AGB. Linear models explained more than 60% of variation of forest canopy volume, while exponential models explained more than 65% for forest canopy volume and adjusted forest volume. Linear and exponential models describe trend independent variable and dependent variable how they relate each other. For this study exponential models showed that forest volume increased with AGB but reached a point where did not increase further while AGB was increasing. There are other studies that applied empirical models and specifically to linear and exponential regression models. Lawrence & Ripple (1998) used linear regression model to assess the relationship between vegetation indices and aboveground biomass and the performance of the model with r^2 ranged 0.55 to 0.70. Anaya, et al., (2009) applied exponential model for more appropriate description of biomass increase as the percentage of tree percentage increases with the 90% confidence intervals. Hall, et al., (2006) used exponential regression as the best model performance for predicting height and crown closure by using Landsat ETM+ bands. Steininger, (2000) explored AGB estimation by using exponential regression model of tropical secondary forests using Landsat TM data and found saturation problem for AGB estimation in advanced succession forest at 15kg m^{-2}. This is the same to forest canopy volume to the prediction of biomass which saturates which canopy growth reaches its maximum growth but still biomass is increasing. The saturation problem is found too in RADR remote sensing with different polarizations and characteristics of vegetation stand structure and ground conditions. As (Luckman, et al., 1997) found that the longer-wavelength (L-band) SAR image was able to discriminated AGB at a certain threshold.

Prediction of AGB from remote sensing technique and combination with different variable have been applied with several studies. The aim of combining several variables was to add values to dependent variable during relationship assessment. Forest canopy volume and forest canopy density were combined but did not have influence in improving relationship with AGB. Lu (2005) conducted a study which combined image spectral reflectance with image texture which improved relationship as seen presented in Figure 6.3. Cutler et al. (2012) combined SAR backscatter and Landsat TM spectral reflectance and improved relationship from (r) = 0.23 (Malaysia), 0.05 (Thailand) and 0.16 (Brazil) to 0.79, 0.79 and 0.84 respectively.

Table 2. Summary of aboveground biomass estimation models using Landsat TM derived variables.

Variables	Study areas	Models	R^2	Beta Value
Spectral responses	Altamira	− 49.892 − 202.045 ND54	0.404	
	Pedras*	95.196 − 5.852 TM5	0.683	
	Bragantina	68.116 − 1.832 TM4	0.701	
	Machadinho (SF)	66.772 − 1.392 TM4	0.746	
	Machadinho (MF)	102.414 − 5.496 TM5	0.158	
Textures	Altamira	89.461 − 151.495 VARtm2_9	0.708	
	Pedras*	35.109 − 6.455 KUtm3_5	0.493	
	Bragantina	21.038 − 3.766 VARtm5_15	0.304	
	Machadinho (SF)	16.462 − 0.227 VARtm4_15	0.232	
	Machadinho (MF)	13.457 + 1.929 CONtm5_19	0.392	
Combination of spectral and texture	Altamira	122.288 − 1.078 KT1 − 128.913 VARtm2_9	0.772	− 0.28 (sp), − 0.72 (txt)
	Pedras*	65.239 − 10.189 TM7 − 3.816KUtm3_5	0.748	− 0.58 (sp), − 0.42 (txt)
	Bragantina	64.037 − 1.651 TM4 + 1.405 SKtm4_9	0.780	− 0.76 (sp), 0.29 (txt)
	Machadinho (SF)	48.082 − 0.806 TM4 − 0.098 VARtm4_15	0.755	− 0.71(SP), − 0.24(txt)
	Machadinho (MF)	75.331 − 4.321 TM5 + 1.789 CONtm5_19	0.498	− 0.31(sp), 0.65(txt)

Note: * Ponta de Pedras; SF and MF: successional forest and mature forest; sp and text: the variables of spectral signatures and textures; TM4, TM5, and TM7: Landsat TM bands 4, 5, and 7; ND54 is the ratio (TM5 − TM4)/(TM5 + TM4); KT1: the first component from the tasselled cap transform based on Landsat TM images; VARtma_b: variance texture measure with TM band a and associated b × b window size; KU, SK, and CON: Kurtosis, skewness, and contrast texture measures.

Aboveground biomass estimation in Brazil

Figure 6.3. Table of summary of the results of the study of estimating aboveground biomass by combining spectral reflectance and canopy texture. Source: (Lu, 2005).

6.6. Relevance of the Research for Biomass Estimation

Under UNFCCC through REDD+ program is to find the best method that high accuracy in estimation AGB. Results from this study show that non-sliced smoothed forest canopy volume can be used to predict AGB for 71% - linear and 78% - exponential model under a forest canopy of 2m*2m. also, from the study can help the quantification and assessing the amount of foliage materials that is contained with the forest canopy. Together with that, applying ALS LiDAR full waveform will assist assessing canopy density by identifying empty pixels within a canopy.

Furthermore, compared to vegetation indices studies that have been conducted, this study has estimated more amount of biomass. Example the study conducted by Adan (2017) used vegetation indices from Sentinel 2 to estimate aboveground biomass exponential regression for Red Edge Ratio Vegetation Indices (RERVI) with correlation coefficient of 0.737. The study model of exponential performs better for 0.78 coefficient correlation for the canopy of 2m pixel size smoothed, which is almost the same to Cutler et al. (2012) study its model was 0.77 correlation coefficient which combined between spectral reflectance and SAR textures for Malaysian forests.

Also, the study has shown some improvements compared with the study done by Jiménez et al. (2017) the estimated aboveground biomass by combining LiDAR data and Landsat ETM+ vegetation indices from different conditions. Unfortunately, most of Jiménez et al., (2017) results were not promising because coefficient of determination (r^2) ranged from 0.49 to 0.65.

6.7. Limitations of the Study

Throughout the whole process of conducting this study, there were some challenges and limitations that have affected the quality of results in one way or another. Individual tree and plot centre location collection were not accurate due to GPS shift errors. these types of errors had effects on matching individual trees with ALS CHM with maximum values that were used to extract tree height from the CHM. In other words, it was not entirely clear whether some trees had been assigned to tree heights that were not theirs because of GPS location shift errors.

Secondly, the segmentation of tree crowns for the identification of individual trees in tropical rainforests was a challenging process. This was because tropical rainforests have different layers of trees and different tree species that affected segmentation due to differences in spectral reflectance under multiresolution. The outcome of this was over or under-segmentation of canopies which later will affect CHM maximum value calculation.

Analysis of forest canopy density using Forest Canopy Density Mapper (FCD Mapper) had either underestimated or overestimated of forest canopy density because selection to some parameters in FCD mapper was very subjective depending on the decision of the analyser. Also, failure of FCD mapper to use 16 bits caused the less of information through conversion process to 8 bits.

7. CONCLUSION AND RECOMMENDATION

7.1. Conclusion

The study calculated forest volume from four different conditions in three forest canopy height sizes which were combined with forest canopy volume to obtain adjusted forest canopy volume. The conditions are:

- Non-sliced and non-smoothed, pixel size 0.5m*0.5m, 1m*1m and 2 m*2m
- Non-sliced and smoothed, pixel size 0.5m*0.5m, 1m*1m and 2 m*2m
- Sliced and non-smoothed, pixel size 0.5m*0.5m, 1m*1m and 2 m*2m
- Sliced and smoothed, pixel size 0.5m*0.5m, 1m*1m and 2 m*2m

In addition, AGB was estimated from the DBH field measured and tree height extracted from LiDAR data which was computed by a general allometric equation developed for tropical rainforests by Chave et al., (2014)(J Chave et al., 2005). Forest canopy volume, adjusted forest canopy volume and AGB were used to assess the relationship. The best model was adopted to produce AGB map for the whole study area

Research Question 1.
What is the forest volume derived from ALS and FCD mapper in a tropical rainforest?

38 sample plots spatially distributed were estimated forest canopy volume with an area of 500m^2 each. The total amount of forest canopy volume 94,720,245.07 m^3 for 1.9 ha (38 plots of 500 m^2 each) was estimated which is equal to 49,852,760.56 m^3 per ha. Estimated forest canopy volume was multiplied by forest canopy density derived from FCD mapper and got adjusted forest canopy volume of 73,351,827.2 m^3 for 1.9 ha, which is equal to 38,606,224.84 m^3 per ha.

Research Question 2.
What is aboveground biomass of the field plots (AGB_{field}) used in this research?

Field measured DBH from 38 field plots and tree height extracted from LiDAR data were computed by a general allometric equation for tropical rainforest biomass estimation. The hectare with lowest biomass was 64.6 tons and the highest was 745 tons. Total AGB calculated was 15025.98 tons for 1.9 ha (38 plots of 500m^2 each).

Research Question 3.
What is the relation between forest volume derived from ALS and FCD mapper and AGB_{field}?

The relationship between forest canopy volume, adjusted forest canopy volume with AGB were strong because the models explained the presence of AGB through forest canopy volume more than 60% in all models. All linear and exponential model were significant with alpha (p-value) <0.05.

Research Question 4.
How accurately does the AGB map predict the actual AGB in the field?

The model with a high coefficient of determination, lowest RMSE and p-value than others was selected to produce a predicted map of AGB in the whole study area. exponential model from non-sliced smoothed regression analysis estimated by 78% present of AGB through forest canopy volume.

7.2. Recommendation

For further improvement of biomass researches, the following recommendations are worth to be considered:

i. The use of more accurate GPS for taking individual and plot centre locations to avoid errors that could be caused by location shifts of individual and central locations. Alternatively, studies could determine the effects caused by error shifts with GPS.

ii. Future researches may try to investigate the combination of canopy volume from ALS point clouds and forest texture from SAR images. This can even be done in the same study area as a desktop study because all data are already available (ALS data, SAR images and field data).

iii. Lastly, future studies can try to investigate the volume from TLS point clouds do they relate to aboveground biomass through voxel method. Because TLS captures the whole tree and allows for the estimation of foliage and tree trunk volumes.

LIST OF REFERENCES

Achad Frederic & Hansen Methew C. (2016). *Global Forest Monitoring from Earth Observation - Google Books*. (Achad Frederic & Hansen Methew C., Ed.) (1st ed.). Florida: CRC Press.

Adan, M. S. (2017). *Derived Vegetation Indices and Terrestrial Laser Scanner To Estimate Above- Ground Biomass / Carbon in Ayer Hitam Tropical Forest Derived Vegetation Indices and Terrestrial Laser Scanner To Estimate Above- Ground Biomass / Carbon in Ayer Hitam Tropical Ra*. University of Twente - Faculty of Geoinformation Science and Earth Observation; Unpublished Msc. Thesis.

Anaya, A. Jesus, Chuvieco, Emilio, Orueta, P. A. (2009). Aboveground biomass assessment in Colombia: A remote sensing approach. *Forest Ecology and Management*, *257*, 1237–1246. https://doi.org/10.1016/j.foreco.2008.11.016

Antunes, S. (2013). *DIY Instruments for Amateur Space: Inventing Utility for Your Spacecraft ... - Sandy Antunes - Google Books*. (B. Jepson, Ed.) (First Edition). Tokyo: O'Reilly Press.

Araújo, T. M., Higuchi, N., & Andrade de Carvalho Júnior, J. (1999). Comparison of formulae for biomass content determination in a tropical rain forest site in the state of Pará, Brazil. *Forest Ecology and Management*, *117*(1–3), 43–52. https://doi.org/10.1016/S0378-1127(98)00470-8

Babst, F., Bouriaud, O., Alexander, R., Trouet, V., & Frank, D. (2014). Toward consistent measurements of carbon accumulation: A multi-site assessment of biomass and basal area increment across Europe. *Dendrochronologia*, *32*(2), 153–161. https://doi.org/10.1016/j.dendro.2014.01.002

Barizan, R. S. (1997). *Studies on the Early Establishment of Dipterocarp Seedlings in a Malaysian Logged Hill Forest.* University of Stirling, Scotland, Phd. Thesis.

Basuki, T. M., van Laake, P. E., Skidmore, A. K., & Hussin, Y. A. (2009). Allometric equations for estimating the above-ground biomass in tropical lowland Dipterocarp forests. *Forest Ecology and Management*, *257*(8), 1684–1694. https://doi.org/10.1016/j.foreco.2009.01.027

Brown, S. (1997). *Estimating Biomass and Biomass Change of Tropical Forests: A Primer - Sandra Brown, Food and Agriculture Organization of the United Nations - Google Books* (134 No. ISSN 0258-6150).

Chandrashekhar, M. B., Saran, S., Raju, P. L. N., & Roy, P. S. (2005). Forest Canopy Density Stratification: How Relevant is Biophysical Spectral Response Modelling Approach? *Geocarto International*, *20*(1), 15–21. https://doi.org/10.1080/10106040508542332

Chave, J., Andalo, A. C., Brown, A. S., Cairns, A. M. A., Chambers, J. Q., Eamus, A. D., … Kira, T. (2005). Tree allometry and improved estimation of carbon stocks and balance in tropical forests. *Oecologia*, *145*, 87–99. https://doi.org/10.1007/s00442-005-0100-x

Chave, J., Muller-Landau, H. C., Baker, T. R., Easdale, T. A., Hans Steege, T. E. R., & Webb, C. O. (2006). Regional and phylogenetic variation of wood density across 2456 neotropical tree species. *Ecological Applications*, *16*(6), 2356–2367. https://doi.org/10.1890/1051-0761(2006)016[2356:RAPVOW]2.0.CO;2

Chave, J., Réjou-Méchain, M., Búrquez, A., Chidumayo, E., Colgan, M. S., Delitti, W. B. C., … Vieilledent, G. (2014). Improved allometric models to estimate the aboveground biomass of tropical trees. *Global Change Biology*, *20*, 3177–3190. https://doi.org/10.1111/gcb.12629

Corlett, R., & Primack, R. B. (2011). *Tropical rain forests: An Ecological and Biogeographical Comparison.* (second Edi). West Sussex: Wiley-Blackwell.

Cummings D.L, Kauffman J. Boone, Perry David A, H. R. F. (2002). Above ground biomass and structure of rainforests in the Southwestern Brazilian Amazon. *Forest Ecology and Management*, *163*, 293–307. https://doi.org/doi.org/10.1016/S0378-1127(01)00587-4

Cutler M.E.J, Boyd D.S., Foody G.M, V. A. (2012). Estimating tropical forest biomass with a combination of SAR image texture and Landsat TM data: An assessment of predictions between regions. *ISPRS Journal of Photogrammetry and Remote Sensing* , *70*, 66–77. https://doi.org/http://dx.doi.org/10.1016/j.isprsjprs.2012.03.011

Dittmann, S., Thiessen, E., & Hartung, E. (2017). Applicability of different non-invasive methods for tree mass estimation: A review. *Forest Ecology and Management*. https://doi.org/10.1016/j.foreco.2017.05.013

Djomo, A. N., & Chimi, C. D. (2017). Tree allometric equations for estimation of above, below and total biomass in a tropical moist forest: Case study with application to remote sensing. *Forest Ecology and Management*, *391*, 184–193. https://doi.org/10.1016/j.foreco.2017.02.022

Dong, J., Kaufmann, R. K., Myneni, R. B., Tucker, C. J., Kauppi, P. E., Liski, J., … Hughes, M. K. (2003). Remote sensing estimates of boreal and temperate forest woody biomass: Carbon pools, sources, and sinks. *Remote Sensing of Environment*, *84*(3), 393–410. https://doi.org/10.1016/S0034-4257(02)00130-X

Drake, J. B., Dubayah, R. O., Clark, D. B., Knox, R. G., Blair, J. B., Hofton, M. A., … Prince, S. (2002). Estimation of tropical forest structural characteristics, using large-footprint lidar. *Remote Sensing of Environment*, *79*(2–3), 305–319. https://doi.org/10.1016/S0034-4257(01)00281-4

Drake B. Jason, Dubayah O. Ralph, Clark B. David, Knox G. Robert, Blair Bryan J. Hofton A. Michelle, Chazdon L. Robin, Weishmpel F. John, P. D. S. (2000). Estimation of tropical forest structural characteristics using large-footprint lidar, *79*, 305–319. https://doi.org/https://doi.org/10.1016/S0034-4257(01)00281-4

Eckert, S. (2012). Improved forest biomass and carbon estimations using texture measures from worldView-2 satellite data. *Remote Sensing*, *4*(4), 810–829. https://doi.org/10.3390/rs4040810

Edson, C., & Wing, M. G. (2011). Airborne light detection and ranging (LiDAR) for individual tree stem location, height, and biomass measurements. *Remote Sensing*, *3*(11), 2494–2528. https://doi.org/10.3390/rs3112494

Englhart, S., Keuck, V., & Siegert, F. (2012). Modeling aboveground biomass in tropical forests using multi-frequency SAR data-A comparison of methods. *IEEE Journal of Selected Topics in Applied Earth Observations and Remote Sensing*, *5*(1), 298–306. https://doi.org/10.1109/JSTARS.2011.2176720

FAO. (2010). *Global Forest Resources Assessment*. Rome.

Farid, A., Goodrich, D. C., Bryant, R., & Sorooshian, S. (2008). Using airborne lidar to predict Leaf Area Index in cottonwood trees and refine riparian water-use estimates. *Journal of Arid Environments*, *72*(1), 1–15. https://doi.org/10.1016/j.jaridenv.2007.04.010

Foody, G. M., Boyd, D. S., & Cutler, M. E. J. (2003). Predictive relations of tropical forest biomass from Landsat TM data and their transferability between regions. *Remote Sensing of Environment*, *85*(4), 463–474. https://doi.org/10.1016/S0034-4257(03)00039-7

Gideon Neba, S., Kanninen, M., Eba'a Atyi, R., & Sonwa, D. J. (2014). Assessment and prediction of above-ground biomass in selectively logged forest concessions using field measurements and remote sensing data: Case study in South East Cameroon. *Forest Ecology and Management*, *329*, 177–185. https://doi.org/10.1016/j.foreco.2014.06.018

Godinho, S., Gil, A., Guiomar, N., Neves, N., & Pinto-Correia, T. (2016). A remote sensing-based approach to estimating montado canopy density using the FCD model: a contribution to identifying HNV farmlands in southern Portugal. *Agroforestry Systems*, *90*, 23–34. https://doi.org/10.1007/s10457-014-9769-3

Goslee, K., Walker, S. M., Grais, A., Murray, L., Casarim, F., & Brown, S. (2012). *Leaf Technical Guidance Series for the Development of a Forest Carbon Monitoring System for REDD+*.

Grau, E., Durrieu, S., Fournier, R., Gastellu-Etchegorry, J. P., & Yin, T. (2017). Estimation of 3D vegetation density with Terrestrial Laser Scanning data using voxels. A sensitivity analysis of influencing parameters. *Remote Sensing of Environment*, *191*, 373–388. https://doi.org/10.1016/j.rse.2017.01.032

Hadi, F., Wikantika, K., & Sumarto, I. (2004). Implementation of Forest Canopy Density Model to Monitor Forest Fragmentation in Mt . Simpang and Mt . Tilu Nature Reserves , West Java , Indonesia Implementation of Forest Canopy Density Model to Monitor Forest Fragmentation in Mt . Simpang and Mt . Tilu. In *3rd FIG Regional Conference* (pp. 1–9). Jakarta, Indonesia.

Hall, R., Skakun, R., Arsenault, E., & Case, B. (2006). Modeling forest stand structure attributes using Landsat ETM+ data: Application to mapping of aboveground biomass and stand volume. *Forest Ecology and Management*, *225*, 378–390. https://doi.org/10.1016/j.foreco.2006.01.014

Hamilton G, J. (1988). *Forest mensuration handbook*. (Forest Commission, Ed.) (Third). London: Forestry Commission.

Haven, P. (1988). *Diversity at risk: Tropical forests*. (E. O. Wilson & F. M. Peter, Eds.) (First Edit). Washington: National Academies Press (US).

Holdaway, R. J., Mcneill, S. J., Mason, N. W. H., & Carswell, F. E. (2014). Propagating uncertainty in plot-based estimates of forest carbon stock and carbon stock change. *Ecosystems*, *17*, 627–640. https://doi.org/10.1007/s10021-014-9749-5

Hyyppä, J., Hyyppä, H., Leckie, D., Gougeon, F., Yu, X., & Maltamo, M. (2008). Review of methods of small footprint airborne laser scanning for extracting forest inventory data in boreal forests. *International Journal of Remote Sensing*, *29*(5), 1339–1366. https://doi.org/10.1080/01431160701736489

IPCC. (1996). *Intergovernmental Panel on Climate Change Good Practice Guidance for Land Use, Land-Use Change and Forestry IPCC National Greenhouse Gas Inventories Programme*.

Jiménez, E., Vega, J. A., Fernández-Alonso, J. M., Vega-Nieva, D., Ortiz, L., López-Serrano, P. M., & López-

Sánchez, C. A. (2017). Estimation of aboveground forest biomass in Galicia (NW Spain) by the combined use of LiDAR, LANDSAT ETM+ and National Forest Inventory data. *iForest*, *10*, 590–596. https://doi.org/10.3832/ifor1989-010

Joshi, C. (2006). *Mapping cryptic invaders and invasibility of tropical forest ecosystems: Chromolaena odorata in Nepal. Phd Thesis*. Wegeningen.

Karna, Y. K., Hussin, Y. A., Gilani, H., Bronsveld, M. C., Murthy, M. S. R., Qamer, F. M., … Baniya, C. B. (2015). Integration of WorldView-2 and airborne LiDAR data for tree species level carbon stock mapping in Kayar Khola watershed, Nepal. *International Journal of Applied Earth Observation and Geoinformation*, *38*, 280–291. https://doi.org/10.1016/j.jag.2015.01.011

Koukoulas S, B. A. (2005). Mapping individual tree location, height and species in broadleaved deciduous forest using airborne LIDAR and multi-spectral remotely sensed data. *International Journal of Remote Sensing*, *26*(3), 431–455. https://doi.org/10.1080/0143116042000298289

Kumar, L., Sinha, P., Taylor, S., & Alqurashi, A. F. (2015). Review of the use of remote sensing for biomass estimation to support renewable energy generation. *Journal of Applied Remote Sensing*, *9*(1), 97696. https://doi.org/10.1117/1.JRS.9.097696

Kumar, S. S. (2011). *Modelling the Relationship Between Tree Canopy Projection Area and Aboveground Carbon Stock Using High Resolution Geoeye Satellite Images*. Faculty of Geoinformation Science and Earth Observation (ITC) - University of Twente, Enschede, Unpublished Msc. Thesis.

Laurance, W. F., Laurance, S. G., Ferreira, L. V, RankindeMerona, J. M., Gascon, C., Lovejoy, T. E., & Merona, J. M. R. (1997). Biomas collapse in Amazonian forest fragments. *Science*, *278*(5340), 1117–1118. https://doi.org/DOI: 10.1126/science.278.5340.1117

Lawrence, R. L., & Ripple, W. J. (1998). Comparisons among Vegetation Indices and Bandwise Regression in a Highly Disturbed, Heterogeneous Landscape: Mount St. Helens, Washington. *Remote Sensing of Environment*, *64*, 91–102.

Le Quéré, C., Moriarty, R., Andrew, R. M., Peters, G. P., Ciais, P., Friedlingstein, P., … Bozec, Y. (2015). Global carbon budget 2014. *Earth Syst. Sci. Data*, *7*, 47–85. https://doi.org/10.5194/essd-7-47-2015

Lefsky, M. A., Cohen, W. B., Acker, S. A., Parker, G. G., Spies, T. A., & Harding, D. (1999a). Lidar remote sensing of the canopy structure and biophysical properties of douglas-fir Western Hemlock Forests. *Remote Sensing of Environment*, *70*, 339–361.

Lefsky, M. A., Cohen, W. B., Acker, S. A., Parker, G. G., Spies, T. A., & Harding, D. (1999b). Lidar remote sensing of the canopy structure and biophysical properties of Douglas-fir western hemlock forests. *Remote Sensing of Environment*, *70*(3), 339–361. https://doi.org/10.1016/S0034-4257(99)00052-8

Lemmens, M. (2017). The Fierce Rise of Airborne Lidar. Retrieved January 19, 2018, from https://www.gim-international.com/content/article/the-fierce-rise-of-airborne-lidar

Liang, X., Kankare, V., Hyyppä, J., Wang, Y., Kukko, A., Haggrén, H., … Vastaranta, M. (2016). Terrestrial laser scanning in forest inventories. *ISPRS Journal of Photogrammetry and Remote Sensing*, *115*, 63–77. https://doi.org/10.1016/j.isprsjprs.2016.01.006

Lim, K., Treitz, P., Wulder, M., St-Onge, B., & Flood, M. (2003). LiDAR remote sensing of forest structure. https://doi.org/10.1191/0309133303pp360ra

Lu, D. (2005). Aboveground biomass estimation using Landsat TM data in the Brazilian Amazon. *International Journal of Remote Sensing*. https://doi.org/10.1080/01431160500142145

Lu, D. (2006). The potential and challenge of remote sensing-based biomass estimation. *International Journal of Remote Sensing*, *27*(7), 1297–1328. https://doi.org/10.1080/01431160500486732

Lu, D., Mausel, P., Brondizio, E., & Moran, E. (2002). Above-ground biomass estimation of successional and mature forests using TM images in the Amazon basin. *Symposium on Geospatial Theory, Processing and Aplications*, 183–196. https://doi.org/10.1007/978-3-642-56094-1_14

Luckman, A., Baker, J., Kuplich, M. T., Yanasse, C. da C. F., & Frery, A. C. (1997). A Study of the Baekseatter and Biomass for Relationship Regenerating Spaeeborne SAR between Radar Tropical Forest Instruments. *Remote Sensing of Enviroment*, *60*(1–13).

Mohammadi, J., Shataee, S., & Babanezhad, M. (2011). Estimation of forest stand volume, tree density and biodiversity using landsat ETM+ data, comparison of linear and regression tree analyses. *Procedia Environmental Sciences*, *7*, 299–304. https://doi.org/10.1016/j.proenv.2011.07.052

Mon, M. S., Mizoue, N., & Zaw Htun, N. (2012). Estimating forest canopy density of tropical mixed deciduous vegetation using Landsat data: A comparison of three classification approaches. *International Journal of Remote Sensing*, *33*(4), 1042–1057. https://doi.org/10.1080/01431161.2010.549851

Muluken, N. B. (2017). *Intergrating Airborne LiDAR and Terrestrial Laser Scanner Forest Parameters for Accurate Estimation of Aboveground Biomass/Carbon in Ayer Hitam Tropical Forest Reserve, Malaysia*. Faculty of Geo-

information Science and Earth Observation, University of Twente - Enschede, Unpublished Msc. Thesis.
Muukkonen, P., & Heiskanen, J. (2005). Estimating biomass for boreal forests using ASTER satellite data combined with standwise forest inventory data. *Remote Sensing of Environment*, *99*(4), 434–447. https://doi.org/10.1016/j.rse.2005.09.011
Muukkonen, P., & Heiskanen, J. (2007). Biomass estimation over a large area based on standwise forest inventory data and ASTER and MODIS satellite data: A possibility to verify carbon inventories. *Remote Sensing of Environment*, *107*(4), 617–624. https://doi.org/10.1016/j.rse.2006.10.011
Nandin-Erdene, T. (2011). *Object Based Image Analysis of Geo-eye VHR Data to Model Aboveground Carbon Stock in Himalayan Mid-Hill Forests, Nepal*. Faculty of Geoinformation and Earth Observation (ITC) - University of Twente, Enschede, Unpublished Msc. Thesis.
Nascimento, M. T., Reinaldo, A., Barbosa, I., Villela, D. M., & Proctor, J. (2007). Above-ground biomass changes over an 11-year period in an Amazon monodominant forest and two other lowland forests. *Plant Ecology*, *192*, 181–191. https://doi.org/10.1007/s11258-007-9303-z
Nelson, R. (1984). Determining forest canopy characteristics wing airborne laser data. *Remote Sensing of the Environment*, *15*(3), 201–212. https://doi.org/10.1016/0034-4257(84)90031-2
Nelson, R., Oderwald, R., & Gregoire, T. G. (1997). Separating the ground and airborne laser sampling phases to estimate tropical forest basal area, volume, and biomass. *Remote Sensing of Environment*, *60*(3), 311–326. https://doi.org/10.1016/S0034-4257(96)00213-1
Nie, S., Wang, C., Zeng, H., Xi, X., & Li, G. (2017). Above-ground biomass estimation using airborne discrete-return and full-waveform LiDAR data in a coniferous forest. *Ecological Indicators*, *78*, 221–228. https://doi.org/10.1016/j.ecolind.2017.02.045
Nogueira, E. M., Yanai, A. M., Saldanha De Vasconcelos, S., Lima De Alencastro Graça, P. M., & Fearnside, P. M. (2017). Carbon stocks and losses to deforestation in protected areas in Brazilian Amazonia. *Regional Environmental Change*, *18*, 261–270. https://doi.org/10.1007/s10113-017-1198-1
Olivas, P. C., Oberbauer, S. F., Clark, D. B., Clark, D. A., Ryan, M. G., O 'brien, J. J., & Ordõ Nez, H. (2013). Comparison of direct and indirect methods for assessing leaf area index across a tropical rain forest landscape. *Agricultural and Forest Meteorology*, *177*, 110–116. https://doi.org/10.1016/j.agrformet.2013.04.010
OSU. (2017). Vegetation Structure with LiDAR | Remote Sensing Laboratory. Retrieved August 14, 2017, from http://remotesensing.forestry.oregonstate.edu/vegetation-structure-lidar
Petersson, H., Holm, S., Ståhl, G., Alger, D., Fridman, J., Lehtonen, A., … Mäkipää, R. (2012). Individual tree biomass equations or biomass expansion factors for assessment of carbon stock changes in living biomass – A comparative study. *Forest Ecology and Management*, *270*, 78–84. https://doi.org/10.1016/J.FORECO.2012.01.004
Phan, T. H. D., Brouwer, R., Davidson, M. D., & Hoang, L. P. (2017). A comparative study of transaction costs of payments for forest ecosystem services in Vietnam. *Forest Policy and Economics*, *80*, 141–149. https://doi.org/10.1016/j.forpol.2017.03.017
Popescu, C. sorin, & Kaiguang, Z. (2008). A voxel-based lidar method for estimating crown base height for deciduous and pine trees. *Remote Sensing of Environment*, *112*, 767–781. https://doi.org/10.1016/j.rse.2007.06.011
Quinn Gerry P., K. M. J. (2002). *Experimental Design and Data analysis for Biologists*. London: Cambridge University Press.
Rajpar, M. N., & Zakaria, M. (2014). Ajas assessing the effects of logging activities on Avian richness and diversity in different aged post - harvested hipp dipterocarp tropical rainforest of Malaysia. *American Journal of Applied Sciences*, *11*(9), 1519–1529. https://doi.org/10.3844/ajassp.2014.1519.1529
Ribeiro, S. C., Fehrmann, L., Soares, C. P. B., Jacovine, L. A. G., Kleinn, C., & de Oliveira Gaspar, R. (2011). Above- and belowground biomass in a Brazilian Cerrado. *Forest Ecology and Management*, *262*(3), 491–499. https://doi.org/10.1016/j.foreco.2011.04.017
Rikimaru, A., Roy, P. S., & Miyatake, S. (2002a). Tropical forest cover density mapping. *Tropical Ecology*, *43*(1), 39–47.
Rikimaru, Roy, P. S., & Miyatake, S. (2002b). Rikimaru , P . S . Roy and S . Miyatake , 2002 . Tropical forest cover density mapping . Tropical. *Tropical Ecology*, *43*(1), 39–47.
Sadadi, O. (2016). *Accuracy of Measuring Tree Height Using Airborne LiDAR and Terrestrial Laser Scanner and Its Effect on Estimating Forest Biomass and Carbon Stock in Ayer Himatan Tropical Rain Forest Reserve, Malaysia*. Faculty of Geo-information Science and Earth Observation (ITC) - University of Twente, Unpublished Msc. Thesis.
Shrestha, S. K. (2011a). *Carbon Stock Estimation Using Very High Resolution satellite Imagery and Individual Crown Segementatin. (A Case Study of Broadleaved and Needle Leaved Forest of Dolakha, Nepal)*. Faculty of Geo-information Science and Earth Observation Technology (ITC) - University of Twente, Enschede,

Unpublished Msc. Thesis.
Shrestha, S. K. (2011b). *CARBON STOCK ESTIMATION USING VERY HIGH RESOLUTION SATELLITE IMAGERY AND INDIVIDUAL CROWN SEGMENTATION. (A CASE STUDY OF BROADLEAVED AND NEEDLE LEAVED FOREST OF DOLAKHA, NEPAL)*. (Msc) Faculty of Geoinformation Science and Earth Observation (ITC) - University of Twente, Enschede.
Steininger, M. . (2000). Satellite estimation of tropical secondary forest above-ground biomass: data from Brazil and Bolivia. *International Journal of Remote Sensing*, *21*(6–7), 1139–1159. https://doi.org/10.1080/014311600210119
Stovall, A. E. L., Vorster, A. G., Anderson, R. S., Evangelista, P. H., & Shugart, H. H. (2017). Non-destructive aboveground biomass estimation of coniferous trees using terrestrial LiDAR. *Remote Sensing of Environment*, *200*(July), 31–42. https://doi.org/10.1016/j.rse.2017.08.013
Van Laar Anthonie, A. A. (2007). *Forest Mensuration*. (T. P. and M. T. Klaus von Gadow, Ed.) (12th ed.). Dordrecht, Netherlands: Springer.
Van Leeuwen, M., Hilker, T., Coops, N. C., Frazer, G., Wulder, M. A., Newnham, G. J., & Culvenor, D. S. (2011). Assessment of standing wood and fiber quality using ground and airborne laser scanning: A review. *Forest Ecology and Management*, *261*(9), 1467–1478. https://doi.org/10.1016/j.foreco.2011.01.032
van Leeuwen, M., & Nieuwenhuis, M. (2010). Retrieval of forest structural parameters using LiDAR remote sensing. *European Journal of Forest Research*, *129*(4), 749–770. https://doi.org/10.1007/s10342-010-0381-4
Wilkes, P., Lau, A., Disney, M., Calders, K., Burt, A., Gonzalez de Tanago, J., … Herold, M. (2017). Data acquisition considerations for Terrestrial Laser Scanning of forest plots. *Remote Sensing of Environment*, *196*, 140–153. https://doi.org/10.1016/j.rse.2017.04.030

APPENDICES

Appendix 1; Field data collection sheet.

DATA COLLECTION SHEET, BERKELAH FOREST RESERVE, MALAYSIA.								
Author:			**Plot radius:**		**Slope: (%)**		**Date:**	
Plot centre	**Latitude:**			**Longitude:**			**Plot No:**	
Canopy Density (%)								
Photography			Name of Person					
Tree No:	Latitude	Longitude	Species	DBH (cm)	Stem height	Tree shapes	Crown diam. (m)	Canopy density (%)

Appendix 2; Forest Canopy Volume and Forest Canopy Foliage Volume of different conditions in (m3)

Plot No	Not sliced non-smoothed forest canopy 2m	Not sliced smoothed forest canopy 2m	Sliced non-smoothed forest canopy 2m	Sliced smoothed forest canopy 2m	Not sliced non-smoothed forest canopy 1m	Not sliced smoothed forest canopy 1m	Sliced non-smoothed forest canopy 1m	Sliced smoothed forest canopy 1m	Not sliced non-smoothed forest canopy 0.5m	Not sliced smoothed forest canopy 0.5m	Sliced non-smoothed forest canopy 0.5m	Sliced smoothed forest canopy 0.5m
1	5776	6919.5	5860	9324.5	5443	5695.6	5044	6906.5	4520.7	4705.5	4025.9	6131.8
2	10516	10375.2	10464	10618.5	9608	9566.5	9511	9989.1	8601.4	8644.0	8342.7	9376.3
3	5184	5152.3	4088	5343.3	4851	4831.3	3757	4511.8	4402.9	4412.7	3253.5	4182.9
4	9732	9742.0	9700	9778.4	8800	8806.1	8733	8884.4	8166.1	8168.5	7847.2	8400.8
5	13840	13631.8	13840	13676.0	13488	13503.9	13481	13519.1	12950.2	12971.8	12961.5	13034.1
6	12872	12868.6	12872	12868.6	12724	12724.0	12724	12724.0	12169.8	12170.2	12169.3	12177.7
7	15024	14878.9	15024	14878.9	14482	14439.9	14482	14439.9	14248.7	14238.9	14248.7	14224.0
8	12528	12633.9	12528	12633.9	11825	11849.3	11818	11856.5	11124.6	11132.3	11079.5	11197.2
9	12704	12816.4	12704	12816.4	12337	12358.7	12261	12461.0	11542.7	11550.5	11412.4	11732.9
10	12728	12707.5	12728	12707.5	12059	12066.0	12051	12077.2	11735.2	11734.2	11718.5	11761.2
11	11012	11122.1	11012	11127.1	10161	10215.4	10082	10453.9	9518.4	9576.8	9351.6	9859.7
12	8180	8087.9	8180	8096.8	7688	7658.5	7598	7739.8	7264.2	7272.4	6993.1	7497.0
13	10876	10749.4	10876	10765.6	10133	10078.3	10127	10096.4	9456.7	9439.6	9375.0	9545.5
14	10784	10742.5	10756	10761.5	10271	10262.0	10263	10272.2	9856.2	9864.0	9789.1	9957.7
16	11712	11821.1	11712	11821.1	11014	11066.5	11014	11066.5	10784.9	10799.0	10734.7	10855.0
17	12672	12591.7	12672	12592.6	12189	12187.3	12189	12187.3	11575.3	11575.1	11563.6	11588.1
18	13144	12988.7	13132	13048.4	12619	12566.6	12609	12613.6	11979.9	11973.7	11951.1	12018.2
19	12156	12205.3	12156	12205.3	11568	11591.6	11568	11591.6	11132.0	11139.5	11132.0	11144.4
20	12332	12389.7	12332	12421.2	11722	11733.1	11707	11758.7	11178.5	11184.0	11147.0	11227.5
21	14276	14253.0	14276	14253.0	13741	13743.3	13741	13743.3	13196.6	13195.5	13188.2	13218.4
22	13040	13077.7	13040	13077.7	12650	12671.7	12644	12684.1	12079.0	12091.7	12032.9	12172.1
23	13992	13906.6	13992	13906.6	13170	13169.0	13170	13169.0	12535.4	12556.0	12520.8	12590.5
24	14716	14680.5	14716	14680.5	14186	14173.0	14186	14173.0	13557.8	13555.6	13554.6	13558.0
25	14696	14511.3	14696	14663.1	12988	13307.5	12988	13316.0	12695.0	12971.9	13075.2	13127.2
26	11852	11841.6	11852	11841.6	11647	11626.1	11647	11626.1	11476.9	11483.0	11476.9	11479.5
27	6008	6243.2	5732	6812.7	5594	5908.4	5138	6232.5	5310.1	5554.9	4747.5	6028.9
28	11460	11553.6	11460	11553.6	10793	10807.9	10717	10871.3	10282.3	10287.1	10131.7	10450.6
29	10652	10623.6	10620	10662.3	10253	10253.2	10174	10392.6	9581.8	9626.1	9449.9	9844.3
30	13916	13875.1	13916	13875.1	13294	13289.4	13286	13302.2	12972.0	12965.2	12966.2	12970.5
31	6156	6204.4	5888	9321.6	5327	5344.1	4976	5912.2	4888.7	4997.9	3997.9	5649.4
32	9320	9321.6	9320	9321.6	9008	9022.3	8978	9050.8	8574.0	8580.3	8530.3	8611.3
33	14300	14085.8	14300	14085.8	13835	13775.9	13835	13775.9	13477.8	13463.2	13475.7	13452.7
34	8428	8484.1	8292	9084.5	7949	7987.4	7780	8332.2	7453.3	7493.7	7153.5	7974.1
35	9520	9297.9	9520	9321.8	8655	8618.3	8655	8625.3	7945.3	7949.0	7822.6	8010.7
37	7124	7285.5	7080	7386.8	6114	6236.5	5861	6594.0	5695.9	5783.2	5359.4	6282.2
38	10792	10759.9	10792	10764.0	9879	9858.2	9851	9900.1	9465.1	9471.7	9374.1	9535.2
39	3348	3244.4	1320	4132.8	2723	2706.2	962	2464.0	2151.7	2356.7	490.3	1920.6
40	8636	8649.5	8636	8652.8	8174	8169.4	8174	8169.4	7730.5	7730.8	7704.2	7741.7
Total	**416004**	**416323.8**	**412084**	**424883.1**	**392962**	**393868.3**	**387782**	**397483.3**	**373277.6**	**374666.0**	**366148.0**	**380530.1**
Aver-age	**10947.5**	**10955.9**	**10844.3**	**11181.1**	**10341.1**	**10365.0**	**10204.8**	**10460.1**	**9823.1**	**9859.6**	**9635.5**	**10014.0**

Appendix 3; Adjusted Forest Canopy Volume and Adjusted Forest Canopy Foliage Volume of different conditions in (m3)

Plot No	Not sliced non-smoothed forest canopy 2m	Not sliced smoothed forest canopy 2m	Sliced non-smoothed forest canopy 2m	Sliced smoothed forest canopy 2m	Not sliced non-smoothed forest canopy 1m	Not sliced smoothed forest canopy 1m	Sliced non-smoothed forest canopy 1m	Sliced smoothed forest canopy 1m	Not sliced non-smoothed forest canopy 0.5m	Not sliced smoothed forest canopy 0.5m	Sliced non-smoothed forest canopy 0.5m	Sliced smoothed forest canopy 0.5m
1	4938.5	5916.2	5010.3	7972.4	4653.8	4869.8	4312.6	5905.1	3865.2	4023.2	3442.2	5242.7
2	8991.2	8870.8	8946.7	9078.8	8214.8	8179.3	8131.9	8540.7	7354.2	7390.6	7133.0	8016.7
3	3395.5	3374.8	2677.6	3499.8	3177.4	3164.5	2460.8	2955.2	2883.9	2890.3	2131.1	2739.8
4	6374.5	6381.0	6353.5	6404.8	5764.0	5768.0	5720.1	5819.3	5348.8	5350.4	5139.9	5502.5
5	10449.2	10292.0	10449.2	10325.3	10183.4	10195.4	10178.2	10206.9	9777.4	9793.7	9785.9	9840.7
6	11005.6	11002.6	11005.6	11002.6	10879.0	10879.1	10879.0	10879.1	10405.2	10405.5	10404.8	10412.0
7	12845.5	12721.4	12845.5	12721.4	12382.1	12346.1	12382.1	12346.1	12182.7	12174.2	12182.7	12161.5
8	10711.4	10802.0	10711.4	10802.0	10110.4	10131.1	10104.4	10137.3	9511.5	9518.1	9473.0	9573.6
9	10861.9	10958.0	10861.9	10958.0	10548.1	10566.6	10483.2	10654.2	9869.0	9875.7	9757.6	10031.6
10	9609.6	9594.2	9609.6	9594.2	9104.5	9109.8	9098.5	9118.3	8860.1	8859.3	8847.5	8879.7
11	8314.1	8397.2	8314.1	8400.9	7671.6	7712.6	7611.9	7892.7	7186.4	7230.5	7060.4	7444.1
12	5357.9	5297.6	5357.9	5303.4	5035.6	5016.3	4976.7	5069.5	4758.0	4763.4	4580.5	4910.6
13	7123.8	7040.8	7123.8	7051.5	6637.1	6601.3	6633.2	6613.1	6194.2	6183.0	6140.6	6252.3
14	8141.9	8110.6	8120.8	8125.0	7754.6	7747.8	7748.6	7755.5	7441.4	7447.3	7390.7	7518.1
16	10013.8	10107.1	10013.8	10107.1	9417.0	9461.9	9417.0	9461.9	9221.1	9233.1	9178.2	9281.0
17	10834.6	10765.9	10834.6	10766.7	10421.6	10420.2	10421.6	10420.2	9896.9	9896.7	9886.9	9907.9
18	8609.3	8507.6	8601.5	8546.7	8265.4	8231.1	8258.9	8261.9	7846.8	7842.7	7828.0	7871.9
19	10393.4	10435.6	10393.4	10435.6	9890.6	9910.8	9890.6	9910.8	9517.9	9524.3	9517.9	9528.4
20	11777.1	11832.1	11777.1	11862.2	11194.5	11205.1	11180.2	11229.5	10675.4	10680.7	10645.3	10722.3
21	12206.0	12186.3	12206.0	12186.3	11748.6	11750.5	11748.6	11750.5	11283.1	11282.2	11275.9	11301.7
22	11149.2	11181.4	11149.2	11181.4	10815.8	10834.3	10810.6	10844.9	10327.6	10338.4	10288.2	10407.1
23	11963.2	11890.2	11963.2	11890.2	11260.4	11259.5	11260.4	11259.5	10717.8	10735.4	10705.3	10764.9
24	12582.2	12551.8	12582.2	12551.8	12129.0	12117.9	12129.0	12117.9	11591.9	11590.0	11589.2	11592.1
25	12565.1	12407.2	12565.1	12536.9	11104.7	11377.9	11104.7	11385.2	10854.2	11091.0	11179.3	11223.8
26	8948.3	8940.4	8948.3	8940.4	8793.5	8777.7	8793.5	8777.7	8665.0	8669.7	8665.0	8667.0
27	4536.0	4713.6	4327.7	5143.6	4223.5	4460.8	3879.2	4705.6	4009.1	4194.0	3584.4	4551.8
28	8652.3	8723.0	8652.3	8723.0	8148.7	8160.0	8091.3	8207.9	7763.1	7766.8	7649.4	7890.2
29	8042.3	8020.8	8018.1	8050.1	7741.0	7741.2	7681.4	7846.4	7234.2	7267.7	7134.7	7432.4
30	10506.6	10475.7	10506.6	10475.7	10037.0	10033.5	10030.9	10043.1	9793.9	9788.7	9789.5	9792.8
31	4032.2	4063.9	3856.6	6105.6	3489.2	3500.4	3259.3	3872.5	3202.1	3273.6	2618.6	3700.3
32	6104.6	6105.6	6104.6	6105.6	5900.2	5909.6	5880.6	5928.3	5616.0	5620.1	5587.3	5640.4
33	9366.5	9226.2	9366.5	9226.2	9061.9	9023.2	9061.9	9023.2	8828.0	8818.4	8826.6	8811.5
34	5520.3	5557.1	5431.3	5950.4	5206.6	5231.8	5095.9	5457.6	4881.9	4908.4	4685.5	5223.0
35	6235.6	6090.1	6235.6	6105.8	5669.0	5645.0	5669.0	5649.6	5204.2	5206.6	5123.8	5247.0
37	4666.2	4772.0	4637.4	4838.3	4004.7	4084.9	3839.0	4319.1	3730.8	3788.0	3510.4	4114.9
38	7068.8	7047.7	7068.8	7050.4	6470.7	6457.1	6452.4	6484.6	6199.6	6203.9	6140.0	6245.5
39	2192.9	2125.1	864.6	2707.0	1783.6	1772.6	630.1	1613.9	1409.4	1543.6	321.1	1258.0
40	5656.6	5665.4	5656.6	5667.6	5354.0	5351.0	5354.0	5351.0	5063.5	5063.6	5046.2	5070.8
Total	**321743.4**	**322151.0**	**319148.6**	**328394.7**	**304247.7**	**305005.6**	**300661.2**	**307815.4**	**289171.5**	**290232.8**	**284246.4**	**294772.9**
Average	**8466.9**	**8477.7**	**8398.6**	**8642.0**	**8006.5**	**8026.5**	**7912.1**	**8100.4**	**7609.8**	**7637.7**	**7480.2**	**7757.2**

Appendix 4; Summary of regression statistics between smoothed 0.5m pixel sliced forest canopy foliage volume and aboveground biomass

Regression statistics summary of sliced and smoothed 0.5m pixel forest canopy foliage volume and above-ground biomass

Regression Statistics	
Multiple R	0.83445
R Square	0.696308
Adjusted R Square	0.687872
Standard Error	103.6046
Observations	38

ANOVA

	df	*SS*	*MS*	*F*	*Significance F*
Regression	1	885988.8	885988.8	82.54101	7.56E-11
Residual	36	386421.2	10733.92		
Total	37	1272410			

	Coefficients	*Standard Error*	*t Stat*	*P-value*
Intercept	-145.016	61.81404	-2.346	0.024601
Forest Canopy Volume	0.002698	0.000297	9.085208	7.56E-11

Appendix 5; Summary of regression statistics between sliced none smoothed 0.5m pixel forest canopy foliage volume and aboveground biomass

Regression statistics summary of sliced non-smoothed 0.5m pixel forest canopy foliage volume and aboveground biomass

Regression Statistics	
Multiple R	0.831932
R Square	0.692111
Adjusted R Square	0.683559
Standard Error	104.318
Observations	38

ANOVA

	df	*SS*	*MS*	*F*	*Significance F*
Regression	1	880649.4	880649.4	80.9254	9.7E-11
Residual	36	391760.6	10882.24		
Total	37	1272410			

	Coefficients	*Standard Error*	*t Stat*	*P-value*
Intercept	-55.0946	52.8622	-1.04223	0.304254
Forest Canopy volume	0.002338	0.00026	8.995854	9.7E-11

Appendix 6; Summary of regression statistics between non-sliced smoothed 0.5m pixel forest canopy foliage volume and aboveground biomass

Regression statistics summary of non-sliced smoothed 0.5m pixel forest canopy volume and aboveground biomass

Regression Statistics	
Multiple R	0.835193
R Square	0.697548
Adjusted R Square	0.689147
Standard Error	103.3929
Observations	38

ANOVA

	df	*SS*	*MS*	*F*	*Significance F*
Regression	1	887567	887567	83.02715	7.01E-11
Residual	36	384842.9	10690.08		
Total	37	1272410			

	Coefficients	*Standard Error*	*t Stat*	*P-value*
Intercept	-120.404	59.04228	-2.03928	0.048815
Forest Canopy Volume	0.002616	0.000287	9.111924	7.01E-11

Appendix 7; Summary of regression statistics between non-sliced none smoothed 0.5m pixel forest canopy volume and aboveground biomass

Regression statistics summary of non-sliced non-smoothed 0.5m pixel forest canopy volume and aboveground biomass

Regression Statistics	
Multiple R	0.833958
R Square	0.695486
Adjusted R Square	0.687027
Standard Error	103.7448
Observations	38

ANOVA

	df	*SS*	*MS*	*F*	*Significance F*
Regression	1	884942.9	884942.9	82.22103	7.94E-11
Residual	36	387467.1	10762.97		
Total	37	1272410			

	Coefficients	*Standard Error*	*t Stat*	*P-value*
Intercept	-111.736	58.40788	-1.91302	0.063725
Forest Canopy Volume	0.002581	0.000285	9.067581	7.94E-11

Appendix 8; Summary of regression statistics between sliced smoothed 1m pixel forest canopy foliage volume and aboveground biomass

Regression statistics summary of sliced 1m pixel smoothed forest canopy foliage volume and aboveground biomass

Regression Statistics	
Multiple R	0.839611
R Square	0.704946
Adjusted R Square	0.69675
Standard Error	102.1205
Observations	38

ANOVA

	df	*SS*	*MS*	*F*	*Significance F*
Regression	1	896980.4	896980.4	86.0116	4.47E-11
Residual	36	375429.5	10428.6		
Total	37	1272410			

	Coefficients	*Standard Error*	*t Stat*	*P-value*
Intercept	-170.333	63.21207	-2.69463	0.010639
Forest Canopy Volume	0.002704	0.000292	9.274244	4.47E-11

Appendix 9; Summary of regression statistics between sliced none smoothed 1m pixel forest canopy foliage volume and aboveground biomass

Regression statistics summary of sliced 1m pixel none smoothed forest canopy foliage volume and aboveground biomass

Regression Statistics	
Multiple R	0.832137
R Square	0.692452
Adjusted R Square	0.683909
Standard Error	104.2603
Observations	38

ANOVA

	df	*SS*	*MS*	*F*	*Significance F*
Regression	1	881082.3	881082.3	81.05474	9.51E-11
Residual	36	391327.7	10870.21		
Total	37	1272410			

	Coefficients	*Standard Error*	*t Stat*	*P-value*
Intercept	-92.7739	56.80198	-1.63329	0.111126
Forest Canopy Volume	0.002392	0.000266	9.003041	9.51E-11

Appendix 10; Summary of regression statistics between non-sliced smoothed 1m pixel forest canopy volume and aboveground biomass

Regression statistics summary of sliced 1m pixel smoothed forest canopy volume and aboveground biomass

Regression Statistics	
Multiple R	0.839948
R Square	0.705513
Adjusted R Square	0.697333
Standard Error	102.0223
Observations	38

ANOVA

	df	*SS*	*MS*	*F*	*Significance F*
Regression	1	897702.1	897702.1	86.24659	4.32E-11
Residual	36	374707.9	10408.55		
Total	37	1272410			

	Coefficients	*Standard Error*	*t Stat*	*P-value*
Intercept	-151.719	61.19561	-2.47924	0.017984
Forest Canopy Volume	0.002639	0.000284	9.286904	4.32E-11

Appendix 11; Summary of regression statistics between non-sliced none smoothed 1m pixel forest canopy volume and aboveground biomass

Regression statistics summary of sliced 1m pixel none smoothed forest canopy volume and aboveground biomass

Regression Statistics	
Multiple R	0.838166
R Square	0.702523
Adjusted R Square	0.694259
Standard Error	102.539
Observations	38

ANOVA

	df	*SS*	*MS*	*F*	*Significance F*
Regression	1	893896.8	893896.8	85.01762	5.19E-11
Residual	36	378513.1	10514.25		
Total	37	1272410			

	Coefficients	*Standard Error*	*t Stat*	*P-value*
Intercept	-145.373	60.96443	-2.38456	0.02249
Forest Canopy Volume	0.002615	0.000284	9.2205	5.19E-11

Appendix 12; Summary of regression statistics between sliced smoothed 2m pixel forest canopy foliage volume and aboveground biomass

Regression statistics summary of sliced 2m pixel smoothed forest canopy foliage volume and aboveground biomass

Regression Statistics	
Multiple R	0.835944
R Square	0.698802
Adjusted R Square	0.690435
Standard Error	103.1783
Observations	38

ANOVA

	df	*SS*	*MS*	*F*	*Significance F*
Regression	1	889162.7	889162.7	83.52272	6.5E-11
Residual	36	383247.3	10645.76		
Total	37	1272410			

	Coefficients	*Standard Error*	*t Stat*	*P-value*
Intercept	-266.286	74.31361	-3.58328	0.000997
Forest Canopy Volume	0.002959	0.000324	9.139076	6.50E-11

Appendix 13; Summary of regression statistics between non-sliced none-smoothed 2m pixel forest canopy foliage volume and aboveground biomass

Regression statistics summary of sliced 2m pixel none smoothed forest canopy foliage volume and aboveground biomass

Regression Statistics	
Multiple R	0.829267
R Square	0.687683
Adjusted R Square	0.679008
Standard Error	105.0654
Observations	38

ANOVA

	df	*SS*	*MS*	*F*	*Significance F*
Regression	1	875015.2	875015.2	79.26763	1.26E-10
Residual	36	397394.8	11038.74		
Total	37	1272410			

	Coefficients	*Standard Error*	*t Stat*	*P-value*
Intercept	-122.951	60.66626	-2.02668	0.050151
Forest Canopy Volume	0.00239	0.000268	8.903237	1.26E-10

Appendix 14; Summary of regression statistics between non-sliced smoothed 2m pixel forest canopy volume and aboveground biomass

Regression statistics summary of sliced 2m pixel smoothed forest canopy volume and aboveground biomass

Regression Statistics	
Multiple R	0.845926
R Square	0.715591
Adjusted R Square	0.707691
Standard Error	100.2614
Observations	38

ANOVA

	df	*SS*	*MS*	*F*	*Significance F*
Regression	1	910525.4	910525.4	90.57838	2.29E-11
Residual	36	361884.5	10052.35		
Total	37	1272410			

	Coefficients	*Standard Error*	*t Stat*	*P-value*
Intercept	-196.789	64.31525	-3.05975	0.004168
Forest Canopy Volume	0.002703	0.000284	9.517268	2.29E-11

Appendix 15; Summary of regression statistics between non-sliced none smoothed 2m pixel forest canopy volume and aboveground biomass

Regression statistics summary of sliced 2m pixel none smoothed forest canopy volume and aboveground biomass

Regression Statistics	
Multiple R	0.836284
R Square	0.699371
Adjusted R Square	0.69102
Standard Error	103.0808
Observations	38

ANOVA

	df	*SS*	*MS*	*F*	*Significance F*
Regression	1	889886.8	889886.8	83.74898	6.28E-11
Residual	36	382523.2	10625.64		
Total	37	1272410			

	Coefficients	*Standard Error*	*t Stat*	*P-value*
Intercept	-174.063	64.43637	-2.70131	0.010464
Forest Canopy Volume	0.002601	0.000284	9.151447	6.28E-11

Appendix 16; Summary of regression statistics between smoothed 0.5m pixel sliced adjusted forest canopy foliage volume and aboveground biomass

Regression statistics summary of sliced smoothed 0.5m pixel adjusted forest canopy foliage volume and aboveground biomass

Regression Statistics	
Multiple R	0.815021
R Square	0.66426
Adjusted R Square	0.654934
Standard Error	108.9341
Observations	38

ANOVA

	df	*SS*	*MS*	*F*	*Significance F*
Regression	1	845211	845211	71.22581	4.7E-10
Residual	36	427199	11866.64		
Total	37	1272410			

	Coefficients	*Standard Error*	*t Stat*	*P-value*
Intercept	-33.0088	53.75239	-0.61409	0.543018
Adjusted Forest Canopy Volume	0.002762	0.000327	8.439539	4.70E-10

Appendix 17; Summary of regression statistics between sliced none smoothed 0.5m pixel adjusted forest canopy foliage volume and aboveground biomass

Regression statistics summary of sliced non-smoothed 0.5m pixel adjusted forest canopy foliage volume and aboveground biomass

Regression Statistics	
Multiple R	0.823794
R Square	0.678636
Adjusted R Square	0.66971
Standard Error	106.5763
Observations	38

ANOVA

	df	*SS*	*MS*	*F*	*Significance F*
Regression	1	863503.6	863503.6	76.0226	2.12E-10
Residual	36	408906.4	11358.51		
Total	37	1272410			

	Coefficients	*Standard Error*	*t Stat*	*P-value*
Intercept	14.69879	46.96346	0.312984	0.756099
Adjusted Forest Canopy Volume	0.002545	0.000292	8.719094	2.12E-10

Appendix 18; Summary of regression statistics between non-sliced smoothed 0.5m pixel adjusted forest canopy foliage volume and aboveground biomass

Regression statistics summary of non-sliced smoothed 0.5m pixel adjusted forest canopy volume and above-ground biomass

Regression Statistics	
Multiple R	0.819034
R Square	0.670816
Adjusted R Square	0.661673
Standard Error	107.8652
Observations	38

ANOVA

	df	*SS*	*MS*	*F*	*Significance F*
Regression	1	853553.6	853553.6	73.3615	3.28E-10
Residual	36	418856.4	11634.9		
Total	37	1272410			

	Coefficients	*Standard Error*	*t Stat*	*P-value*
Intercept	-19.7706	51.53607	-0.38363	0.703511
Adjusted Forest Canopy Volume	0.002718	0.000317	8.565133	3.28E-10

Appendix 19; Summary of regression statistics between non-sliced none smoothed 0.5m pixel adjusted forest canopy volume and aboveground biomass

Regression statistics summary of non-sliced non-smoothed 0.5m pixel adjusted forest canopy volume and above-ground biomass

Regression Statistics	
Multiple R	0.819788
R Square	0.672052
Adjusted R Square	0.662943
Standard Error	107.6625
Observations	38

ANOVA

	df	*SS*	*MS*	*F*	*Significance F*
Regression	1	855126.2	855126.2	73.77364	3.06E-10
Residual	36	417283.8	11591.22		
Total	37	1272410			

	Coefficients	*Standard Error*	*t Stat*	*P-value*
Intercept	-16.02	50.9869	-0.3142	0.755184
Adjusted Forest Canopy Volume	0.002703	0.000315	8.589158	3.06E-10

Appendix 20; Summary of regression statistics between smoothed 1m pixel sliced adjusted forest canopy foliage volume and aboveground biomass

Regression statistics summary of sliced smoothed 1m pixel adjusted forest canopy foliage volume and aboveground biomass

Regression Statistics	
Multiple R	0.815037
R Square	0.664285
Adjusted R Square	0.654959
Standard Error	108.9301
Observations	38

ANOVA

	df	*SS*	*MS*	*F*	*Significance F*
Regression	1	845242.3	845242.3	71.23367	4.69E-10
Residual	36	427167.7	11865.77		
Total	37	1272410			

	Coefficients	*Standard Error*	*t Stat*	*P-value*
Intercept	-44.1409	54.9969	-0.80261	0.427469
Adjusted Forest Canopy Volume	0.002713	0.000321	8.440004	4.69E-10

Appendix 21; Summary of regression statistics between sliced none smoothed 1m pixel adjusted forest canopy foliage volume and aboveground biomass

Regression statistics summary of sliced non-smoothed 1m pixel adjusted forest canopy foliage volume and above-ground biomass

Regression Statistics	
Multiple R	0.821541
R Square	0.674929
Adjusted R Square	0.665899
Standard Error	107.1893
Observations	38

ANOVA

	df	*SS*	*MS*	*F*	*Significance F*
Regression	1	858786.7	858786.7	74.74511	2.61E-10
Residual	36	413623.3	11489.54		
Total	37	1272410			

	Coefficients	*Standard Error*	*t Stat*	*P-value*
Intercept	-8.0897	49.80663	-0.16242	0.871882
Adjusted Forest Canopy Volume	0.00255	0.000295	8.645525	2.61E-10

Appendix 22; Summary of regression statistics between non-sliced smoothed 1m pixel adjusted forest canopy foliage volume and aboveground biomass

Regression statistics summary of non-sliced smoothed 1m pixel adjusted forest canopy volume and aboveground biomass

Regression Statistics	
Multiple R	0.81847
R Square	0.669893
Adjusted R Square	0.660724
Standard Error	108.0163
Observations	38

ANOVA

	df	*SS*	*MS*	*F*	*Significance F*
Regression	1	852379.1	852379.1	73.0557	3.45E-10
Residual	36	420030.8	11667.52		
Total	37	1272410			

	Coefficients	*Standard Error*	*t Stat*	*P-value*
Intercept	-35.0583	53.32567	-0.65744	0.515081
Adjusted Forest Canopy Volume	0.002682	0.000314	8.547263	3.45E-10

Appendix 23; Summary of regression statistics between non-sliced none smoothed 1m pixel adjusted forest canopy volume and aboveground biomass

Regression statistics summary of non-sliced non-smoothed 1m pixel adjusted forest canopy volume and aboveground biomass

Regression Statistics	
Multiple R	0.819134
R Square	0.670981
Adjusted R Square	0.661841
Standard Error	107.8383
Observations	38

ANOVA

	df	*SS*	*MS*	*F*	*Significance F*
Regression	1	853762.6	853762.6	73.41608	3.25E-10
Residual	36	418647.4	11629.09		
Total	37	1272410			

	Coefficients	*Standard Error*	*t Stat*	*P-value*
Intercept	-33.164	52.99054	-0.62585	0.535363
Adjusted Forest Canopy Volume	0.002676	0.000312	8.568319	3.25E-10

Appendix 24; Summary of regression statistics between smoothed 2m pixel sliced adjusted forest canopy foliage volume and aboveground biomass

Regression statistics summary of sliced smoothed 2m pixel adjusted forest canopy foliage volume and aboveground biomass

Regression Statistics	
Multiple R	0.79974
R Square	0.639584
Adjusted R Square	0.629573
Standard Error	112.8662
Observations	38

ANOVA

	df	*SS*	*MS*	*F*	*Significance F*
Regression	1	813813.5	813813.5	63.88468	1.71E-09
Residual	36	458596.4	12738.79		
Total	37	1272410			

	Coefficients	*Standard Error*	*t Stat*	*P-value*
Intercept	-82.2706	62.50696	-1.31618	0.196432
Adjusted Forest Canopy Volume	0.002764	0.000346	7.992789	1.71E-09

Appendix 25; Summary of regression statistics between sliced none smoothed 2m pixel adjusted forest canopy foliage volume and aboveground biomass

Regression statistics summary of sliced non-smoothed 2m pixel adjusted forest canopy foliage volume and aboveground biomass

Regression Statistics	
Multiple R	0.817555
R Square	0.668395
Adjusted R Square	0.659184
Standard Error	108.2611
Observations	38

ANOVA

	df	*SS*	*MS*	*F*	*Significance F*
Regression	1	850473.1	850473.1	72.56306	3.75E-10
Residual	36	421936.9	11720.47		
Total	37	1272410			

	Coefficients	*Standard Error*	*t Stat*	*P-value*
Intercept	-25.2788	52.41685	-0.48227	0.632537
Adjusted Forest Canopy Volume	0.002505	0.000294	8.518395	3.75E-10

Appendix 26; Summary of regression statistics between non-sliced smoothed 2m pixel adjusted forest canopy foliage volume and aboveground biomass

Regression statistics summary of non-sliced smoothed 2m pixel adjusted forest canopy volume and above-ground biomass

Regression Statistics	
Multiple R	0.817507
R Square	0.668318
Adjusted R Square	0.659105
Standard Error	108.2738
Observations	38

ANOVA

	df	*SS*	*MS*	*F*	*Significance F*
Regression	1	850374.5	850374.5	72.5377	3.77E-10
Residual	36	422035.5	11723.21		
Total	37	1272410			

	Coefficients	*Standard Error*	*t Stat*	*P-value*
Intercept	-55.7436	55.80879	-0.99883	0.324543
Adjusted Forest Canopy Volume	0.002661	0.000312	8.516906	3.77E-10

Appendix 27; Summary of regression statistics between non-sliced none smoothed 2m pixel adjusted forest canopy volume and aboveground biomass

Regression statistics summary of non-sliced non-smoothed 2m pixel adjusted forest canopy volume and above-ground biomass

Regression Statistics	
Multiple R	0.815852
R Square	0.665615
Adjusted R Square	0.656327
Standard Error	108.714
Observations	38

ANOVA

	df	*SS*	*MS*	*F*	*Significance F*
Regression	1	846935.4	846935.4	71.6604	4.37E-10
Residual	36	425474.5	11818.74		
Total	37	1272410			

	Coefficients	*Standard Error*	*t Stat*	*P-value*
Intercept	-47.6376	55.22986	-0.86253	0.394104
Adjusted Forest Canopy Volume	0.002616	0.000309	8.465247	4.37E-10